TRANSPORTATION RESEARCH RECORD 853

Concrete Analysis and Deterioration

TRANSPORTATION RESEARCH BOARD

NATIONAL RESEARCH COUNCIL

NATIONAL ACADEMY OF SCIENCES
WASHINGTON, D.C. 1982

Transportation Research Record 853
Price $7.20
Edited for TRB by Mary McLaughlin

modes
1 highway transportation
4 air transportation

subject areas
24 pavement design and performance
25 structures design and performance
32 cement and concrete
35 mineral aggregates

Library of Congress Cataloging in Publication Data
Concrete analysis and deterioration.

(Transportation research record; 853)
Reports prepared for the TRB 61st Annual Meeting.
1. Pavements, Concrete–Addresses, essays, lectures. 2. Concrete construction–Addresses, essays, lectures. I. National Research Council (U.S.). Transportation Research Board. II. Series.
TE7.H5 no. 853 [TE278] 380.5s [625.8'4] 82-18833
ISBN 0-309-03357-8 ISSN 0361-1981

Sponsorship of the Papers in This Transportation Research Record

GROUP 2–DESIGN AND CONSTRUCTION OF TRANSPORTATION FACILITIES
R.V. LeClerc, consultant, Olympia, Washington, chairman

Concrete Section
Carl F. Crumpton, Kansas Department of Transportation, chairman

Committee on Performance of Concrete
David Stark, Portland Cement Association, chairman
Charles F. Scholer, Purdue University, secretary
Greg Bobrowski, J. Parke Boyer, Philip D. Cady, Theodore R. Cantor, W.P. Chamberlin, Kenneth C. Clear, James R. Clifton, Glenn William DePuy, Sidney Diamond, James T. Dikeou, Ludmila Dolar-Mantuani, Bernard Erlin, John W. Figg, J.E. Gillott, Richard H. Howe, Stella L. Marusin, Bryant Mather, Katharine Mather, Howard J. McGinnis, Richard C. Meininger, Richard C. Mielenz, W. Grigg Mullen, V. Ramakrishnan, John Ryell, R.K. Smutzer, Samuel S. Tyson, Hollis N. Walker, Richard D. Walker

Committee on Batching, Mixing, Placing, and Curing of Concrete
Richard E. Hay, Federal Highway Administration, chairman
Alfred G. Bishara, E.J. Breckwoldt, Ralph A. Britson, James R. Clifton, Everett R. Davis, Ben E. Edwards, William E. Elmore, Samuel B. Helms, Paul Klieger, Bryant Mather, W. Grigg Mullen, Wade J. Patrick, Robert T. Peterson, V. Ramakrishnan, William T. Stapler, A. Haleem Tahir, William L. Trimm

William G. Gunderman, Transportation Research Board staff

Sponsorship is indicated by a footnote at the end of each report. The organizational units, officers, and members are as of December 31, 1981.

Contents

D-CRACKING: PAVEMENT DESIGN AND CONSTRUCTION VARIABLES
Robert J. Girard, Eugene M. Myers, Gerald D. Manchester, and William L. Trimm 1

EFFORTS TO ELIMINATE D-CRACKING IN ILLINOIS
Marvin L. Traylor 9

RECYCLING PORTLAND CEMENT CONCRETE PAVEMENT
Andrew D. Halverson 14

RELATION BETWEEN PAVEMENT D-CRACKING AND COARSE-AGGREGATE PORE STRUCTURE
D.N. Winslow, M.K. Lindgren, and W.L. Dolch 17

OHIO AGGREGATE AND CONCRETE TESTING TO DETERMINE D-CRACKING SUSCEPTIBILITY
John T. Paxton 20

DURABILITY OF CONCRETE AND THE IOWA PORE INDEX TEST
Vernon J. Marks and Wendell Dubberke 25

CONCRETE EVALUATION BY RADAR THEORETICAL ANALYSIS
A.V. Alongi, T.R. Cantor, C.P. Kneeter, and A. Alongi, Jr. 31

RADAR AS APPLIED TO EVALUATION OF BRIDGE DECKS
T.R. Cantor and C.P. Kneeter 37

EFFECTS OF CONCRETE DETERIORATION ON BRIDGE RESPONSE
David B. Beal and William P. Chamberlin 43

ACCURACY OF THE CHACE AIR INDICATOR
Michael M. Sprinkel 48

Authors of the Papers in This Record

Alongi, A., Jr., Penetradar Corporation, P.O. Box 87, 6865 Walmore Road, Niagara Falls, NY 14304

Alongi, A.V., Penetradar Corporation, P.O. Box 87, 6865 Walmore Road, Niagara Falls, NY 14304

Beal, David B., New York State Department of Transportation, 1220 Washington Avenue, State Campus, Albany, NY 12232

Cantor, T.R., Port Authority of New York and New Jersey, Journal Square Transportation Center, One Path Plaza, Jersey City, NJ 07306

Chamberlin, William P., New York State Department of Transportation, 1220 Washington Avenue, State Campus, Albany, NY 12232

Dolch, W.L., School of Civil Engineering, Purdue University, Civil Engineering Building, West Lafayette, IN 47907

Dubberke, Wendell, Highway Division, Iowa Department of Transportation, 800 Lincoln Way, Ames, IA 50010

Girard, Robert J., Division of Materials and Research, Missouri Highway and Transportation Commission, P.O. Box 270, Jefferson City, MO 65102

Halverson, Andrew D., Minnesota Department of Transportation, Transportation Building, St. Paul, MN 55155

Kneeter, C. P., Port Authority of New York and New Jersey, Journal Square Transportation Center, One Path Plaza, Jersey City, NJ 07306

Lindgren, M.K., School of Civil Engineering, Purdue University, Civil Engineering Building, West Lafayette, IN 47907

Manchester, Gerald D., Division of Materials and Research, Missouri Highway and Transportation Commission, P.O. Box 270, Jefferson City, MO 65102

Marks, Vernon J., Highway Division, Iowa Department of Transportation, 800 Lincoln Way, Ames, IA 50010

Myers, Eugene W., Division of Materials and Research, Missouri Highway and Transportation Commission, P.O. Box 270, Jefferson City, MO 65102

Paxton, John T., Bureau of Testing, Ohio Department of Transportation, 1600 West Broad Street, Columbus, OH 43223-1298

Sprinkel, Michael M., Virginia Highway and Transportation Research Council, Box 3817, University Station, Charlottesville, VA 22903

Traylor, Marvin L., Bureau of Materials and Physical Research, Illinois Department of Transportation, 126 East Ash Street, Springfield, IL 62706

Trimm, William L., Division of Materials and Research, Missouri Highway and Transportation Commission, P.O. Box 270, Jefferson City, MO 65102

Winslow, D.N., School of Civil Engineering, Purdue University, Civil Engineering Building, West Lafayette, IN 47907

D-Cracking: Pavement Design and Construction Variables

ROBERT J. GIRARD, EUGENE W. MYERS, GERALD D. MANCHESTER, AND WILLIAM L. TRIMM

Reported map cracking and D-cracking problems observed on portland cement concrete (PCC) pavements in Missouri from the late 1930s to 1981 are briefly discussed. Investigations involving studies in the laboratory and constructed pavements have contributed significantly to a better understanding of the deterioration process and its cause. Type, characteristics, and maximum size of coarse aggregate; source of cement; design of concrete mix; and type of base have been or are being studied in the field or laboratory to determine their influence to frost susceptibility of concrete. Missouri has increased the service life of its PCC pavements. This has been accomplished by (a) not using river and glacial gravels in construction of PCC pavements and (b) subjecting limestones that have a known history of D-cracking problems to increased quality restrictions, which has resulted in some ledges and entire quarries and formations being eliminated. However, D-cracking remains and, in terms of required maintenance and service life, is still a problem.

"Map cracking" and "D-cracking" are terms that have been used in Missouri to discuss the phenomenon of concrete pavement deterioration that occurs when a frost-susceptible aggregate is used in a freeze-and-thaw environment. Map cracking was used in the earliest recorded field surveys to describe visual surface deterioration of gravel aggregate pavements, and D-cracking has been used in recent years to describe visual surface deterioration of limestone aggregate pavements.

D-cracking today is defined as cracking in a slab surface in a pattern that appears first in an orientation parallel to transverse and longitudinal joints and cracks, continues around corners, and may progress into the central area of the slab. Staining, a slight darkening of the concrete at joints or cracks, may precede D-cracking.

As noted above, D-cracking is a phenomenon of concrete pavements. On the Missouri highway system, there are no known concrete bridge decks that exhibit D-cracking.

MAP CRACKING

Early History

The first concrete pavement in Missouri was constructed in 1913 on MO-30 (Gravois Road) in St. Louis. It was 20 ft wide and 1 mile long. By 1922, Missouri had 121 miles of concrete pavement, and, prior to 1928, 1200 miles of two-lane (16-, 18-, and 20-ft) pavement and 359 miles of 9-ft pavement. The coarse aggregates used in these concrete pavements were gravel, crushed flint, or limestone. Crushed flint is a colloquialism used in the identification of crushed chert fragments produced as residue from mining and processing of lead and zinc ores.

In 1930, personnel of the Missouri Highway Department and the Portland Cement Association surveyed all concrete pavements constructed before 1928 (1). Numerous types of pavement distress were reported from this survey; however, the emphasis of the report was on structural cracking and joint blowups. No deterioration other than structurally related was mentioned.

After this report was finished, correspondence indicated that a new type of deterioration, noted on several projects, was becoming important. This deterioration, referred to as map cracking, was considered to be a defect that was peculiar to individual projects and would be confined to those respective locations.

One pavement constructed in 1925, which used river gravel as the coarse aggregate, was partially replaced and the remainder was resurfaced by 1936. The reason for reconstruction of this pavement, after an effective service life of only 11 years, was excessive map-cracking deterioration. Costs for maintenance patching of map-cracked areas on this and other isolated projects had become excessive as early as 1931. Field observations recorded during the 1930s noted that the occurrence of map cracking was much more pronounced on pavements that contained either chert gravel or 2-in crushed flint than on pavements that contained limestone as coarse aggregate. Not all projects constructed with chert gravel were map-cracked. In some instances, map-cracked and non-map-cracked areas were noted within the same project when both areas were constructed with the same coarse aggregate.

Period from 1940 to Late 1950s

In 1940, the map-cracking problem became significant statewide in terms of maintenance costs and rideability. A limited investigation, consisting of a sampling of projects that showed joint distress and a search of correspondence regarding various projects, indicated that deterioration was not simply due to one factor. Map cracking was apparently caused by a combination of conditions and not necessarily the same combination of conditions between projects.

The 13 variables listed below were extracted from the field survey data collected from 1927 to 1940 and studied:

1. Climate--A well-defined trend was found in the variance of freezing cycles from North to South, and the intensity of joint deterioration pointed toward a correlation with freeze-and-thaw cycles.
2. Topography--Topography was considered an indirect influence related to drainage.
3. Moisture and drainage--Deterioration was greater in areas of the projects where drainage was poor.
4. Type of subgrade soil--No correlation was established between map-cracking deterioration and type of subgrade soil except for soils that retain high moisture contents.
5. Type of coarse aggregate--Type of coarse aggregate was determined to be the single most significant contributing factor in map-cracking deterioration. With few exceptions, all severe map cracking had been found in pavements that contained either chert gravel or 2-in crushed flint as coarse aggregate. Some difference was noted, however, between crushed limestones produced from different formations.
6. Fine aggregate--Fine aggregate was determined to have little influence on the problem of map-cracking deterioration.
7. Brand of cement--Observations in Missouri did not indicate that the brand of cement caused variance in the amount of deterioration.
8. Concrete proportions--Variations in mix design did not appear to influence the deterioration process.
9. Quality of concrete--Density of concrete did not appear to be a cause of deterioration in itself, but when honeycombing was present the deterioration process was accelerated.
10. Pavement design--Deterioration was found in

all pavement designs. Neither uniform nor variable thickness of pavement, bar mat or wire-mesh reinforcement, or the use or nonuse of subgrade paper prevented deterioration.

11. Method of curing--No correlation was found between curing methods.

12. Weather conditions during construction--Available records indicated that projects completed in cooler temperatures had less deterioration.

13. Traffic and loading conditions--Traffic did not appear to be responsible for the occurrence of deterioration, although it may influence the rate of progression.

Based on the results of this 1940 field investigation and data contained in correspondence on the map-cracking problem, coarse-fraction river or glacial gravels have not been accepted for use in concrete pavements since 1941. These data also showed that some pavements containing limestone coarse aggregate had a deterioration problem similar to map cracking but it was not severe or extensive enough to cause concern.

Extensive laboratory experimentation was begun on freeze and thaw of concrete specimens that contained various coarse aggregates, mix designs, and air entrainment. Gravels were found to be extremely frost susceptible when used in a stream-wet or partially saturated condition, regardless of the mix design or the use of air-entraining agents. Observations from field surveys were reduced to the probable cost of maintenance per mile of pavement with various types of coarse aggregates. Comparisons of these results continued to reinforce the previous decision to eliminate the use of gravels in portland cement concrete (PCC) pavements.

Missouri experienced a lull in concrete pavement construction during the 1940s and early 1950s. During this period, some laboratory work was conducted to determine the feasibility of beneficiation of limestones to eliminate deleterious particles based on specific gravity. No specific work was conducted on the problem of map cracking, which was then thought to have been remedied.

D-CRACKING

Construction Program Booms in Late 1950s

A significant increase in construction during the late 1950s and 1960s resulted in many new miles of Interstate and primary highways being placed into service. Because of the heavy demand for coarse aggregate, many new quarry sites were developed. The aggregates used in the new pavements were limestones that met specifications in existence at the time. By 1965, many of the newer concrete pavements located in the northwest and west-central area of the state exhibited deterioration that was identified as D-cracking. Preliminary field surveys indicated that concrete pavements constructed with several different limestones had an alarming rate of incidence of D-cracking. Field surveys conducted extensively from 1965 through 1967 projected that the design service life of many of these projects would not be realized. Where annual field survey data were available, they showed the problem to be accelerating and becoming a very expensive maintenance problem. One particular coarse aggregate was identified as a frost-susceptible aggregate. Because of its abundance in the northwest part of the state, it was designed as the prime source for data analysis in both the field surveys and laboratory freeze-and-thaw studies.

Addition of Special Provisions to Missouri Specifications: 1967-1977

Missouri had for many years approved limestone coarse aggregate for use in PCC pavement construction by first sampling and testing material by individual ledges for quality. A ledge is normally established by natural-parting seams of shale or the configuration of the rock itself. The crushed product is then sampled and tested for acceptance for quality requirements, gradation, specific gravity, absorption, weight per cubic foot, and deleterious substances. To attack the deterioration problem, the State of Missouri, based on analysis of field survey data, revised the specifications to identify and restrict the use of frost-susceptible limestones.

Beginning in 1967, special provisions added to the specifications were imposed on all contracts for concrete pavement construction in the northwest and west-central areas of the state. The following modifications to the specifications were made:

1. Maximum size of coarse aggregate was reduced from the existing 2-in gradation requirements to the following:

Sieve Size	Percent Passing
1 in	100
0.75 in	90-100
0.375 in	15-40
No. 4	0-5

2. Quality guidelines were revised for each ledge of limestone in each quarry to meet the following standards:

Property	Value
Water alcohol freeze loss	10% max
Bulk specific gravity	2.60 min
Absorption	1.5% max

These revised quality guidelines eliminated the use of a number of ledges and some entire formations and quarries previously approved for coarse aggregate for concrete pavement.

3. A moisture barrier of 4-mil polyethylene sheeting was placed between the base and the concrete pavement. For evaluation purposes, projects with this design feature were required to leave 10 percent of the main-line pavement as a control section without the polyethylene moisture barrier.

4. With the reduction in size of coarse aggregate, sand content was increased from 33 percent to approximately 45 percent by volume of the total aggregate fraction.

In conjunction with the above special provision, a three-phase investigation (2-4) was initiated: (a) a laboratory study to evaluate freeze-and-thaw resistance of concrete by using Bethany Falls limestone from eight different sources; (b) a laboratory study to evaluate freeze-and-thaw resistance of concrete by using Bethany Falls limestone from one source with 11 type 1 cements, each from a different source; and (c) a field study to evaluate pavement performance based on the special provision outlined above.

The first phase of the investigation was designed to determine whether frost resistance of laboratory concrete could be correlated with the physical properties of the coarse aggregates used. The freeze-and-thaw test method, similar to Procedure B of ASTM C-666, was modified to include only one cycle per week, which consisted of a 16-h freeze, and storage in water between cycles. Eleven Bethany Falls

Figure 1. Location of sampling sites and test section.

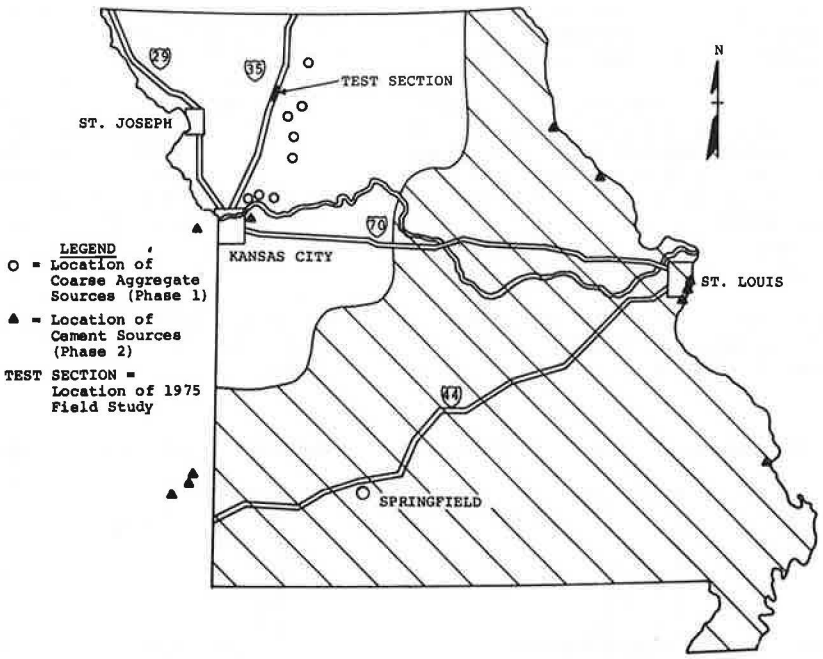

Figure 2. Failure of specimens.

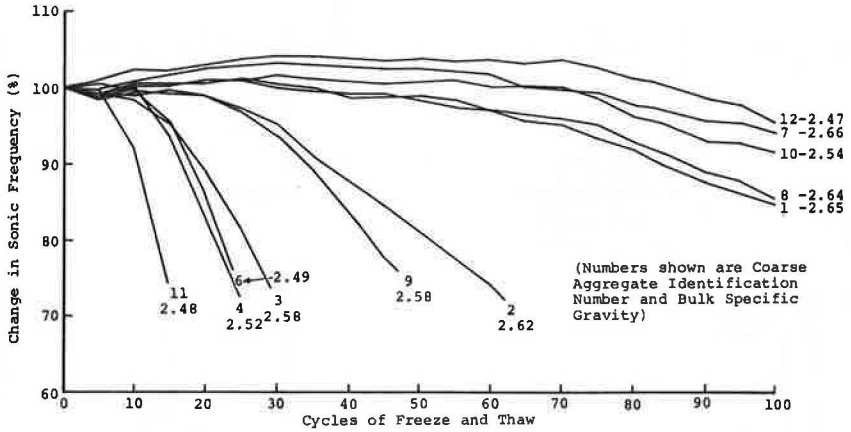

coarse aggregates from the D-crack-susceptible area of the state were sampled from various locations, as shown in Figure 1. Samples were picked by ledges in anticipation of obtaining two samples from each of the bulk-specific-gravity groups of >2.63, 2.63-2.56, 2.55-2.51, and <2.51. The main variables in the design of concretes were air-entrainment and non-air-entrainment, and sand contents were 33, 37, and 45 percent of total aggregate fraction based on the air-entrained design.

Results from this study indicated the following:

1. Frost susceptibility of concrete specimens increased as bulk specific gravity of coarse aggregate decreased, as shown in Figure 2. There were two exceptions: Coarse aggregates 10 and 12 were determined to be of an oolitic pelletal limestone structure rather than finely crystalline or microcrystalline calcitic limestone as determined for the other coarse aggregates. These two coarse aggregates are not typical of the Bethany Falls limestone stratum. These results proved that the bulk-specific-gravity limitation of 2.60 in the special provisions was beneficial.

2. Gravity gradation of the coarse aggregate, based on bulk specific gravity (vacuum-saturated surface dry), influenced frost resistance of the aggregate. An almost unlimited array of gravity gradations may exist for any particular "mean" gradation. Gravity gradations of the various samples of coarse aggregates in this study are shown in Figures 3 and 4.

3. Permanent dilation of concrete specimens after the first 10 freeze-and-thaw cycles was found to be a good indicator of ultimate failure of concrete specimens. As shown in Figure 5, the slope of the curves at the end of 10 freeze-and-thaw cycles could be used to rank the aggregates in order of ultimate failure.

4. Increased sand content of the aggregate fraction, from 33 to 45 percent, indicated a trend toward increased frost resistance of concrete. However, as shown in Figures 6 and 7, the actual difference in the number of cycles at ultimate failure may be small.

5. Air entrainment added to the resistance of the concrete, but the actual difference in the number of freeze-and-thaw cycles required for failure of specimens was small, as shown in Figures 6 and 7.

The second phase of this study, also a laboratory study, was to determine whether source of cement was

related to frost susceptibility of Bethany Falls limestone. Field surveys made immediately prior to 1967 on limestone pavements indicated that the rate of deterioration was different for projects with different brands of cement. However, the concrete mix designs of the surveyed projects were not the same, nor was the coarse aggregate from the same source. This study was designed to use a Bethany Falls limestone from a known frost-susceptible source with various brands of cement. The coarse aggregate used for this study had a 2.60 bulk specific gravity and was used in a 1-in maximum-size gradation.

Twelve cements, meeting AASHTO M85 and representing type 1 production, were obtained from sources distributed as shown in Figure 1. Cement sources located in western Missouri and eastern Kansas were those normally used in the area where the deterioration problem exists.

The design of concrete used in this study included both air-entrainment and non-air-entrainment. The gradation and volume of coarse aggregate were held constant. A limited experiment on the effect of high-alkali cement was included, in which a cement with 0.8 percent alkali equivalent was used.

The results of this study produced the following conclusions:

1. Failure of the concrete specimens was significantly different between cements, as shown in Figures 8 and 9 (the X cement is the high-alkali cement).

Figure 3. Gravity gradation of coarse aggregate from west-central Missouri.

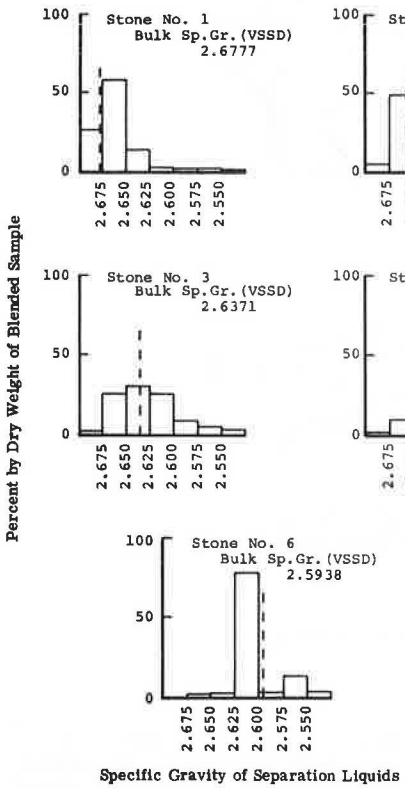

Figure 4. Gravity gradation of coarse aggregate from northwestern Missouri.

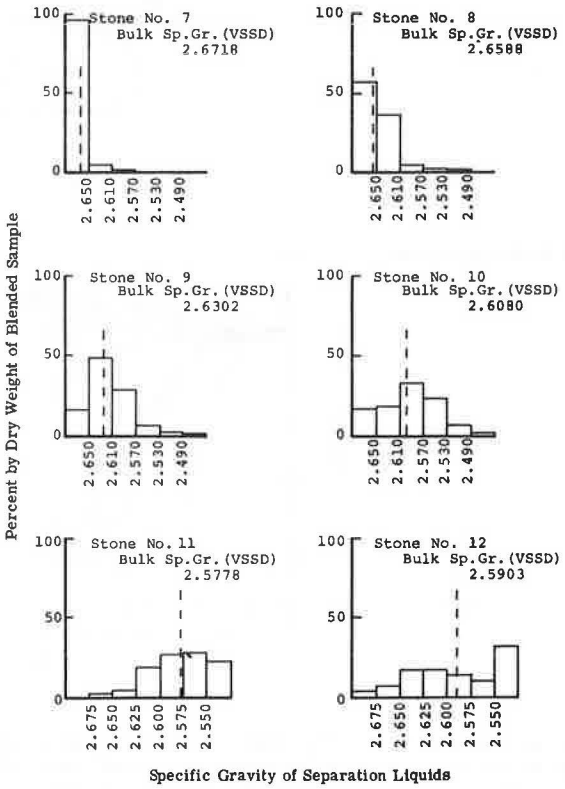

Figure 5. Expansion of concrete specimens.

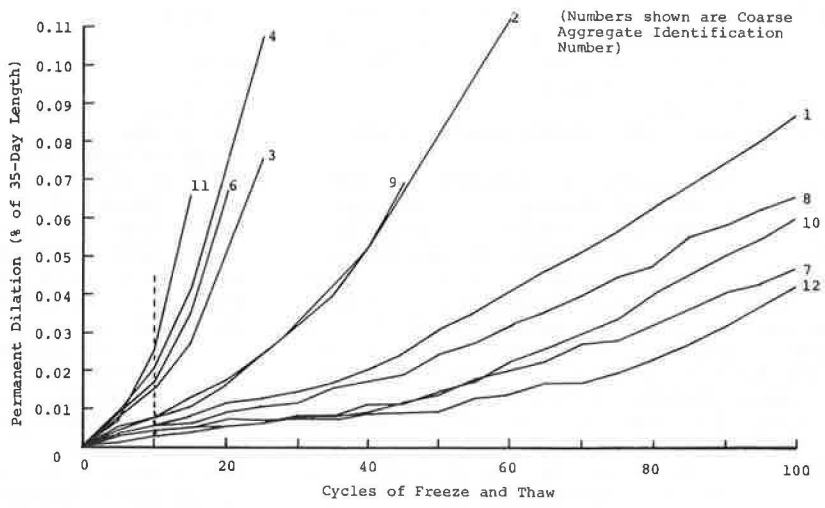

Figure 6. Failure of air-entrained concrete specimens with various sand contents.

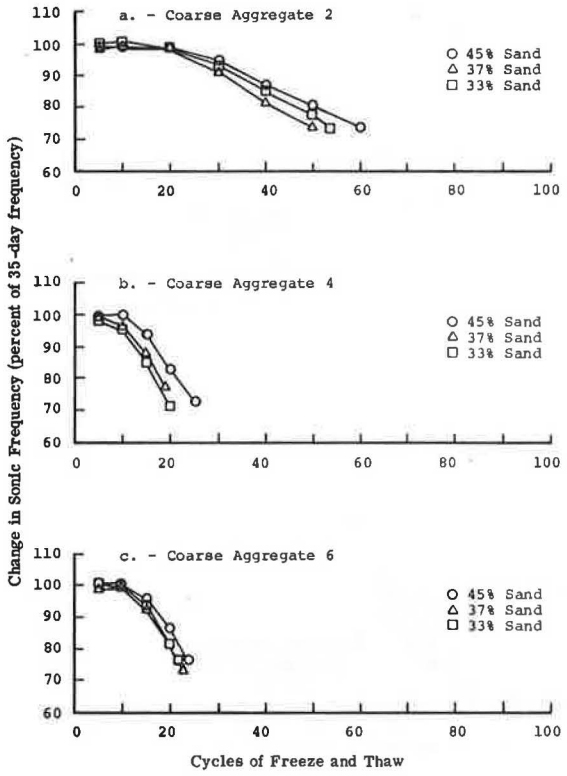

Figure 7. Failure of non-air-entrained concrete specimens with various sand contents.

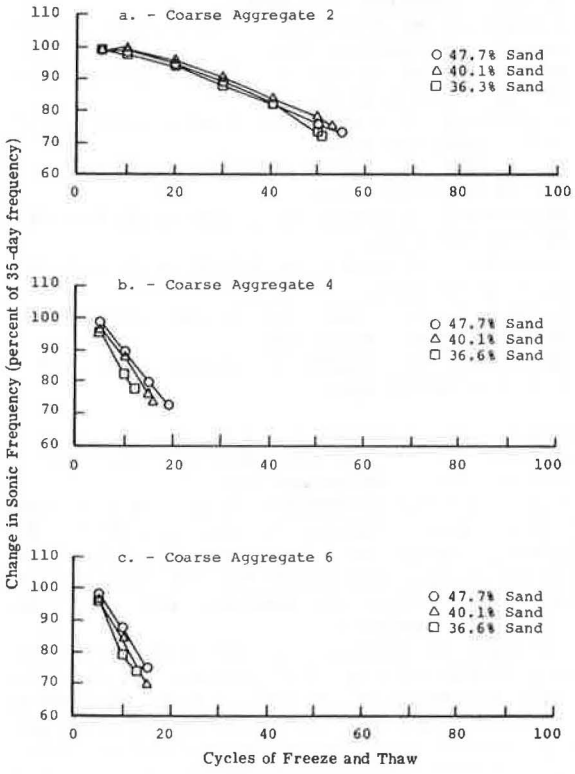

Figure 8. Failure of air-entrained concrete specimens.

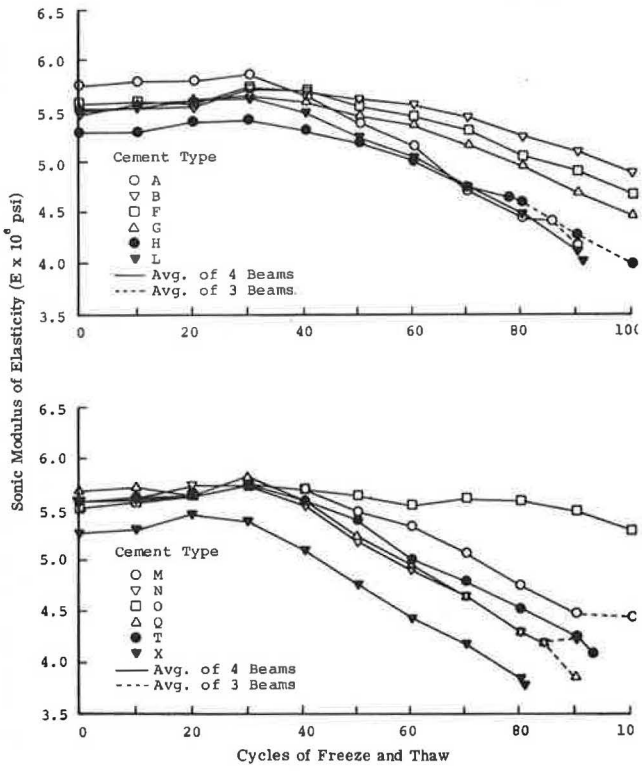

Figure 9. Failure of non-air-entrained concrete specimens.

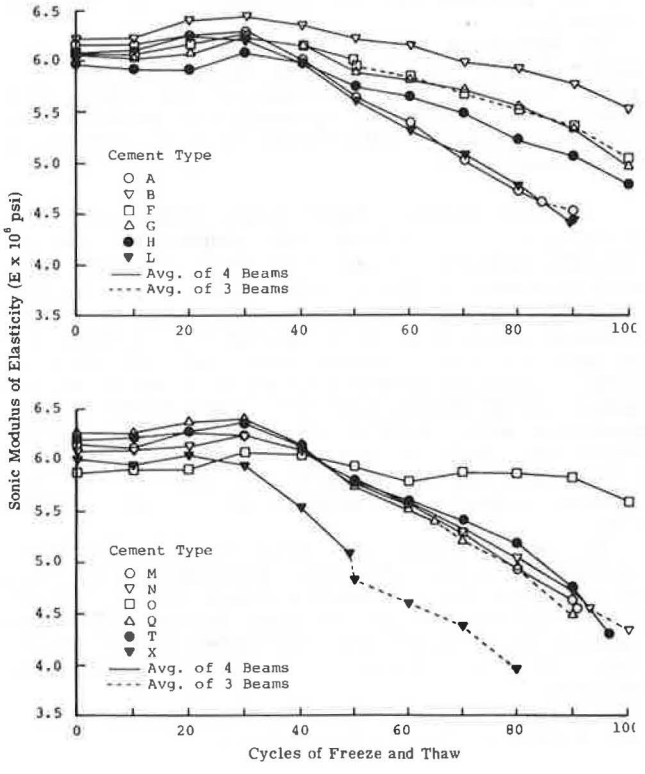

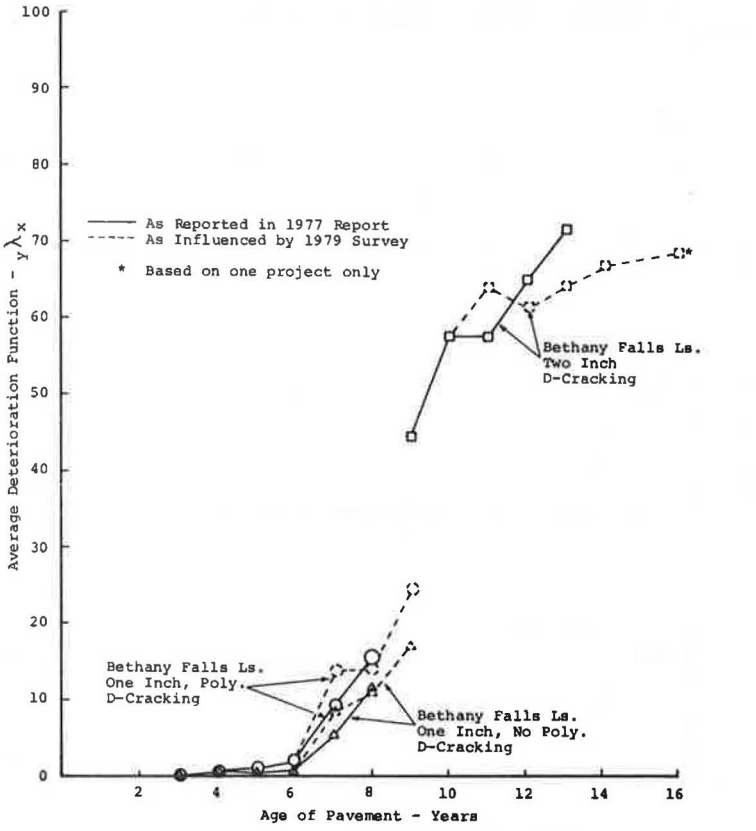

Figure 10. D-cracking on PCC pavement with Bethany Falls limestone as coarse aggregate.

2. The effect of air-entrainment on the durability of specimens was not significant, as shown in Figure 10.
3. Specimens made with high-alkali cement (X) failed before the same brand of cement with low alkali content (L) regardless of air-entrainment levels. This relation, although not perfect, did point to possible interaction of the effects of high-alkali cement.

The third phase, a field study, investigated the occurrence of D-cracking with respect to age of concrete pavements constructed under the 1967 special provisions. Twenty-eight projects, which had the 1-in maximum-size coarse aggregate and polyethylene sheeting moisture barrier placed under all or part of the pavement, were included in this study. Thirteen projects constructed prior to the specification change with 2-in maximum-size coarse aggregate were included for comparative purposes. Therefore, analysis was accomplished by testing within projects for effects of polyethylene and between projects for effects of coarse-aggregate size.

To reduce observation data to a mathematical equivalent, a parameter was established that would be influenced by a weighted relation of the area of D-cracking visible at the sawn joints. This parameter was labeled the "deterioration function" (λ). The mathematics of the parameter were as follows:

$$y^{\lambda_x} = A + 0.8B + (0.8)^2C + (0.8)^3D + \ldots + (0.8)^7H \quad (1)$$

where

y = calendar year in which survey was made,
x = project identification code,
A = percentage of cracks or joints with 25 ft² or more of affected area,
B = percentage of cracks or joints with 15-25 ft² of affected area,
C = percentage of cracks or joints with 10-15 ft² of affected area,
D = percentage of cracks or joints with 5-10 ft² of affected area,
E = percentage of cracks or joints with 2-5 ft² of affected area,
F = percentage of cracks or joints with 1-2 ft² of affected area,
G = percentage of cracks or joints with 0.5-1 ft² of affected area, and
H = percentage of cracks or joints with 0-0.5 ft² of affected area.

The limits of the deterioration function were 0 for clear pavement to 100 for all observed joints that had 25 ft² or more of deterioration.

This phase of the D-cracking study was designed as a 10-year study. However, the age span of the 28 polyethylene projects (4-9 years) at the completion of the study caused evaluation of the data to be restrained. Generally, the analysis was based on trends of the older projects.

The conclusions reported at the termination of this study indicated that PCC pavement constructed with 1-in maximum-size Bethany Falls limestone coarse aggregate and a 4-mil polyethylene moisture barrier exhibited D-cracking at an earlier age than identical pavement without polyethylene. A 1980 addendum to this study (5) indicated that the conclusions in 1977 were basically sound. The rate of

increase in D-cracking was adjusted slightly upward for polyethylene sections and remained essentially the same for no-polyethylene sections for the Bethany Falls limestone. Curves in the lower-right-hand portion of Figure 10 show the relative change from the original reported data to those with the addendum, for the 1-in maximum-size gradation.

Data obtained for 2-in maximum-size Bethany Falls coarse-aggregate projects, shown in Figure 10, could not be directly correlated with those obtained for the 1-in maximum size because of lack of comparable age of pavement at the time the survey began. With available data, D-cracking was observed as occurring at a higher yearly rate of increase for the 2-in than for the 1-in maximum-size coarse aggregate. Extrapolation of the D-cracking curve for the 2-in maximum size indicates that D-cracking started at an earlier age than it did for the 1-in maximum size. Again, the 1980 addendum to this study (shown as broken lines) indicated that the average yearly increase was estimated high in the original study. The fact that the projects with the revised requirements for quality control and reduced coarse-aggregate size tend to have lesser amounts of D-cracking at nine years of age than the projects with 2-in maximum-size coarse aggregate indicates that the special-provision changes are of significant benefit. The first observation of significant D-cracking was generally made at 5.5-6 years of age regardless of pavement design for 1-in maximum-size coarse aggregate.

Based on results of the third-phase field study, it was decided to

1. Eliminate the polyethylene sheeting moisture barrier,
2. Continue using 1-in maximum size for frost-susceptible coarse aggregate with increase in sand content of the total aggregate fraction, and
3. Continue using revised quality controls for approval of frost-susceptible coarse aggregate.

Roadway Design Variables to Reduce D-Cracking: 1977

In 1975, Missouri initiated another field study to determine the effectiveness of certain design variables in preventing or reducing the occurrence of D-cracking in PCC pavement. The project selected for incorporating various design variables was constructed in 1977 on I-35 in Daviess County (Figure 1). The project site was located in the area susceptible to D-cracking. Shoulder design throughout the project limits included a type 4, permeable, open-graded aggregate for drainage. The following design variables were included:

1. Bethany Falls limestone coarse aggregate, 1-in maximum size;
2. Bethany Falls limestone coarse aggregate from the same source as above, 0.5-in maximum size;
3. Burlington limestone coarse aggregate, 2-in maximum size, produced from a source in central Missouri some 100 miles from the project and with no known history of a D-cracking problem;
4. Pavement constructed with and without polyethylene moisture barrier; and
5. Four different types of base using crushed limestone aggregate: (a) type 3 base (impermeable, dense-graded), (b) bituminous base (impermeable, dense-graded), (c) type 4 base, bituminous-treated (permeable, open-graded), and (d) type 1 base, cement-treated (impermeable, dense-graded).

The plan layout and material descriptions of the test sections are shown in Figure 11. Each test section was placed on tangent with a cross-section design, as shown in Figure 12.

The variables included in this study should provide additional information on the ability to eliminate the occurrence or reduce the magnitude of D-cracking based on (a) maximum size and type of coarse aggregate, (b) type of base, and (c) use or nonuse of polyethylene moisture barrier.

This project is not of sufficient age to make conclusions at this time. No D-cracking had been observed on any of the test sections as of the August-September 1981 survey.

Pavements With or Without Controlled Drainage

Profile design of all projects mentioned thus far in this paper has allowed surface water to drain to or across the shoulders into earth ditches on either side of the roadway surface. The type of shoulder, either earth or aggregate, has not significantly influenced the D-cracking problem. In the Kansas City area, however, many projects built in the late 1950s, middle 1960s, and 1970s were constructed with a concrete curb-and-gutter design with a drop inlet and pipe drainage system. Several of these projects have long sections that are constructed in cut areas or depressed sections. Observations of these pavements indicated little or no D-cracking. The ability of the drainage system to effectively carry the bulk of the surface water away from the pavement should reduce the subbase or base moisture conditions. Effective reduction of the available moisture in the base materials should reduce the yearly rate of D-cracking. Continued observation of these projects should give more insight as to the ultimate effectiveness of the drainage systems in reducing the D-cracking problem.

Cement Studies by Battelle Columbus Laboratories

Based on knowledge gained from the previously mentioned laboratory studies and field observations, the D-cracking problem was postulated to be a function of moisture migration within the concrete. Battelle Columbus Laboratories was contracted by the States of Missouri, Iowa, and Kansas, in cooperation with the Federal Highway Administration, to investigate and determine whether such a correlation existed between cement sources (6).

Phase A of the project studied movement of moisture into and from hardened cement pastes and dimensional changes that accompany the moisture changes. It was established that statistically significant differences did exist between moisture change and related linear dimensional change behavior in the 32 cements studied.

Phase B continued with a study of moisture migration in simulated concretes. Sixteen of the 32 cements were selected for study based on the results of phase A. The broad objective of phase B was to determine the influence of cement in controlling resistance to destructive freezing action in concretes that contain D-crack-prone aggregates. Missouri submitted for test in this study a sample of the D-crack-susceptible Bethany Falls limestone. Only 8 of the 16 cements were used with the Bethany Falls limestone in the freeze-and-thaw behavior test.

The results of this phase indicated that, under the conditions of the study, cement source did not significantly influence the onset of potentially disruptive forces during freezing of concretes that contained D-crack-prone limestone aggregates, even though cement source did have a statistically significant influence on the moisture migration properties of the concretes. That is, under a given set of environmental conditions, the time at which ex-

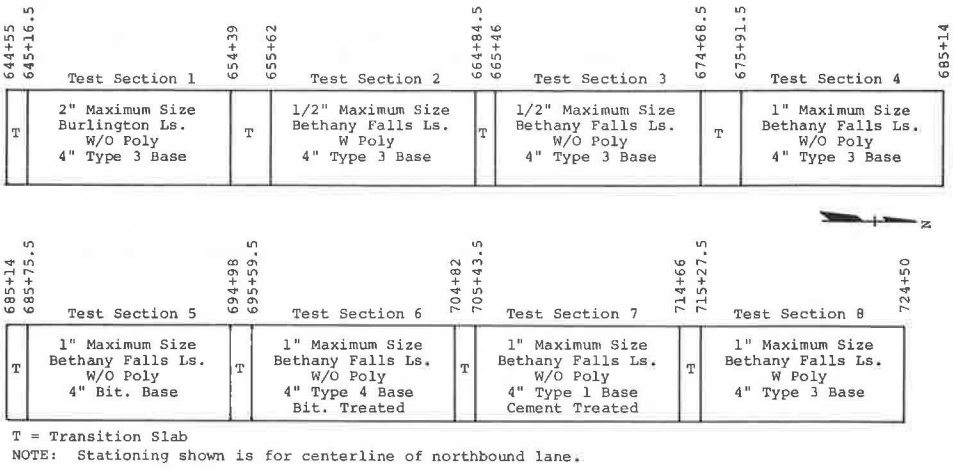

Figure 11. Layout and description of test sections for northbound lane, I-35, Daviess County.

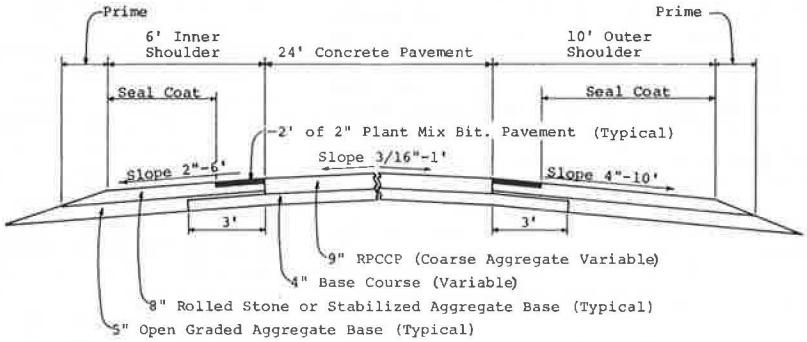

Figure 12. Typical cross section of test areas.

pansion of the aggregate particles commences in concretes that are subjected to freezing is not influenced by cement source. It was possible, however, to ascertain qualitatively that, once expansion of the aggregate particles does begin, the magnitude of dilation can influence the amount of structural damage that occurs in the concrete. Cement sources did have an effect on the magnitude of dilation during freezing in concretes prepared with the Bethany Falls limestone in the laboratory. The practical significance of these observed effects remains questionable.

Present research has answered some questions and raised others regarding the effect of cement source on the D-cracking of concretes prepared with limestone aggregates.

Pennsylvania State University Study on Upgrading of Low-Quality Aggregate

Missouri has also been interested in research concerning the upgrading of low-quality coarse aggregates and has participated in committees that have such responsibilities. The most recent research done under such circumstances is work completed by Pennsylvania State University and published in a National Cooperative Highway Research Program report (7). Three aggregates were selected for inclusion in this study with regard to the D-cracking problem, one of which was from Missouri. This aggregate, Bethany Falls limestone, was the same aggregate used in the field study currently under way on I-35 in Daviess County.

Research conducted in the Pennsylvania State University study was basically oriented toward use of impregnation treatments on the aggregate prior to its incorporation into the concrete. According to the report (7), "All of the impregnants tested were successful in controlling D-cracking as determined by expansion during rapid freeze and thaw cycling." However, reductions in strength, mix-design adjustments, paste-aggregate bond, cost/benefit ratios, and many other aspects must also be researched before an impregnation treatment is applied to a particular construction project.

Suggestions from this study were that further laboratory studies be carried out before a field evaluation program is instituted in order to optimize the choice of methods and treatment materials. Specifically, it was suggested that an expanded range of treatment materials for aggregates sensitive to freeze-thaw and D-cracking be investigated in order to identify the least costly, but most effective, treatment materials.

SUMMARY

This paper presents a history of D-cracking problems in Missouri, including changes made in source and type of coarse aggregates, mix design, and construction design over a period from 1913 to 1981. Chert gravel and glacial gravels have not been used since 1941. Since 1967, each aggregate source and limestone formation in the D-crack-susceptible area of the state has been subjected to increased quality requirements. Reduced coarse-aggregate size has been beneficial, but D-cracking persists and is still a problem in terms of required early maintenance and service life.

Missouri will continue to investigate possible beneficiation processes when D-cracking-susceptible aggregates are used. However, the processes must be effective in terms of material costs, reduced maintenance, and increased service life. Missouri will

continue to express interest in the efforts of other organizations to successfully eliminate or significantly reduce the rate of deterioration of PCC pavements.

ACKNOWLEDGMENT

The opinions, findings, and conclusions expressed in this paper are those of the Missouri Highway and Transportation Department.

REFERENCES

1. Concrete Road Condition Survey in State of Missouri. Missouri State Highway Department and Portland Cement Assn., Jefferson City, MO, May 1931.
2. Investigation of "D" Cracking in PCC Pavements: Phase 1. Missouri State Highway Department, Jefferson City, Missouri Cooperative Highway Research Program, Rept. 71-3, May 1971.
3. Investigation of "D" Cracking in PCC Pavements: Phase 2. Missouri State Highway Department, Jefferson City, Missouri Cooperative Highway Research Program, Rept. 72-4, March 1972.
4. Investigation of "D" Cracking in PCC Pavements: Phase 3. Missouri State Highway Department, Jefferson City, Missouri Cooperative Highway Research Program, Rept. 77-5, Jan. 1977.
5. Investigation of "D" Cracking in PCC Pavements: 1980 Addendum to Phase 3 Report 77-5. Missouri State Highway Department, Jefferson City, May 1980.
6. D.R. Lankard and others. Influence of Cement on Moisture Migration in Paste and Concrete as Related to the Durability of Concrete. FHWA, Rept. FHWA-RD-74-54, June 1974.
7. P.D. Cady and others. Upgrading of Low-Quality Aggregates for PCC and Bituminous Pavements. NCHRP, Rept. 207, July 1979.

Publication of this paper sponsored by Committee on Performance of Concrete.

Efforts to Eliminate D-Cracking in Illinois

MARVIN L. TRAYLOR

Severe D-cracking on Interstate pavements prompted the Illinois Department of Transportation to initiate a program to identify and eliminate the use of D-cracking aggregate. More than 200 crushed-stone and gravel sources were evaluated by using both the Iowa pore index and ASTM C-666 freeze-thaw tests. Shortcomings in the Iowa pore index test have resulted in its use being limited to a screening test. The results of the freeze-thaw program have formed the basis for a specification that the state believes will guarantee the durability of future pavements.

D-cracking had been observed for years in Illinois but had not been considered a serious problem until 1978. In that year, two sections of D-cracked Interstate pavement had deteriorated seriously and required immediate rehabilitation. One section, 9 miles long and 10 years old, received a 5-in bituminous overlay, and the other section, 8 miles long and 11 years old, received a 6-in bituminous overlay. Both sections were continuously reinforced concrete pavement, designed for a 20-year life. As a result of these failures, the Illinois Department of Transportation (DOT) initiated a program to identify and eliminate the use of D-cracking aggregate.

BACKGROUND INVESTIGATION

The first step in the investigation was a review of the technical literature on D-cracking. The literature review, combined with visits to the University of Illinois, the Portland Cement Association (PCA) Laboratories, and the Iowa DOT, provided the Illinois DOT with some basic knowledge of the D-cracking problem. The following items summarize the principal findings:

1. The coarse aggregate is responsible for D-cracking, and sedimentary aggregates are the most susceptible. Once the distress is initiated, it cannot be stopped.
2. Fine aggregates, cement type, drainage systems, and type of subbase have no significant effect on the occurrence of D-cracking.
3. The distress is a result of freeze-thaw stresses, and serious deterioration may occur even without traffic loading.
4. The pore structure of the aggregate is thought to be the characteristic that determines the degree of susceptibility.
5. Removal of moisture or prevention of freezing and thawing would eliminate D-cracking. Neither has been accomplished economically in the field.
6. Reducing the top size of the coarse aggregate lessens the rate of D-cracking and may eliminate the problem altogether with marginal aggregate.
7. A laboratory freeze-thaw test developed by PCA has been successful in predicting the susceptibility of aggregate to D-cracking.
8. A rapid evaluation of D-cracking susceptibility (the Iowa pore index test) has been developed by the Iowa DOT.

Since the only known means of controlling D-cracking was the elimination of susceptible aggregate, a program was established to identify the degree to which the various aggregate sources in Illinois were vulnerable to the distress. Both the PCA freeze-thaw procedure and the Iowa pore index test were selected for use in the evaluation. In January 1979, the necessary equipment for both tests was ordered. At the same time, based on the knowledge that top-size reduction often improved aggregate performance, Illinois issued its first D-cracking specification, which restricted all concrete paving aggregate to a maximum top size of 1 in. (Previously, 1.5-in top-size material had been the standard paving aggregate.) The Illinois DOT realized that this first specification was needlessly restrictive for some aggregates and not severe enough for others. However, because of the state's inability to differentiate between durable and nondurable aggregates, it was a necessary safeguard.

FIELD PERFORMANCE SURVEY

While the necessary equipment for the laboratory

Figure 1. Performance plot for an aggregate source.

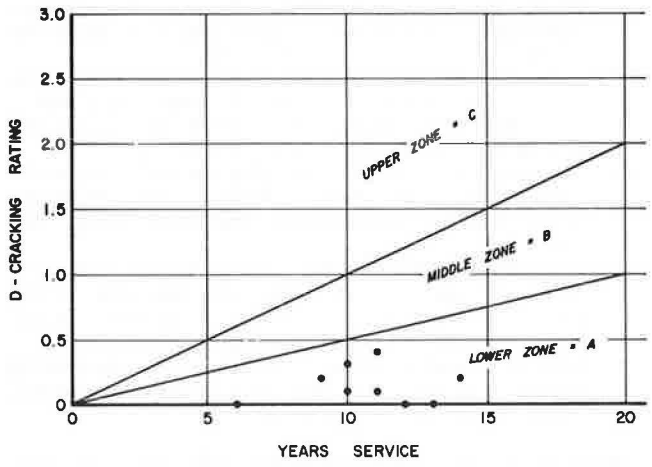

testing program was being acquired, a statewide survey was scheduled to determine the extent and severity of D-cracking. A simple rating scale of zero (no D-cracking) to three (severe D-cracking) was used. Photographs depicting the distress in various stages of development were used to standardize the rating. The survey covered more than 3000 miles of pavement and showed that D-cracking was present in all areas of the state. Only 42 percent of the mileage surveyed was free of D-cracking. Forty percent had low-level D-cracking, 12 percent had intermediate-level D-cracking, and 6 percent was severely D-cracked.

In addition to assigning present condition ratings, the construction records for each mile of pavement were retrieved and the following information was compiled by construction sections: (a) location (county, route, and station limits), (b) length, (c) year built, (d) concrete thickness, (e) pavement type (jointed or continuously reinforced), (f) subbase type and thickness, (g) subsurface drainage type, and (h) coarse-aggregate source.

Since D-cracking is a progressive distress, a means of tempering current condition with the age of the pavement was needed before an evaluation could be made of the aggregate's performance. The fact that each construction section used a single source for the coarse aggregate, so that there was a uniform degree of distress throughout the section, made this task quite simple. First, the condition ratings for each mile of pavement within a construction section were averaged. This value was used to represent the condition of the entire section. Next, all construction sections containing the same coarse aggregate were grouped and a plot for each source was developed, as shown in Figure 1. Each dot on the graph represents one construction section (normally 5-10 miles of pavement).

Plots such as the one shown in Figure 1 were used to assign each aggregate source a field performance rating. If the majority of the construction sections fell in the lower zone, indicating very little D-cracking had developed in their 20-year design life, the source received an A-rating. If the majority of the construction sections fell in the middle zone, the aggregate was considered marginal and given a B-rating. Finally, if the majority of the sections fell in the upper zone, the aggregate source was considered unsatisfactory and given a C-rating. The example shown in Figure 1 received an A-rating.

The field survey, record search, and data analysis were completed by March 1979. Forty crushed-stone (limestone and dolomite) and 31 gravel sources had been rated. Some sources had been used in as many as 25 construction sections, whereas others appeared only once. The relative performance of the two classes of aggregates is indicated in the table below:

Aggregate Class	No. of Sources Receiving Rating A	B	C	Total
Crushed stone	25	11	4	40
Gravel	14	8	9	31

In addition to providing performance ratings, the survey revealed the following:

1. Because of its closely spaced shrinkage cracks, continuously reinforced concrete pavement was much more vulnerable to D-cracking than was jointed pavement.
2. Type of subbase, traffic, or drainage appeared to have had no significant effect on the behavior of the coarse aggregate.

IOWA PORE INDEX PROGRAM

In April 1979, the necessary equipment for the Iowa pore index test was in place and samples from aggregate sources had been gathered for testing. Illinois has roughly 400 crushed-stone and 600 gravel sources, but only 82 crushed-stone and 70 gravel sources are qualified for concrete aggregate. The other sources have been rejected on the basis of Los Angeles abrasion, $NaSO_4$ soundness, or deleterious count. The D-cracking program would test only those sources that had passed these normal quality tests and were currently qualified as concrete aggregate.

The Iowa pore index test measures certain characteristics of an aggregate's pore structure. Twenty-two pounds of washed, oven-dried aggregate (0.75x0.5 in) is placed in the bottom of an air-entrainment pot. The top of the pot has been modified to hold a clear plastic tube calibrated in cubic centimeters. The bottom of the tube is open to the inside of the pot, and the top is connected to a source of air pressure. After the top assembly has been securely fastened in place, water is introduced into the bottom of the pot. The water first fills the spaces among the aggregates and then rises to an established mark on the tube. The system is then sealed and 35 lb of air pressure is applied. This increase in pressure forces the water into the pores of the aggregate, causing the column of water to fall, rapidly at first, and then slowly stabilize (see Figure 2). The height of water in the tube is observed, and readings are taken after 30 s, 1, 2, 5, 10, and 15 min. The pore index is the volume of water (in cubic centimeters) that is forced into the aggregate during the time interval from 1 to 15 min after the air pressure is activated. A high pore index is supposed to indicate a nondurable aggregate.

By June 1979, all concrete aggregate sources in Illinois had been evaluated by use of the Iowa pore index test. The process was found to be fast and economical, and the results were easy to reproduce. Indices ranged from a low of 6 to a high of 150. An attempt was then made to correlate the field performance ratings with the results of the Iowa pore index test. The number of sources available for correlation was limited because many of the sources whose performance had been rated were no longer producing aggregate and many of the current sources had no field performance rating. However, 15 crushed-stone and 9 gravel sources were available for correlation. The geologic differences between gravels and crushed stones suggested that the corre-

Figure 2. Pore index determination.

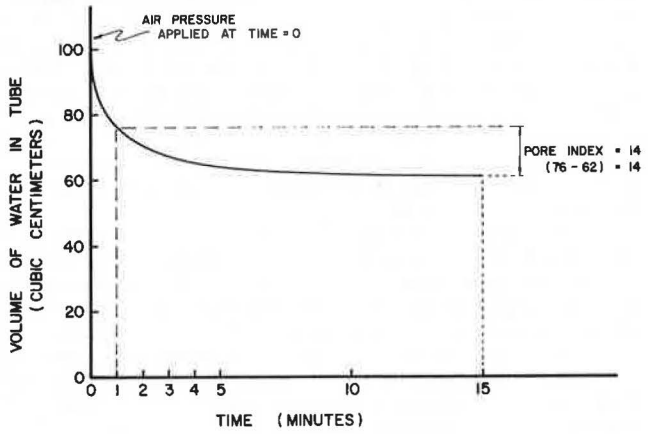

Figure 3. Pore index versus field performance.

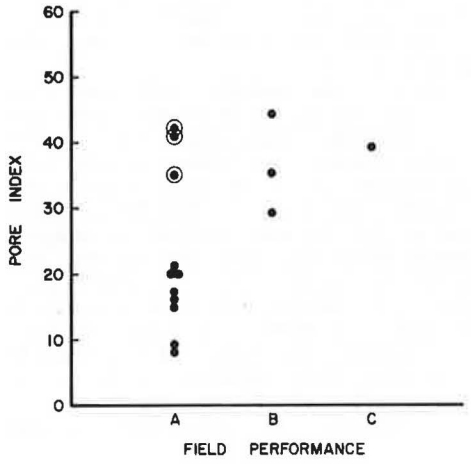

lation be analyzed separately.

Crushed Stone

A plot of the Iowa pore index values versus field performance rating is shown in Figure 3. Although the data are limited, a trend can be identified. Lower values from the Iowa pore index test are associated with good field performance, and high pore indices are associated with poor field performance. However, three points (circled on the plot) appear to be contrary to this trend. Pavements built over the past 20 years with these three aggregates have shown little evidence of D-cracking, yet the pore indices for the current production ledges are extremely high. There are two possible explanations of this fact: Either (a) the pore index test is not an accurate indicator, or (b) the aggregate that is being produced now is of lesser quality than that used in the surveyed pavements.

Gravel

A plot of pore index versus field performance for gravels did not indicate any discernible trends, and the test was discontinued for gravels.

Based on the early results of the pore index testing in June 1979, the Illinois DOT developed and released its second specification aimed at eliminating D-cracking aggregate. The major points of this specification were the following:

1. Crushed-stone top size was controlled by the Iowa pore index, as shown below:

Pore Index	Top Size (in)
0-25	1.5
26-35	1
>35	0.75

2. Because the Iowa pore index test was not effective for gravel and gravel had generally demonstrated poor performance, gravel top size was restricted to 0.75 in.

There were some obvious problems with using the Iowa pore index test for predicting performance. They were as follows:

1. Although the correlation between the pore index and performance showed promise for crushed stone, there were several sources with high pore indices that had excellent performance histories.
2. The test did not appear useful for gravels.
3. The test could not indicate to what extent a reduction in top size would improve performance.

In spite of these shortcomings, the Illinois DOT felt that this new specification was a step closer to identifying the problem aggregates and imposing restrictions only where warranted. However, because of questions concerning the validity of the test, no aggregate sources were rejected. The specification was considered temporary until more data were available.

FREEZE-THAW TESTING

By July 1979, the Illinois DOT's two new freeze-thaw cabinets were operational. They were custom built by a local manufacturer to meet ASTM C-666 requirements. Cycles are controlled by programmable modules that use a step function to approximate the desired rise and fall rates for temperature. Once programmed, all functions are completely automatic and require no operator. The modules also constantly record the temperature at several locations inside the cabinets on both circular charts and digital printout tapes.

Although the equipment is sophisticated, the test is quite simple in principle. The aggregate is cast in a concrete beam that is cured, measured, subjected to a series of freeze-thaw cycles, and remeasured. A small increase in length indicates a durable aggregate, and a large increase indicates a nondurable aggregate. The following paragraphs give a general description of the test procedures. The actual test specifications can be obtained from the author.

A sample of the aggregate is obtained from stockpiles at the source, separated over a nest of sieves, and recombined to a standard laboratory gradation. It is then batched, by using a standard cement, sand, and air-entraining agent. The resulting concrete is formed into three 3x4x15-in beams, cured for two weeks, brought to 73°F, and measured to establish initial lengths.

The beams are placed in the freeze-thaw cabinets and exposed to eight freeze-thaw cycles (0°-40°F) each day. Water covers the beams during the thawing phase but is evacuated during the freezing phase of each cycle. The actual cycle is shown in Figure 4. A complete test consists of 350 freeze-thaw cycles.

Periodically, the beams are removed from the cabinets, warmed to 73°F, and measured. After each measurement, the length change, expressed as a percentage of the original length, is calculated and plotted. Total time for the test, including the 14

days for curing, is approximately nine weeks. Figure 5 shows the test results for two sources. Group 1, with the lower expansions, is superior to group 2.

After several weeks of equipment shakedown, the first freeze-thaw tests were scheduled during August 1980. The first sources tested were selected to represent the full range of field performance. Both crushed stones and gravels were included. The initial results were encouraging for both types of aggregate. Those with excellent field performance showed almost no increase in length (<0.005 percent). Those with marginal performance records lengthened 0.06-0.15 percent. Those with poor field performance had expansion in excess of 0.20 percent. The test appeared to have performed as well for gravels as for crushed stones. Since the early results showed such promise, the program proceeded with a goal of testing every source of concrete aggregate in the state.

Figure 4. Freeze-thaw cycles.

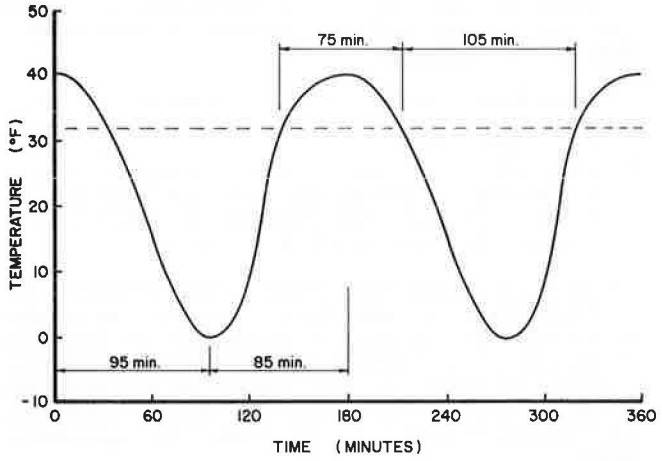

Figure 5. Typical freeze-thaw test results.

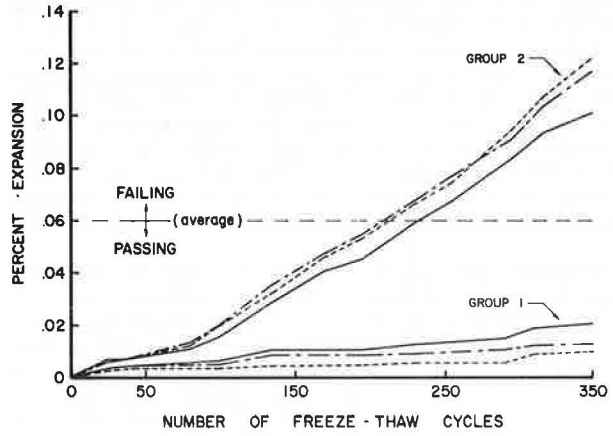

Figure 6. Effect of reduced top size on expansion.

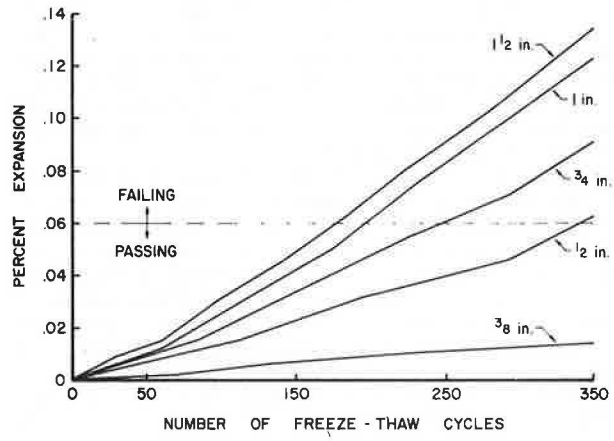

In the early stages of testing, each source was evaluated in at least three different gradations (1.5-, 1-, and 0.75-in top sizes). The improvement that resulted from reducing top size for one limestone source is dramatically shown in Figure 6. However, since each test took nine weeks to complete and the objective was to stop the placement of susceptible aggregates in pavements as soon as possible, the program was soon streamlined. The 1.5-in top-size gradation was tested first. If this gradation passed the expansion criteria (established at 0.06 percent after 350 cycles), smaller gradations were not tested. However, if the largest gradation failed, successively smaller top-size gradations (down to 0.75 in) were tested until the expansion criteria were met.

Many of the crushed-stone quarries have more than one production ledge. Since early testing with the pore index had indicated that significant variability could exist between two ledges in the same quarry, each production ledge of each source was identified and tested separately. The 82 quarries contained a total of 137 separate production ledges. With the additional 70 gravel pits, 207 sources had to be evaluated, several in more than one gradation.

By June 1981, all sources had been evaluated. Each gravel pit and each production ledge of each quarry received a rating that indicated the maximum top-size material they could produce (1.5, 1, or 0.75 in).

The following observations were made during testing:

1. The two freeze-thaw cabinets could be used interchangeably with no significant effect on results.
2. The rate of expansion during the 350-cycle test was quite uniform, which suggested that the number of cycles could be reduced.
3. The three replicate beams for each crushed-stone source behaved very similarly. The variability among the beams was quite small even when total expansion was high.
4. The effect of top-size reduction for crushed stone was reflected in the freeze-thaw plots. The degree of improvement varied from source to source. One source had to be reduced to 0.25-in top size before passing the expansion criteria.
5. Many of the limestone quarries received different ratings for separate production ledges.
6. All dolomites (Illinois classifies carbonates with ≥11.0 percent MgO as dolomites) passed the freeze-thaw criteria at the 1.5-in top size.
7. The three quarries that had good field performance but high pore indices passed the freeze-thaw test in the 1.5-in top size.
8. Triplicate beams cast from a single gravel sample showed considerable variability.
9. Reducing the top size of gravels did not always reduce expansions.
10. An occasional large piece of chert or limonite sometimes caused one of the gravel beams to expand rapidly and eventually break while the two remaining beams showed only moderate expansion.

A comparison of average expansion (for 1-in top-size gradation) versus field performance is shown in Figure 7. This plot displays the same sources that were used in Figure 3. Comparison of Figures 3 and 7 indicates that the freeze-thaw test produced the better correlation. A plot of freeze-thaw expansion (for 1-in top-size gradation) versus pore index is shown in Figure 8. This figure indicates the lack of agreement between the two tests. It does show, however, that all crushed stones with a pore index of 18 or less passed the freeze-thaw test, which suggests that the Iowa pore index may be useful as a screening test.

D-CRACKING SPECIFICATION

In July 1981, the Illinois DOT issued the third version of its D-cracking specification. The Iowa pore index test was replaced by the freeze-thaw test. Each aggregate source was permitted to produce material with a top size up to the rating received from the freeze-thaw test. If the material had not passed the expansion criteria when tested in the 0.75-in top size, it was no longer allowed for concrete pavement. The effect this specification had on the Illinois aggregate industry is shown below (the quarries with more than one rating are shown under the largest top-size rating they received):

Aggregate Class	No. of Sources Receiving Rating, Top Size (in) 1.5	1	0.75	Rejected	Total
Crushed stone	65	9	4	4	82
Gravel	12	11	27	20	70

Figure 7. Freeze-thaw results versus field performance.

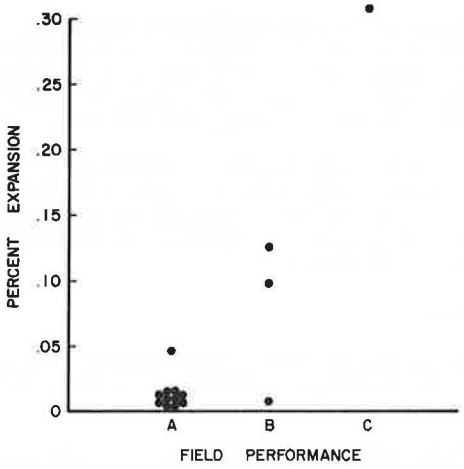

Figure 8. Freeze-thaw results versus pore index.

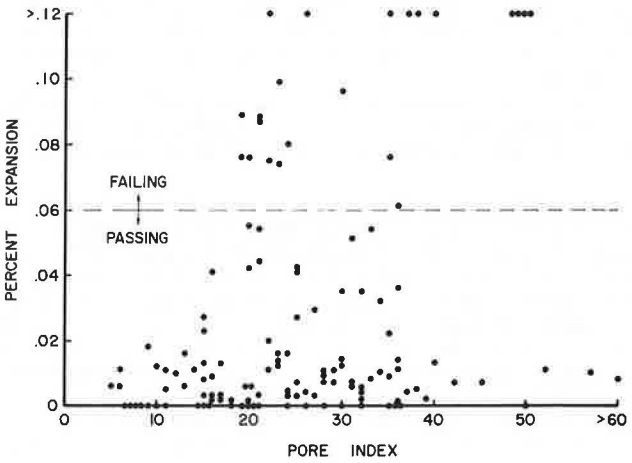

Figure 9. Effect of freeze-thaw specification on Illinois crushed-stone producers.

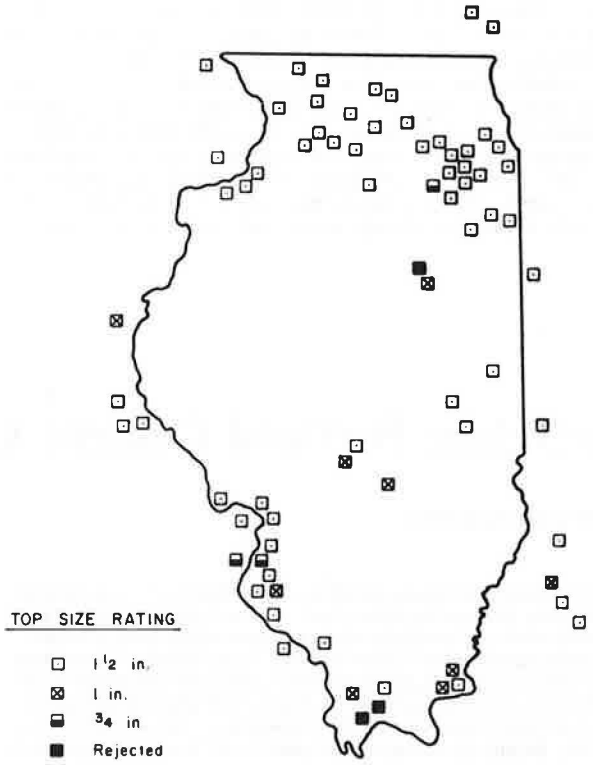

Figure 10. Effect of freeze-thaw specification on Illinois gravel producers.

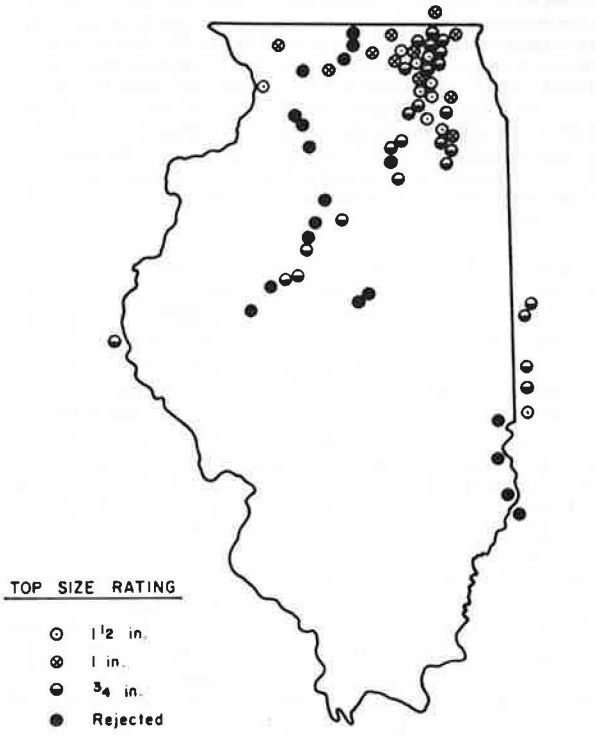

The maps shown in Figures 9 and 10 indicate the geographic impact of this rating system.

After all sources had been rated and the freeze-thaw specification established, a second round of testing was started. For crushed stones, agreement with the initial results has been excellent. However, for gravels, especially those with moderate to high expansion, differences between the initial and follow-up tests were quite pronounced. The problem has been attributed to the extreme variability within the gravel deposits themselves. Obtaining samples that are "representative" is extremely difficult, and pronouncing judgment on the basis of one freeze-thaw test has proved inadequate. Therefore, numerous samples will be taken from production throughout the next year, after which the additional freeze-thaw results will be analyzed and new ratings will be issued. The Iowa pore index, although no longer used as an acceptance test, has proved to be an effective screening test and is still used to determine when a crushed-stone deposit has changed, which makes it necessary to do additional freeze-thaw testing.

The current freeze-thaw specification should eliminate the use of D-cracking aggregates in construction. The freeze-thaw test, although expensive and time-consuming, has proved to be extremely versatile. Since it can be used to evaluate any type of aggregate, each source can be judged by its performance rather than its geologic origin or geographic location.

Although the test is now being used to evaluate routinely processed aggregates, it can also be used to evaluate aggregate improvement techniques. The effectiveness of reduced top size, heavy media, new crushing processes, or additives can be judged by comparing freeze-thaw plots before and after treatment.

Publication of this paper sponsored by Committee on Performance of Concrete.

Recycling Portland Cement Concrete Pavement

ANDREW D. HALVERSON

Quality aggregates for highway construction are in short supply in many parts of Minnesota. Although the current total supply is adequate, the distribution of sources results in localized shortages. It is sometimes necessary to import high-quality aggregates from distant locations. Haul distances can increase aggregate prices substantially, add to the overall project cost, and require the expenditure of sizable amounts of energy. One available source of aggregate is existing portland cement concrete (PCC) pavement currently in need of reconstruction. Reusing this aggregate would result in cost savings in aggregate-short areas, conserve natural resources, and conserve energy in the form of fuel savings when aggregates must be acquired from distant sources. A research study is described that was undertaken to determine the feasibility of recycling PCC pavement, evaluate the new recycled pavement, determine the cost-effectiveness of recycling versus conventional paving, and determine the amount of energy consumed and natural resources conserved. Economic and engineering factors led to the selection of a 16-mile segment of US-59 from Worthington to Fulda in southwestern Minnesota for the study. The in-place roadway, which was constructed in 1955 and consisted of 9-, 7-, 9-in-thick, 24-ft-wide, nonreinforced, D-cracked concrete pavement with soil shoulders, was broken, salvaged, and crushed. Material passing the no. 4 sieve was used for base stabilization and shoulder aggregate, and material retained on the no. 4 sieve but passing the 0.75-in sieve was used as the coarse aggregate for concrete paving. The project results are evaluated based on pavement performance and energy and cost comparisons.

High-quality aggregates for use in highway construction are in short supply in many parts of the country, including portions of Minnesota. Although the total supply is adequate to meet the country's needs, the distribution of sources is such that many local areas experience shortages. In these areas, it is often necessary to import high-quality aggregates from distant locations. Depending on the length of haul, aggregate prices can increase substantially and add significantly to the total project costs. In addition, sizable quantities of energy are expended in the form of fuel for hauling vehicles.

One available source of high-quality aggregates in aggregate-short areas is the many pavements in need of reconstruction. Some of these pavements have exceeded their design life and have failed due to overuse, some have simply become geometrically outdated, and others are exhibiting some form of premature distress due to inadequate design, use of marginal materials, or poor construction practices.

Many of these roads still contain durable aggregates. Reusing these aggregates would not only conserve natural resources but, in aggregate-short areas, could also result in energy and construction cost savings.

In November 1980, the Minnesota Department of Transportation (DOT) completed a major recycling project. That project can be discussed in terms of three distinct activities: selection, experimental work, and project evaluation.

PROJECT SELECTION

In September 1976, during the initial search for a recycling project, candidate projects were selected on the basis of several criteria:

1. The roadway should have adequate vertical and horizontal alignment to preclude extensive regrading.
2. The existing right-of-way should be sufficient to allow reconstruction without further land acquisition. The existing roadway should be in such an advanced state of deterioration that the reconstruction is either programmed or imminent, and the project should be located in an area of aggregate scarcity.
3. If the existing pavement is rigid, it should be nonreinforced; if it is flexible, it should be thick enough to minimize new material requirements.

In 1977, a 16-mile segment of US-59 in southwestern Minnesota was selected for a recycling project. The existing roadway had been constructed in 1955, and was a 9-, 7-, 9-in-thick, 24-ft-wide, nonreinforced concrete pavement with soil shoulders. The pavement had been placed on a minimum of 3 in of gravel base, which in turn had been placed over an in-place bituminous surface. The roadway exhibited no frost heaves, but the pavement exhibited extensive D-cracking, a series of crescent-shaped cracks on the pavement surface that usually start at the

intersection of pavement joints and progress to the center of the concrete panel. In Minnesota, this distress is physical in nature and is associated with poor-quality aggregates that absorb moisture and fail through freeze-thaw action. D-cracking exists in about 63 of Minnesota's 87 counties. Nearly 1700 miles, or 14 percent, of the 12 350 miles of Interstate and trunk highways appear to be affected.

In the case of US-59, the coarse aggregate in the concrete was from a local deposit of glacial gravel. The cause of the D-cracking was a limestone-dolomite material that constituted 55-60 percent of this aggregate. The maximum particle size was 2 in.

Early in 1978, a surface determination was made for reconstructing US-59. On the basis of this evaluation, an 8-in-thick, recycled, nonreinforced concrete pavement appeared to be the most economical alternative. In November 1979, the Minnesota DOT let a construction project to crush the distressed pavement, use the material passing the no. 4 sieve for base stabilization and shoulder aggregate, and use the material passing the 0.75-in sieve and retained on the no. 4 sieve as the coarse aggregate for reconstructing the concrete pavement. The winning bid of $5.1 million was submitted by Arcon Construction Company. This included $425 000 for two bridges that were replaced.

EXPERIMENTAL WORK

During the planning for the US-59 recycling project, the Minnesota DOT removed a 3-ft-wide section across the full width of the roadway. This material was crushed and examined for quality. The material was then used in trial mixes. Initially, five concrete mix designs, made up of various combinations of recycled and virgin materials, were identified.

One mix was designed to use recycled coarse and fine aggregates. One mix used recycled coarse aggregate and natural sand. One mix was designed to contain recycled coarse aggregate and natural sand and substitute fly ash for 10 percent of the cement. Another mix used recycled coarse aggregate and natural sand and 20 percent fly ash replacing 15 percent of the cement. The final mix was a control mix with a natural coarse aggregate and sand and 20 percent fly ash replacing 15 percent of the cement. It was found that the material passing the no. 4 sieve was very angular, and the trial mixes that used this material vastly increased the water demand to get workability. The result was that the cement requirement was very high. The decision to use the minus no. 4 material for base stabilization and to use natural sand in the concrete was made at this time.

The concrete mix design that used recycled coarse aggregate and natural sand and 20 percent fly ash substituting for 15 percent of the cement was selected for use on the US-59 recycling project. Its cement content was the lowest of the recycled concrete alternatives, and the amount of water required to produce concrete with 1-2 in of slump was also the lowest.

The gradation specified for the recycled coarse aggregate called for 95-100 percent passing the 0.75-in sieve and allowed up to 10 percent passing the no. 4 sieve.

Computations of the total coarse aggregate available on crushing assumed (a) 5 percent of the material wasted in salvage and crushing, (b) 1200 tons lost in yield, and (c) 500 tons of stockpile loss. This indicated that an adequate supply of recycled coarse aggregate would be available to make a design of 40 percent sand and 60 percent coarse aggregate feasible for the recycling options.

Another study of recycled concrete is currently under way. In the initial phase of this study, four concrete mixes were evaluated. Data existed on a mix that used virgin material from a source near US-59. One concrete mix was produced that had recycled coarse aggregate and natural sand, and another mix had recycled coarse aggregate and natural sand and fly ash substituting for 10 percent of the cement. These were compared with a previously tested mix that used an Ohio non-D-cracking aggregate.

Freeze-thaw testing was done on the recycled concretes to determine the potential for D-cracking activity. Freeze-thaw testing was done in a Weber cabinet with a large compressor. This unit is capable of 28 freeze-thaw cycles in a 24-h period, but it is operated at 12 cycles. Since the rate of freezing and thawing is not variable, and to ensure uniform conditioning, a timed delay is included at 0°F and a somewhat longer delay at 40°F. The beams of the four concrete designs were subjected to as many as 603 freeze-thaw cycles.

The recycled concretes showed some reduced D-cracking potential when compared with the natural aggregates, and the concrete in which fly ash substituted for 10 percent of the cement showed greatly reduced potential.

Initially, 3x4x16-in beams for freeze-thaw testing were cast one day, stripped and set in lime soak the next day, and soaked for 14 days. Once removed from the lime soak, beams were held in a freezer at 0°F until they could be freeze-thaw tested. Currently, beams are placed in lime soak for 28 days, allowed to air dry for one day, and moist cured for 30, 90, 150, and 210 days. They are then placed in the freezer at 0°F until they can be freeze-thaw tested.

Reconstruction of US-59 took place in 1980. Breaking and salvage of the in-place roadway began in May. Bituminous overlays originally placed by maintenance forces were removed with an elevating scraper. This was done in the afternoon when the overlay was warm. Smaller patches and joint filler were easily removed by using a small loader with a boom attached to the bucket and a tooth on the boom. The operator placed the tooth in the joint and, with the loader in reverse, dragged out the joint filler. Cleanup was done by hand and completed in June.

The in-place concrete was broken by using a shop-fabricated pavement breaker pulled by a crawler loader. The pavement breaker consisted of a two-wheel, rubber-tired trailer with a pile hammer attached. At the bottom of the pile hammer was a 14x18-in metal shoe that impacted and broke the pavement. The pile hammer was rated at 18 200 ft·lb and operated at 88-92 blows/min. Four passes were made per 12-ft lane. The speed at which the pavement breaker was pulled varied. The pavement broke more easily next to the edge or next to a previous pass of the machine. The breaker was pulled faster in those areas. The contractor attempted to break the concrete into 2-ft-square pieces. Breaking into smaller pieces made salvage more difficult. In order to avoid damage to in-place culverts, the contractor used a drop hammer to break the pavement in those locations.

The broken concrete was picked up by a power shovel with a wider-than-normal bucket. The contractor originally used two power shovels for salvage but, after a short trial, switched to one. Production was not affected, and eventually the salvage operation reached 0.5 mile/day.

Overbreakage and small pieces of concrete missed by the power shovel were gathered by a small dozer.

This was modified by adding teeth to the dozer blade. This allowed the operator to rake the material to the shovel without accumulating a significant amount of gravel base. The base was then shaped with a blade and compacted to protect it from the rain. Concrete salvage was completed in July.

Broken concrete was stockpiled at the crushing plant. A dozer worked the stockpile. A rubber-tired loader charged the 36x48-in single-toggle primary crusher. The contractor added a 1-in screen at the primary crusher to remove gravel base picked up with the pavement. The primary crusher reduced the material to less than 6 in in size. As this was moved by belt to the screening plant, reinforcing steel was removed by hand. Screened material was separated into stockpiles of minus no. 4 and no. 4 sieve to minus 0.75-in material. Of the minus 0.75-in material, the maximum natural aggregate particle size was on the order of 0.625 in, since all particles included some sand cement paste.

Oversized concrete from the screening plant was fed to a 54-in secondary cone crusher and then rescreened. Crushing began in May and was completed in July.

Concrete paving began in July 1980. Concrete was produced by a 9-yd^3, dual-drum central mix plant. The paving was preceded by an autograder that fine-graded the stabilized base. Concrete was supplied to a belt placer, which was followed by a conventional slip-form paver. Surface texture was applied with an astro-turf drag to enhance skid resistance. The final piece of equipment placed transverse tining and sprayed membrane curing compound.

The nonreinforced concrete pavement has random repeat spacing of skewed panels, 13, 16, 14, and 19 ft in length. Effective spacing is 15.5 ft. Joints are skewed 2 ft in 12 ft.

Paving of the northbound and southbound lanes was completed on September 9, 1980, and turn lanes were completed on September 24. On September 18, the last of the recycled aggregate was used and the contractor switched to natural aggregate of the same maximum size. The concrete contained 22 259 yd^3 of recycled aggregate and 640 yd^3 of natural aggregate. The use of natural aggregate does not indicate a shortage of recycled material. Turn lanes were added to the project after the computation of available aggregate was made.

PROJECT EVALUATION

The US-59 project can be evaluated in terms of pavement performance, cost comparison, and energy comparison.

As expected, paving with the recycled concrete was no problem. The recycled concrete finished well, but this has been the experience with all concrete mixes containing fly ash. Minnesota DOT specifications for surface finish allow a 1/8-in variation on a 10-ft straight edge and a 3/16-in edge slump. The pavement satisfactorily met these specifications.

A roughometer test was run on both lanes of US-59 after construction of the shoulders. The roughometer indicates riding quality by recording inches of roughness per mile. A riding quality of $\leq$85 in/mile of roughness is acceptable.

The average roughness for US-59 was 71 in/mile. The construction contract provided a bonus of 50¢/yd^2/lane mile of pavement when the riding quality indicated less than 69 in/mile of roughness. The bonus was awarded on 13 lane miles or 41 percent of the total lane miles of the project. The contractor received about a $41 000 bonus.

The quality of the transverse tining applied to the US-59 project reflects, in part, the condition of the skewed joints in the new pavement. These joints are cut with a saw when the concrete is still not fully cured. The sawing of a skewed joint across transverse tining often results in breaking or raveling of the surface concrete at the edge of the saw cut. The raveling, in turn, produces a rough surface. On this project, the contractor marked the joints and placed a metal strip approximately 6 in wide over the mark for the future saw cut. When the tining was applied, the tines passed over the metal strip, leaving the concrete surface at the joint untined. Since the pavement surface was smooth at the location of the joint, the concrete did not ravel when the cut was made. This is not expected to affect skid number.

A comparison of costs for recycling PCC as opposed to conventional concrete paving was originally assembled by personnel in the Minnesota DOT Estimating Unit and later updated from project records. Table 1 gives the updated project costs that are applicable. The first two items in the table are a direct comparison of the representative cost to remove and dispose of concrete pavement in the area of the state where the project is located and the contract price to remove, crush, and stockpile the old concrete pavement.

As mentioned earlier, recycled stabilizing aggregate was included in this project. The cost indicated is the additional cost for natural material from local sources to replace the recycled material.

Several shoulder designs were used on US-59. All of these used 2 in of bituminous over variable depths of class 5 and class 3 shouldering material. The contract provided for the use of the minus no. 4 material from the crushed concrete pavement and the crushed material from the bituminous overlays as a substitute for virgin material. The incremental cost difference for virgin material is included in the column for conventional concrete paving.

The final items relating to structural concrete reflect the contract amounts for the project as opposed to local costs for conventional concrete. The table also reflects the standard structural concrete used when recycled aggregate was no longer available.

The cost savings resulting from the recycling project were approximately $726 000. This amounts to 14 percent of the total project cost or nearly 16 percent of the grading and paving costs.

Part of the project evaluation compared the energy consumed in recycling with the energy required to construct a conventional pavement. Due to the difficulty in determining energy consumption for

Table 1. Cost saving from recycling concrete on US-59 project.

Item	Quantity	Cost ($)	
		Recycle	Conventional
Remove concrete pavement	229 170 yd^2		401 047
Salvage concrete pavement, crush, and stockpile	229 170 yd^2	595 842	
Stabilizing aggregate	24 238 tons		60 595[a]
Shouldering[b]			
Class 3	23 114 tons		57 785[a]
Class 5	21 238 tons		53 095[a]
Recycled concrete	52 651 yd^3	1 289 950	
Recycled concrete with high early strength	936 yd^3	28 890	
Standard concrete	1308/53 959 yd^3[c]	51 954	2 077 422
Standard concrete with high early strength	31/994 yd^3[c]	1 395	43 736
Total		1 968 031	2 693 680

[a] Differential cost between recycled material and natural aggregate.
[b] Portion of class for which recycled material was available.
[c] Virgin aggregate/total concrete used on project.

specific pieces of equipment, average energy consumption figures were used. Values published by the Asphalt Institute were the primary source.

The construction operations considered were materials removal, production, and transportation. It was assumed that, once the material reached the plant site, the mixing and placing operations balanced each other and only production of the component materials, such as crushing and screening, was significant.

The contractor would have used the same methods to break and remove the D-cracked pavement if it was to have been salvaged or disposed of. There was a net requirement of 130 additional equivalent gallons of gasoline for the concrete recycling option. This was the energy consumed in removal of bituminous pavement.

Overall, materials production for recycled concrete would require more energy than materials production for conventional concrete. This amounts to about 24 500 gal of gasoline.

To complete the evaluation of energy consumed, it was necessary to determine the energy requirements for transporting the construction materials. This determination assumed a constant source whenever possible, and the source was the actual supplier for the project.

The energy requirement for transportation of construction materials was less for the recycling option than for conventional paving. This amounts to a savings of 65 300 gal of gasoline.

A summary of the energy requirements in equivalent gallons of gasoline for recycling versus conventional paving is given in the table. There was an indicated savings of 40 610 gal of gasoline of an estimated 915 860 gal for conventional concrete paving. This would operate 51 automobiles, averaging 15 miles/gal, and traveling the normal 12 000 miles/year for a full year. This, in itself, is not an overwhelming savings, but it should be noted that conventional paving would require disposal of the broken D-cracked pavement. It is possible that the material may have been disposed of at the borrow pit where the contractor's plant was located. If another disposal site were required, additional truck haul would be necessary. The energy requirement would have increased further for conventional construction.

SUMMARY

In summary, the project selection process indicated the desirability of entering into a concrete recycling project on the basis of economic and engineering factors. Experimental work with trial mixes provided the concrete design most desirable for field application, and field application resulted in a project with a surface that has good riding quality. The US-59 recycling project is considered to be a success. The scarcity of quality aggregates in this area of Minnesota is partly responsible for that. In other areas, cost and energy savings may not be realized.

ACKNOWLEDGMENT

This paper reports the results of research conducted in cooperation with the Demonstration Projects Division of the Federal Highway Administration, U.S. Department of Transportation.

I appreciated the invaluable assistance provided by Marvin Mortenson, Leo Warren, and Allen Nippoldt of the Minnesota DOT. The cooperation of others in the Minnesota DOT--the District 7 Office at Mankato, the Office of Design Services, and the Office of Materials Engineering--and the contribution of the project personnel and the contractors were essential to the completion of this paper.

Publication of this paper sponsored by Committee on Performance of Concrete.

Relation Between Pavement D-Cracking and Coarse-Aggregate Pore Structure

D.N. WINSLOW, M.K. LINDGREN, AND W.L. DOLCH

Previous research has developed a relation between the pore structure of a coarse aggregate and the freeze-thaw durability, measured in the laboratory, of concrete made with that aggregate. This has permitted the calculation of an expected durability factor from a knowledge of an aggregate's median pore diameter and total pore volume. This work has been extended to a consideration of in-service pavements, some of which showed D-cracking distress and some of which appeared to be durable. Forty-seven pavement sections were cored, and coarse-aggregate samples were removed and separated lithologically. Their pore-size distributions were determined by mercury intrusion. Criteria involving the expected durability factor and relative amounts of good and bad aggregate fractions in the pavement were correlated with the extent of observed D-cracking. These correlations were distinctly superior to absorption measurements in identifying bad aggregates. It is suggested that the established criteria might be used to predict the performance to be expected from aggregate sources and might be a valuable acceptance standard.

D-cracking is an important durability problem in portland cement concrete (PCC) that is exposed to freezing conditions. It is particularly prevalent in pavements. It occurs when water in the coarse-aggregate pores freezes and causes sufficient expansion to crack the concrete. When D-cracking occurs in a pavement slab, it continues until the entire slab is destroyed. There exists no practical way to stop its progress. The only measure effective against it is the exclusion from the concrete mixture of those aggregates susceptible to the problem. Many agencies that have control over the materials used in paving perform regular tests on the coarse aggregate in an effort to screen out material that will cause D-cracking. Nevertheless, this form of distress still occurs in pavements made from materials that have passed current testing procedures. It is obvious that a more diagnostic test method is required.

In earlier work (1), the relation between the pore structure of an aggregate and its susceptibility to D-cracking was examined. The pore structures of a variety of crushed-stone coarse aggre-

Figure 1. Pore-size distributions of aggregates in a typical pavement core.

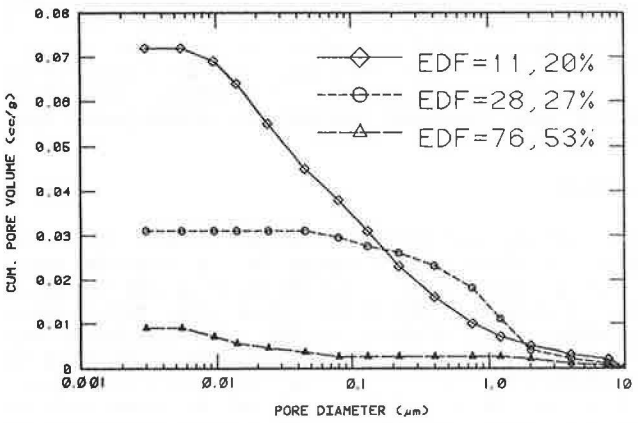

gates were determined by mercury intrusion porosimetry. The D-cracking resistance of the aggregates was determined by freezing and thawing concrete made with them according to a standard testing procedure (ASTM C-666A). Certain aspects of an aggregate's pore structure were found to correlate with the aggregate's freeze-thaw durability, and the following predictive equation was developed:

$$EDF = 0.579/PV + 6.12 \times MD + 3.04 \quad (1)$$

where

EDF = expected durability factor of aggregate (a larger value implies greater durability),
PV = aggregate's total intrudable pore volume of pores larger than 4.5 nm in diameter (cm^3/g), and
MD = median diameter of the intrudable pores larger than 4.5 nm in diameter (μm).

This relation indicates that the resistance to D-cracking is degraded by either a sufficiently large pore volume or a sufficiently small average pore size or a combination of these.

This earlier work was based on freeze-thaw performance observed in the laboratory. However, there was some indication that a knowledge of the pore structure of an aggregate could be used to predict the field performance of a pavement made with that aggregate. Furthermore, it appeared that measuring the pore-size distribution of an aggregate might be a superior diagnostic test for identifying nondurable aggregates. The work reported here was carried out to illuminate these important points.

EXPERIMENTAL PROCEDURES

The general plan of the research was to survey existing PCC highways, to note their condition with respect to D-cracking, and to remove cores from them. The pore-size distributions of the aggregates in the cores were then determined, and the predictive formula was used to find the EDF. Finally, a relation between the observed pavement condition and the measured EDF was established.

This study was restricted to four-lane highways in Indiana that had not been overlaid with a bituminous mixture. The former restriction was made to ease traffic problems while coring, and the latter one was made so that the surface could be observed for indications of D-cracking. Forty-seven pavement sections were surveyed and sampled. Each section was constructed under a separate contract and was typically 10-20 miles in length. All had a maximum coarse-aggregate size of either 1.5 or 2.5 in, and the coarse aggregate was either crushed stone or gravel. The distribution of pavement ages at the time of sampling is given below:

Age (years)	No. of Sections Sampled
0-5	1
6-10	5
11-15	19
16-20	12
21-25	7
26-30	3

The cores from each section were sawed in half, axially, and one half was crushed. Pieces of the coarse aggregate were removed from the crushed material, adhering mortar was removed when necessary, and the aggregate was washed and oven dried. It was then separated into visually distinct lithologic categories for each core. A typical core containing crushed stone had one to three different types of aggregate present, and a typical core containing gravel had four to eight different types. The sawed face of the uncrushed half of each core was polished and examined to give an approximate percentage of each type of coarse aggregate present in each core.

The pore-size distribution of each type of aggregate removed from the samples was determined by mercury intrusion porosimetry. The average of the contact angles previously reported (1), 124°, was used to calculate the pore diameters. Several pieces of the same aggregate type were tested simultaneously, as described previously (1). The EDF of each type of aggregate in each pavement section was calculated from its pore-size distribution by using the equation presented earlier.

The pore-size distributions of the aggregates from a typical core are shown in Figure 1. A total of 314 such distributions were determined during this research and are given elsewhere (2). A summary of the percentages of each type of aggregate in each core along with their EDFs is also too extensive to present here and may be found in the same report.

ANALYSIS OF DATA

One combined EDF, representative of each pavement segment, had to be obtained from the various EDFs found in that segment. A simple average, or a weighted average, of all EDFs was found to be unsatisfactory for this purpose. This was so because a few large EDF values could overwhelm the average whereas there were still a sufficient number of low-EDF aggregates present to cause distress. It was found that, when a sufficient amount of poor aggregate (low EDFs) was present, the average of only these poor rocks should be used to represent the segment. Conversely, when enough good material (high EDFs) was present, the average of only the good rocks was the appropriate value to represent the pavement.

Thus, the problem of finding a single EDF value that was representative of the aggregate in a pavement had two important aspects. One was to determine the maximum EDF value that a nondurable rock type could have. The second was to determine how much of a poor rock type must be present to cause poor pavement performance. These two questions are not independent, since the amount of poor rock in a segment depends on the definition of poor--i.e., the EDF that divides good from poor.

These two questions were answered simultaneously by a trial-and-error method. First, an EDF that divided good and poor aggregates was chosen. Next, the analysis of each core was used to determine the amount of good and poor aggregate present in each pavement section. Then a maximum limit on the amount of poor aggregate that could be present, without causing distress, was selected.

If a pavement section contained more than this maximum limit of poor aggregate, the average EDF of the poor portion of the aggregate in that section was used to represent the entire pavement section. If a section had less than this limit, the average EDF of the good portion of its aggregate was taken to represent the section.

If the EDF that divides good and poor aggregate had been selected properly, and if the maximum tolerable limit on poor aggregate had also been selected properly, then the resulting representative EDF for the section should have correctly described the actual condition of the pavement. That is, all pavements with a representative EDF below the good-poor dividing line should show D-cracking distress, and all pavements with a representative EDF above the dividing line should be free of D-cracking. If pavement sections with a poor representative EDF were observed to be in good condition, or vice versa, this meant that either the selection of the dividing EDF or the tolerable percentage of poor aggregate, or both, were improper.

The above technique used arbitrarily selected good-poor dividing lines and tolerable limits for poor aggregate plus laboratory measurements on the aggregates to "predict" the condition of each pavement section. This "prediction" was then compared with the observed pavement condition. The selection of both the good-poor division and the tolerable amount of poor aggregate was adjusted until the prediction most closely corresponded to the observed condition for all 47 pavement sections.

RESULTS

The best combination of a good-poor dividing line and maximum acceptable amount of poor aggregate was found to be that in which there was an EDF of 50 and no more than 10 percent of the aggregate had an EDF below this value. In other words, 90 percent of the aggregate should have an EDF greater than 50 if D-cracking is to be avoided. These criteria were found to be equally applicable to crushed stone and to gravel coarse aggregates. They have been shown to apply only during the first 30 years of pavement life. The following table compares observed performance (summer 1979, when the pavements were cored) and predicted performance by using these criteria:

No. of Pavement Sections	Observed Performance	Predicted Performance
29	D-cracked	Nondurable
11	Not D-cracked	Durable
7	Not D-cracked	Nondurable

DISCUSSION OF RESULTS

In this study, no attempt was made to differentiate between aggregates on the basis of how rapidly they will produce a D-cracked pavement. The criteria that were developed are of the "yes-no" variety. They differentiate between aggregates that will produce D-cracking within 30 years and those that will not. The criteria do not allow one to say that a certain aggregate will produce D-cracking within 10 years while another aggregate will require 20 years.

There were not a sufficient number of surveyable pavement sections in each age group to permit the further refinement of a prediction of the time required to display D-cracking. Furthermore, the rate of deterioration caused by a nondurable aggregate is likely to be associated with the environmental conditions surrounding a given slab and not only with the pore structure of the aggregate within the slab, and the criteria that have been presented concern themselves only with an aggregate's pore structure.

There is also an economic consideration that may be rapidly making a prediction of the rate of deterioration an academic exercise. The combination of climbing maintenance costs and increasingly scarce maintenance funds may presage the time when resurfacing a pavement solely because of D-cracking cannot be economically tolerated. Thus, it may not be important whether a pavement deteriorates in 10 or 20 years, since either possibility may be unacceptable.

This study only considered cores with a maximum aggregate size of either 1.5 or 2.5 in. No others were available. Approximately 75 percent of the cores contained 2.5-in maximum sizes. It is not felt that there were a sufficient number of cores with each maximum size to attempt the development of a separate criterion for each. Furthermore, most of the aggregates that were examined would probably not benefit from a reduction in size. In any event, the criteria presented appear to be equally applicable to both maximum sizes.

The results reported here are for either crushed limestone or gravel aggregates. These aggregates had pore sizes that were relatively tightly grouped about their median pore diameter. This median diameter varied over several orders of magnitude for the different aggregates examined. However, whatever the median might be, the pore diameter that separated the largest 25 percent of the pores from the rest was almost always less than five times as large as the median pore diameter. To put it another way, the majority of the pore volume in any aggregate usually resided in pores whose sizes were grouped within an order of magnitude of the median diameter.

Some aggregates, particularly slags, have a much wider spread in pore diameters. Only a few cores containing aggregate with widely spread pore sizes were examined. In these few, it appeared that this spread was advantageous and that it caused the aggregate to be more resistant to D-cracking than its EDF would predict. However, not enough pavements with such aggregates have been investigated quantitatively to include this parameter of their pore structure in the EDF calculation. Therefore, the findings reported here should be restricted, conservatively, to those aggregates for which the 25th percentile pore diameter is less than five times the median, or 50th percentile, pore diameter.

The preceding text table shows the result of applying the 90 percent > EDF = 50 criteria to the 47 pavement sections included in this study. The criteria always predict that an aggregate that actually shows distress is susceptible to distress. Had these criteria been used as a test to screen out susceptible aggregates, these sections would not have contained aggregate that causes D-cracking.

The sections that did not show distress at the time of sampling fall into two categories. The criteria predict that 11 sections should, indeed, be durable with respect to D-cracking. However, the criteria also predict that 7 sections should D-crack, but these 7 sections were not observed to be in distress at the time they were cored. It may be that these sections have had insufficient time to

show distress, or the criteria may be conservative in that they reject all the bad aggregate and also some durable aggregate as well. Continued observation of these sections is required to answer this question.

All the aggregate in all 47 sections passed the durability acceptance test in force at the time of construction: a 24-h absorption test. Yet almost two-thirds of the sections are in distress; 3 are less than 10 years old. The criteria developed in this study consider the median pore size as well as the pore volume of an aggregate rather than merely a measure of the pore volume. Furthermore, they consider that a comparatively small amount of poor material can destroy a pavement even when a large amount of good aggregate is present. For these reasons, they are considered to do a better job of discriminating among aggregates.

If the criteria developed here were used for acceptance testing of aggregate in relation to freeze-thaw durability, it would be necessary to measure a great many pore-size distributions. Even with the advent of automatic instruments to perform the tests, this would be an expensive undertaking. However, the cost of resurfacing D-cracked pavement is vastly more expensive. Compared with this extraordinary maintenance cost, the expense of the more refined testing described here would be small.

CONCLUSIONS

1. The pore structure of the coarse aggregate in a pavement can be used to calculate an EDF that is representative of the pavement.
2. The representative EDF correlates well with the presence or absence of observed pavement D-cracking distress.
3. The pore structure of a potential coarse-aggregate source may be a useful predictor of potential D-cracking problems in pavements made with that aggregate.

ACKNOWLEDGMENT

This research was carried out by the Joint Highway Research Project, Purdue University, in cooperation with the Indiana State Highway Commission and the Federal Highway Administration. Their assistance is appreciated.

REFERENCES

1. M. Kaneuji, D.N. Winslow, and W.L. Dolch. The Relationship Between an Aggregate's Pore Size Distribution and Its Freeze/Thaw Durability in Concrete. Cement and Concrete Research, Vol. 10, 1980, pp. 433-441.
2. M.K. Lindgren. The Prediction of the Freeze/Thaw Durability of Coarse Aggregate in Concrete by Mercury Intrusion Porosimetry. Purdue Univ., West Lafayette, IN, Joint Highway Research Project, Rept. 80/14, 1980.

Publication of this paper sponsored by Committee on Performance of Concrete.

Ohio Aggregate and Concrete Testing to Determine D-Cracking Susceptibility

JOHN T. PAXTON

Several laboratory test methods were analyzed to determine their capability of indicating the D-cracking susceptibility of coarse aggregates. Two methods were modified versions of ASTM C666 A and B, two were unconfined freeze-thaw tests of the aggregate, and the remaining two were standard sodium and magnesium soundness tests. The major modification of the ASTM C666 test methods was to determine the elongation of the test specimens versus routine weight-loss determinations and/or sonic modulus determinations. Results are evaluated by plotting the percentage of expansion versus the number of cycles completed and calculating the area under the curve generated. Although 10 specimens are used in the testing, the 2 high and 2 low test results are removed before final analysis. The correlation of this test method with service records of various aggregates was found to be good; however, when the same coarse aggregates were tested in sodium sulfate, magnesium sulfate, or unconfined freeze and thaw, the results did not correlate well with the service records.

D-cracking in portland cement concrete (PCC) pavements has been and is a serious problem in Ohio. Early in 1969, it was decided that research was needed to investigate the causes of and determine solutions for this problem. In June 1969, the Ohio Department of Transportation (ODOT) entered into a cooperative research agreement for this purpose with the Portland Cement Association (PCA). By March 1972, PCA had published an interim report on D-cracking of concrete pavements in Ohio that indicated that the coarse aggregate in the concrete was a cause of the problem. In addition, this interim report indicated that a freeze-thaw test similar to ASTM C666 could be used to determine the D-cracking susceptibility of coarse aggregates. It was at this time that ODOT decided to conduct research to evaluate the capability of various test methods for indicating which coarse aggregates used in Ohio were likely to cause D-cracking. This paper deals with the results obtained by using these various test methods to test coarse aggregates from 16 sources in Ohio that had service records indicating D-cracking in less than 15 years or no D-cracking in 15 years or more. The aggregate sources and their service records are given in Table 1.

AGGREGATE TESTING BY FREEZE-THAW

Confined

The initial testing undertaken by ODOT was freeze-thaw testing of the coarse aggregate incorporated in a concrete. The freeze-thaw tests used were similar to ASTM C666 methods A and B; however, instead of a determination of the sonic modulus of concrete specimens undergoing freeze-thaw cycling, the expansions of the specimens were checked and recorded throughout the test period. It was determined from the PCA research that the specimens that exhibited the larger expansions were those made with coarse aggre-

gate from sources whose service records showed D-cracking in less than 15 years.

All of the coarse aggregates were sieved into fractions and then recombined in the proportions shown in Figure 1. The fine aggregate, a natural sand, for all concrete mixes was from one source. The gradation and other properties are shown in Figure 1. The fine and coarse aggregates for all concrete were soaked, completely immersed in water, for a period of 16 h prior to mixing. Type 1 cement from a single source was used in all batches. The chemical composition and physical properties are shown in Figure 1. The specimens were 3x4x15-in prisms that had a gage stud embedded in each end. The gage length of the specimens was 14 in. All specimens were moist cured for 24 h at a temperature of 73°F ± 3°F and 13 days in saturated lime water at 73°F ± 3°F. At the end of the curing period, the specimens were cooled to 40°F ± 3°F and the initial length measurements were made by using a length comparator similar to the type specified in ASTM C490.

Table 1. Coarse-aggregate sources used in various tests.

Source	Location	Type of Material	Service Record	
			D-Cracking	No. of Years
Cng-1	Urbana	Gravel	Yes	<15
Cln-1	Melvin	Crushed Stone	No	>15
Del-5	Delaware	Crushed Stone	Yes	<15
Fn-6	Columbus	Gravel	Yes	<15
Kx-13	Fredericktown	Gravel	Yes	<15
Mn-3	Marion	Crushed Stone	Yes	<15
Mi-6	Piqua	Gravel	Yes	<15
My-16	Dayton	Gravel	Yes	>15
Rs-8	Kinnikiniick	Gravel	Yes	<15
Pm-4	Rimer	Crushed Stone	No	>15
Sy-2	Woodville	Crushed Stone	No	>15
Sy-6	Bellevue	Crushed Stone	No	>15
Vt-3	Union	Crushed Stone	No	>15
Wt-1	Carey	Crushed Stone	No	>15
Wt-8	Carey	Crushed Stone	No	>15

The method A procedure of ASTM C666, freezing and thawing in water, was conducted at 8 cycles/day, and expansion measurements were made at intervals of 24 and 32 cycles until the specimens had undergone 250 cycles of testing (see Table 2). The method B procedure of ASTM C666, freezing in air and thawing in water, was conducted at 12 cycles/day, and expansion measurements were made at intervals of 36 and 48 cycles until the specimens had undergone 450 cycles of testing. All of the freeze-thaw testing was conducted in a Conrad Missimer apparatus capable of holding 60 specimens.

The results are given in tabular form in Tables 2 and 3 and are shown graphically in Figures 2 and 3. The results in Tables 2 and 3 are grouped according to the two service record categories. In Figures 2 and 3, the sources that showed D-cracking in less than 15 years are depicted by dashed lines and the sources that showed no D-cracking in 15 years or more are depicted by solid lines. Additional freeze-thaw testing was undertaken, and the same mixing and curing procedures discussed above were used. However, 20 specimens were produced from each batch of concrete, and 10 of these specimens were tested by using method A procedures and the remaining 10 by using method B procedures. At the completion of the testing, the two high and two low test results were removed from the data. The data were then plotted in the form of percentage expansion versus the number of cycles completed. Figures 4 and 5 show the areas generated under the curves at 250 and 350 cycles for methods A and B, respectively. The number of cycles used for methods A and B were chosen to be 250 and 350, respectively, because at this point the separation of the sources that exhibit D-cracking in service from those that do not exhibit D-cracking is apparent. The area under the curve can be computed by integration; however, many small calculators have the capacity to perform this operation. A computer program is in use in Ohio for this operation and is available on request from ODOT.

Figure 1. Materials and mix design for concrete prisms.

Cement Composition

Compound Composition (%)					Cement Composition (%)										
C_3S	C_2S	C_3A	C_4AF	-	CaO	SiO_2	Al_2O_3	Fe_2O_3	MgO	Na_2O	K_2O	SO_3	Loss on Ignition	Insoluble Residue	Blaine cm^2/g
51	23	11.5	8	-	64.61	21.36	6.01	2.61	1.75	0.15	0.78	1.83	0.60	0.21	3424

Fine-Aggregate Gradation

Percent Retained in Sieve Size Indicated						Specific Gravity	Absorption	Na_2So_4 Loss
No.4-No.8	No.8-No.16	No.16-No.30	No.30-No.50	No.50-No.100	-100			
9	23	30	26	8	4	2.66	1.78	2.0

Coarse-Aggregate Gradation

Percent Retained in Sieve Size Indicated				
1.5-1 in.	1-0.75 in	0.75-0.5 in	0.5-0.375 in	0.375-No.4
35	17	28	15	5.0

Mix Design for Concrete Prisms

Cement factor:	6.5 bags/yd^3
Aggregate weights (dry)	Ls Gr
Fine:	1190 1075
Coarse:	1775 1890
Water-cement ratio:	4.8 ± 0.1 gal/bag
Air content:	6 ± 0.5%
Slump:	1.0 - 2.5 in

Table 2. Results of method A freeze-thaw test.

Source of Coarse Aggregate	Expansion by No. of Cycles (%)											
	25	50	75	100	125	150	175	200	225	250	300	350
No D-Cracking in 15 or More Years												
Cln-1	0.002	0.004	0.004	0.010	0.010	0.024	0.037	0.051	0.059	0.091	0.138	–
My-1	0.003	0.006	0.012	0.021	0.019	0.030	0.037	0.038	0.048	0.053	0.088	–
Pm-4	0.006	0.004[a]	0.008[a]	0.009[a]	0.027[b]	–	–	–	–	–	–	–
Sy-2	0.004	0.008[a]	0.010[a]	0.013[a]	0.016[a]	0.023[a]	0.028[a]	0.037[a]	0.048[a]	0.091[a]	0.121[b]	–
Sy-6	0.007	0.018	0.028	0.039	0.053	0.081	0.117[b]	0.145[b]	0.155[b]	0.197[b]	0.305[b]	–
Vt-3	0.003	0.005	0.008	0.014	0.018	0.024	0.031	0.036	0.036	0.041	0.055[a]	–
Wt-1	0.000	0.003	0.008	0.006	0.007	0.008	0.010	0.008[a]	0.016[a]	0.023[a]	0.030[a]	–
Wt-8	0.008	0.011	0.018	0.021	0.063	0.073[a]	0.054[a]	0.057[a]	0.056[a]	0.062[a]	0.048[b]	–
D-Cracking in Less Than 15 Years												
Cgn-1	0.006	0.006	0.008	0.010	0.018	0.023	0.027	0.036	0.098	0.122	0.094[a]	–
Del-5	0.010	0.015	0.020	0.025	0.033	0.044	0.049	0.063	0.073	0.081	0.126	–
Fn-6	0.004	0.004	0.007	0.008	0.016	0.019	0.024	0.036	0.073	0.077	0.131[a]	–
Kx-13	0.010	0.012	0.020	0.029	0.035	0.040	0.048	0.061	0.066	0.092	0.073	–
Mn-3	0.011	0.015	0.020	0.028	0.033	0.045	0.051	0.060	0.075	0.088	0.114	–
Mi-6	0.019	0.023	0.047	0.041[a]	0.051[a]	0.058[a]	0.076[a]	0.088[a]	0.098[a]	0.145[a]	0.160[b]	–
My-16	0.002	0.006	0.009	0.015	0.017	0.033	0.055	0.100	0.103[a]	0.156[a]	–	–
Rs-8	0.007[a]	0.024[b]	0.061[b]	–	–	–	–	–	–	–	–	–

Note: Each value represents the average expansion for three specimens unless otherwise noted.
[a]Two specimens.
[b]One specimen.

Table 3. Results of method B freeze-thaw test.

Source of Coarse Aggregate	Expansion by No. of Cycles (%)											
	25	50	75	100	125	150	200	250	300	350	400	450
No D-Cracking in 15 or More Years												
Cln-1	0.002	0.003	0.004	0.005	–	0.005	–	0.004	0.007	0.005	0.003	0.005
My-1	0.002	0.003	0.003	0.000	0.001	0.003	–	0.005	0.004	0.002	0.004	0.004
Pm-4	0.003	0.004	0.003	0.003	0.011	0.003	–	0.002	0.004	0.002	0.002	0.004
Sy-2	0.003	0.004	0.004	0.002	0.002	0.005	–	0.008	0.008	0.005	0.008	0.008
Sy-6	0.003	0.004	0.006	0.006	0.013	0.007	–	0.007	0.008	0.007	0.008	0.011
Vt-3	0.002	0.003	0.001	0.000	0.001	0.004	–	0.007	0.006	0.003	0.004	0.004
Wt-1	0.003	0.003	0.003	0.000	0.001	0.004	–	0.005	0.005	0.003	0.004	0.005
Wt-8	0.002	0.003	0.002	0.000	0.001	0.003	–	0.006	0.007	0.005	0.005	0.006
D-Cracking in Less Than 15 Years												
Cgn-1	0.002	0.003	0.005	0.005	0.012	0.006	–	0.008	0.009	0.009	0.009	0.012
Del-5	0.006	0.011	0.014	0.016	0.026	0.023	0.033	0.036	0.048	0.053	0.062	0.076
Fn-6	0.003	0.006	0.006	0.008	0.011	0.012	–	0.014	0.016	0.017	0.020	0.025
Kx-13	0.003	0.005	0.006	0.007	0.014	0.014	–	0.014	0.019	0.018	0.023	0.028
Mn-3	0.004	0.007	0.009	0.009	0.011	0.015	0.021	0.028	0.035	0.037	0.046	0.054
Mi-6	0.000	0.002	0.003	0.002	0.009	0.008	–	0.007	0.009	0.008	0.012	0.015
My-16	0.000	0.001	0.002	0.002	0.003	0.004	0.005	0.011	0.016	0.014	0.016	0.019
Rs-8	0.001	0.003	0.004	0.002	0.002	0.004	0.004	0.007	0.010	0.007	0.009	0.009

Note: Each value represents the average expansion for three specimens.

Figure 2. Expansions for freeze-thaw method A.

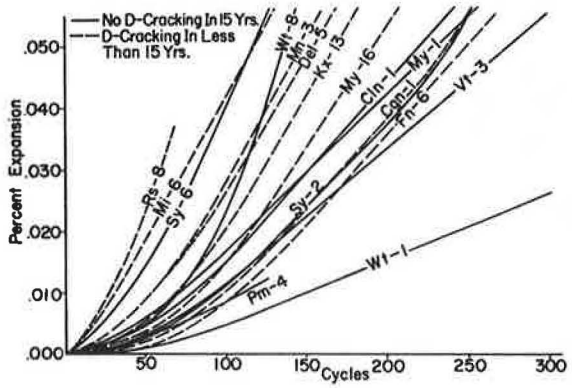

Figure 3. Expansions for freeze-thaw method B.

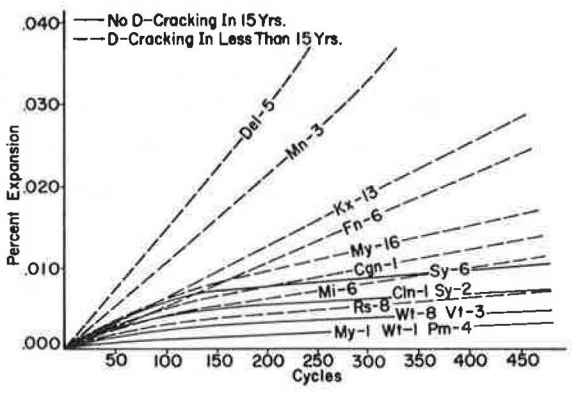

Unconfined

The four tests discussed previously have the disadvantage of requiring considerable time to complete. For this reason, it was decided to investigate other tests that could possibly give comparable results in less time. The New York DOT has such a test method: N.Y. 208A-68, entitled "Freezing and Thawing, Coarse Aggregates". The New York method called for testing material passing the 2-in sieve and retained on the 1.5-in sieve and material passing the 1.5-in sieve and retained on the 1-in sieve. The top size of material used in the earlier freeze-thaw test was the material retained on the 1-in sieve; therefore, it was decided to use this size and the material passing the 1-in sieve and retained on the 0.75-in sieve. The New York method called for using 3000 g of the larger material and 2000 g of the smaller material. In this testing, 2000 g of each of the sizes was tested. The temperatures required by the test method are -10°F ± 2°F and 70°F ± 5°F. The cycle used in New York consists of 17 ± 1 h at -10°F and the remainder of the 24-h cycle is used for thawing to 70°F. The test required that 25 cycles be run. With the equipment available at the ODOT Testing Laboratory, this cycle could be duplicated; in addition, it was found that the ODOT equipment had the capacity to complete four -10°F to 70°F cycles in a 24-h period. It was decided to run the test both ways and compare the results. The aggregates being tested are submerged in a 10 percent sodium chloride solution throughout the entire testing period. With the exceptions noted above, of the amount of material used and the number of cycles performed in a 24-h period, these tests were conducted in accordance with the New York DOT method. The same 16 coarse aggregates were tested by using these two methods, and the results are shown in Figures 6 and 7.

Figure 4. Area under curve for freeze-thaw method A at 250 cycles.

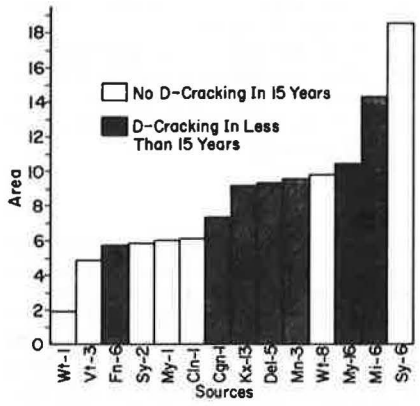

Figure 5. Area under curve for freeze-thaw method B at 350 cycles.

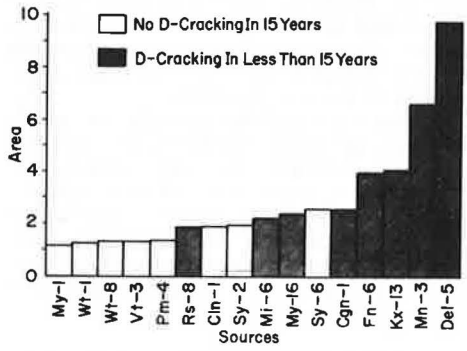

Figure 6. New York aggregate freeze-thaw test: one freeze-thaw cycle per day.

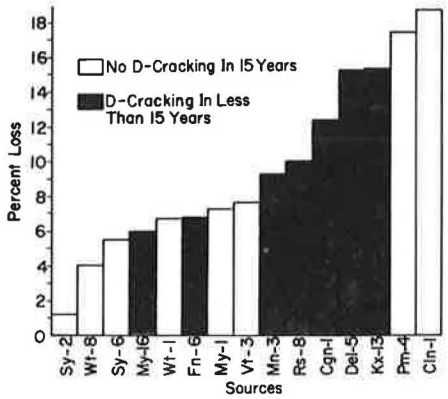

AGGREGATE TESTING FOR SOUNDNESS (SODIUM AND MAGNESIUM SULFATE)

The two other test methods used in this work were the American Association of State Highway and Transportation Officials (AASHTO) methods for testing for sodium sulfate soundness loss and magnesium sulfate soundness loss. The same 16 aggregate sources used in the previous testing were tested by using these two methods. These tests were conducted in accordance with AASHTO T-104, the standard AASHTO method. The results of these tests are shown in Figures 8 and 9. ODOT currently tests aggregates for soundness in sodium sulfate as a normal part of the aggregate specifications.

Figure 7. New York aggregate freeze-thaw test: four freeze-thaw cycles per day.

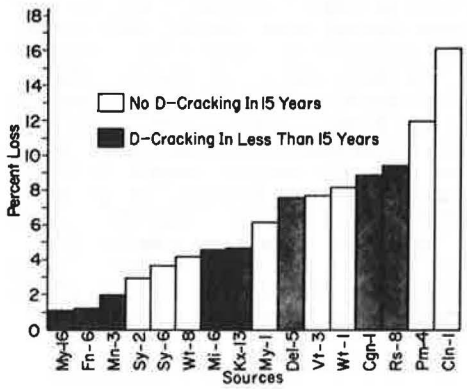

Figure 8. Sodium sulfate soundness test.

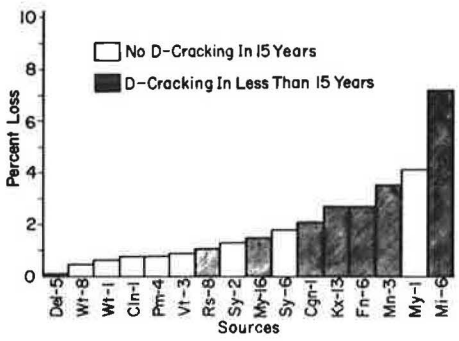

Figure 9. Magnesium sulfate soundness test.

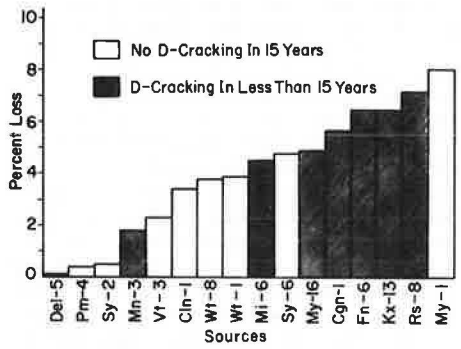

DISCUSSION OF TEST RESULTS

Two major problems that have been encountered in freeze-thaw testing of concrete prisms by using method A of ASTM C666 are the gage pins falling out of the specimens and the specimens breaking before the testing reaches the desired number of cycles. This can be seen in Table 2 in that many of the specimen sets do not contain three specimens at the end of the testing. These two occurrences cannot always be attributed to the coarse aggregate in the specimens. In addition, the containers that hold the specimen and water for this test are a constant maintenance problem because of bulging and cracking caused by the pressures of the frozen water.

The freeze-thaw method B test is the most desirable, since any effect brought about by the containers is eliminated. The major drawback to using method B has been that the expansions produced are small and it is therefore difficult to differentiate between those aggregates that cause D-cracking and those that do not in the same number of cycles as is used with method A. It was found that 12 cycles could be completed in a 24-h period when testing with method B whereas only 8 cycles could be completed in the same period when testing with method A. This made it possible to extend the method B test to obtain the differentiation between the D-cracking and non-D-cracking aggregates. It can be seen in Tables 2 and 3 and Figures 2 and 3 that differentiation and correlation with service record data are obtained for all sources except Rs-8 and Sy-6 as early as 300 cycles; however, it is still very difficult to select a distinct separation point until at least 350 cycles have been completed. At 300 cycles, there is very little difference between the areas and expansions of the good and bad aggregates. At 350 cycles, the area shows good differentiation, but there is still little difference between the expansions. It can be said with a fair degree of confidence, from looking at Figure 5, that, if after 350 cycles of method B testing the prisms have not expanded so that the area under the curve is more than 2.05, the aggregate being tested is not susceptible to D-cracking. No explanation has been found for the behavior of sources Rs-8 and Sy-6.

If one looks at the freeze-thaw testing of the aggregates alone, it can be seen that the correlation with the service record data is not as good as it is with the freeze-thaw testing of the concrete prisms. In examining Figures 6 and 7 it can be seen that, as the number of cycles per 24-h period is increased, the correlation with service record becomes worse because in Figure 7 three of the worst sources show the least loss. In addition, two of the sources, Pm-4 and Cln-1, which have very good service records, show very poor performance in these tests, whereas source Fn-6, which has a poor service record, shows rather good performance.

Both of the soundness tests show fair correlation with service record data; however, source Del-5, which has a very poor service record, does very well in these tests, whereas My-1, which has a very good service record, does very poorly.

CONCLUSIONS

Although the freeze-thaw testing of concrete may not be the only method of determining coarse-aggregate susceptibility to D-cracking, it has the best correlation with the service record data of the eight tests conducted for this work. Method B of ASTM C666 is better for the determination of aggregate susceptibility to D-cracking than method A because any effect of the containers is eliminated. In addition, the determination of the area generated under the curve is more suitable for determining aggregate D-cracking susceptibility than is a comparison of expansions because, once the area generated exceeds the maximum permitted, it will never go below this maximum. In some cases, the expansion will just exceed the maximum and at the next measurement will be just below the maximum.

Freeze-thaw testing of concrete containing these same coarse aggregates has been conducted by the PCA Laboratory, and the performance of the concrete in the test ranked the coarse aggregates in very nearly the same order as did the testing reported here. At least two other laboratories are looking for test methods to determine D-cracking susceptibility, and both are investigating the freeze-thaw of concrete specimens.

Publication of this paper sponsored by Committee on Performance of Concrete.

Durability of Concrete and the Iowa Pore Index Test

VERNON J. MARKS AND WENDELL DUBBERKE

An overview of the problem of D-cracking in portland cement concrete (PCC) is provided, and the Iowa pore index test for determining the quality of coarse aggregate for concrete is evaluated. The Iowa pore index test was developed to evaluate the durability of coarse aggregate. The test measures the amount of water that can be injected into oven-dried aggregate during a period from 1 to 15 min after application of 35 psi (241 kPa) of pressure. The test is very effective in identifying aggregates with substantial pore system of the 0.04- to 0.2-μm-diameter size and correlates very well with aggregate service records. Test results of nonhomogeneous samples can be misleading. Laboratory tests have shown that a small amount (15 percent) of unsound material in the coarse aggregate can produce nondurable concrete. Studies with the scanning electron microscope show that coarse aggregates associated with D-cracking are normally fine grained whereas durable aggregate is either coarse grained or extremely fine grained. The pore-size distribution of coarse aggregates was determined by using a mercury porosimeter. Aggregates associated with D-cracking exhibit a predominance of 0.04- to 0.2-μm-diameter pore sizes.

Very simply, durability is the quality of being able to last. In portland cement concrete (PCC), design, materials, mix proportion, and construction practices are factors that affect durability. The life of PCC pavement is becoming more important due to the severe shortage of highway funds. The only factor to be considered in this paper is the quality of the coarse aggregate. All references to durability relate to the effect of the coarse aggregate and, more specifically, to D-cracking.

D-cracking (see Figures 1 and 2), a type of PCC pavement deterioration attributed to the coarse aggregate in the mixture, was first recognized on Iowa's primary road system in the late 1930s. The term D-cracking dates back to the 1930s and was used in reference to deterioration characterized by the appearance of fine, parallel cracks along joints, random cracks, or free edges of the pavement slab (1). Generally, the first signs of D-cracking are a discoloration or staining at the intersection of the transverse and longitudinal joints.

The Portland Cement Association (PCA) has conducted extensive research on the D-cracking problem. The PCA research has shown that essentially all aggregates that contribute to D-cracking are of sedimentary origin and of both carbonate and silicate composition. These range from essentially pure limestone to dolomite (2). This research has further established that D-cracking in Iowa is a distress that results from freeze-thaw failure in the coarse-aggregate particles.

There are variations between bedded layers, but in general the limestones of southwestern Iowa result in severe D-cracking at a relatively early pavement age. There are many limestone and dolomite beds in northeastern Iowa that have service records of 30 years without any signs of D-cracking. Evidence of D-cracking can appear in as few as three years (3).

OBJECTIVE

The objective of this paper is to provide an overview of the PCC D-cracking problem and an evaluation of the pore index test for determining the quality of coarse aggregate for concrete.

IDENTIFICATION OF PAVEMENT DETERIORATION

Iowa, like many other states, was reluctant at one time to identify pavement deterioration as D-cracking. In the 1960s, severe D-cracking was recognized on major primary pavements. This precipitated an extensive condition inventory of all PCC pavement that has continued to the present.

D-cracking has resulted in rapid failure of the pavement; therefore, any rapid deterioration of originally sound concrete has generally been identified as D-cracking. There have been a few incidents of rapid pavement failure in Iowa in which the entire slab developed crack patterns that, although generally identified as D-cracking, did not exhibit the typical distress progression. This leads to the consideration that there may be other modes of rapid failure not yet identified by research. There is some evidence that the use of deicing salts may accelerate the D-cracking process.

EVALUATION OF COARSE AGGREGATE

Soundness Test

The basic Iowa Department of Transportation (DOT)

Figure 1. Pavement exhibiting severe D-cracking deterioration.

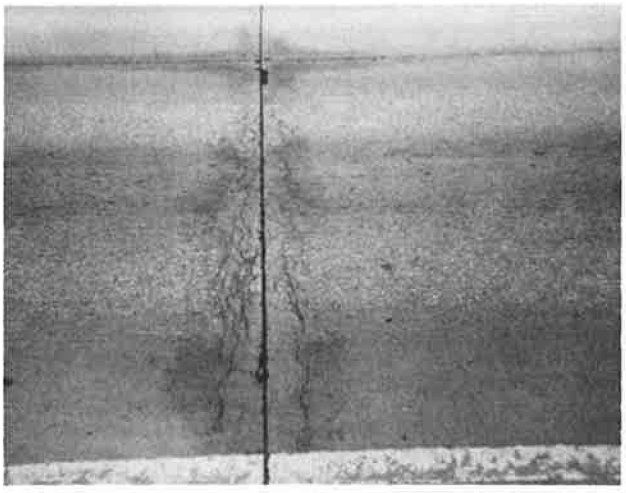

Figure 2. Close-up of D-cracking at intersection of transverse and longitudinal joints.

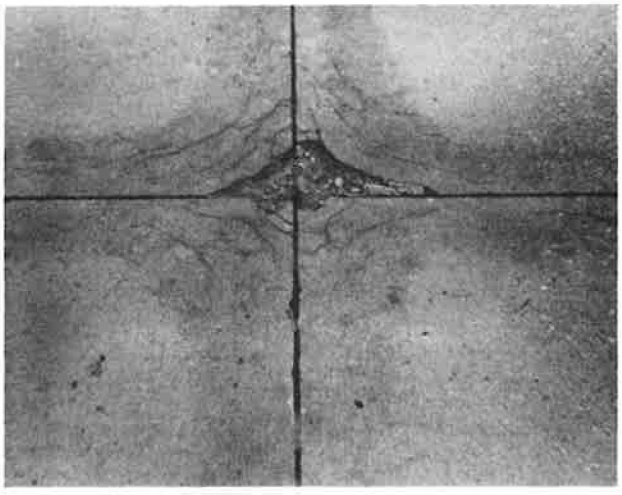

Table 1. Coarse-aggregate data.

Aggregate No.	Producer	Location	Bed(s)	Aggregate Composition	Grain Size	Service Record	Specific Gravity	Absorption (%)	Freeze-Thaw Loss[a] (%)	Durability Factor[b]	Pore Index (mL)
1	Weaver	Alden, IA	3	Limestone	Very coarse	Excellent	2.58	2.8	2	95	13
2	Niemann	Lamont, IA	1-7	Dolomite	Very coarse	Excellent	2.70	1.8	2	96	19
3	Niemann	Festina, IA	1-4	Dolomite	?	Very good	2.69	0.4	1	96	7
4	Cessford	Farmington, IA	3	Argillaceous limestone	Very fine	Very good	2.69	0.5	8	95	21
5	Western material	Kankakee, IL	A	Argillaceous dolomite	Coarse	Very good	2.73	0.8	7	99	44
6	Anderson	Montour, IA	1-7	Oolitic limestone	Medium	Good	2.61	2.0	2	75	18
7	Green	Floyd, IA (Warnholtz)	17D	Argillaceous limestone	Very fine	NA	2.70	2.0	7	97	83
8	Green	Floyd, IA (Warnholtz)	18	Argillaceous dolomite	Fine	NA	2.70	1.8	7	93	65
9	Columbia	Ullin, IL	NA	Limestone	Medium	D-cracking	2.67	0.9	1	17	48
10	Alpha	Prairieburg, IA (Plower)	4	Dolomite	Fine	Severe D-cracking	2.62	3.9	2	21	95
11	Martin Marietta	Waterloo, IA (South)	17-18	Limestone	Medium	Severe D-cracking	2.66	2.0	1	71	44
12	Schildberg	Crescent, IA	25	Limestone	Fine	Severe D-cracking	2.65	1.2	2	48	42
13[c]	Green	Floyd, IA (Warnholtz)	16	Very argillaceous limestone	Fine	NA	NA	NA	31	NA	120
14[c]	–	–	–	Tripolitic chert	Fine	–	2.49	4.4	–	–	82
15[c]	–	–	–	Dense chert	Very fine	–	–	–	–	–	14

[a] Method A.
[b] ASTM C666 method B.
[c] Selected fractions.

"Coarse Aggregate for Concrete" soundness test is a 16-cycle (9-cycle/day) water-alcohol "method A" freeze-and-thaw test that, except for automation, remains essentially as adopted in the 1948 Standard Specifications. An aggregate sample retained on the no. 4 (0.48-cm) sieve is subjected to alternate freezing [2 h to -15°F (-26°C)] and thawing [40 min to 70°F (21°C)] in a 0.5 percent methyl alcohol solution. The percentage passing the no. 8 (0.24-cm) sieve after 16 cycles is reported as loss. The maximum loss of 6 percent allowed by specification has remained unchanged since 1948.

Until the general recognition of D-cracking, this method A freeze-and-thaw test, as referred to by the Iowa DOT, was accepted as the main criterion for the exclusion of coarse aggregates that would contribute to nondurable concrete. Service records have identified concrete that exhibited D-cracking of varying severity and that contained aggregate that had passed the method A freeze-and-thaw test.

It is apparent from a more critical analysis of the method A freeze-and-thaw test that it excludes coarse aggregate primarily on the basis of the amount of shale, clay, and tripolitic chert. In the past, it has been generally accepted that these materials are detrimental to the quality of concrete. The method A freeze-and-thaw test relates to petrography and in general restricts the acceptance of coarse aggregate to materials containing less than 5 percent shale, clay, or tripolitic chert.

Durability Test

Research on the rapid freeze-and-thaw test of concrete beams was initiated in 1962. The procedure used was essentially that described in ASTM C291 (now ASTM C666 method B) for freezing in air and thawing in water. Various preparation or curing treatments were tested, and it was determined that a 90-day cure in the moist room was necessary to ensure "critical" saturation and allow completion of the major portion of the cement hydration to yield the maximum display of subsequent distress of concrete containing nondurable aggregate. After several years of investigation proved that laboratory freeze-and-thaw results correlated well with service records, this test was incorporated into the 1972 Standard Specifications for quarry approval prior to acceptance of coarse aggregate. Both the dynamic modulus and the growth are recorded, and the durability factor at 300 cycles is calculated from the dynamic modulus (see Table 1).

Even though the modified ASTM C666 method B correlates well, there are undesirable features. Concrete beams measuring 4x4x18 in (10.16x10.16x45.72 cm) and made from aggregates with satisfactory service records may fail (durability factor less than 80 percent) if small amounts of deleterious materials (such as tripolitic chert) are present in the aggregate. With a 90-day moist preparation and 38 days (8 cycles/day) for the test, it takes nearly five months to complete the aggregate evaluation.

Other Tests

The Iowa DOT has investigated the use of the absorption-adsorption test to determine the quality of aggregate, and the test was found to be overly restrictive for Iowa aggregates. Aggregates with satisfactory service records would fail the test. Iowa studies of sodium sulphate and magnesium sulphate tests resulted in poor correlation with the aggregate service records.

DEVELOPMENT OF IOWA PORE INDEX TEST

Recognizing that the D-cracking problem was freeze and thaw related (1), and more specifically related to pore sizes (3), Dubberke began investigations of measuring the amounts of water, under low air pressure, that could be injected into oven-dried aggregate. A Washington Press-Ur-Meter (used to measure entrained air in PCC) was modified for use in the test (see Figure 3). During development of the pore

Figure 3. Pore index test apparatus.

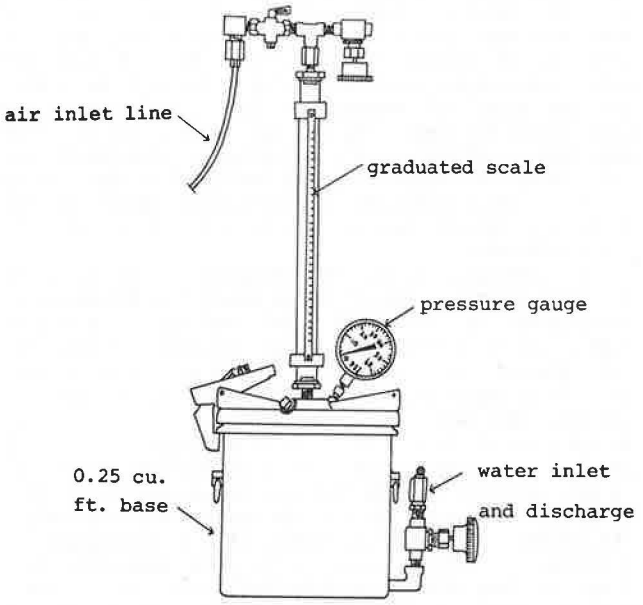

index test (4), pressures ranging from 10 to 60 psi (69-414 kPa) were applied while the incremental amount of water injected into the aggregate during a 2-h period was recorded. This early testing indicated that any pressure in this range could be used by selecting the appropriate corresponding time (a lower pressure requires a longer time). High pressures with some aggregates resulted in such a rapid lowering of the water that accurate manual readings at the beginning of the test were very difficult to obtain. With a pressure of 35 psi (241 kPa), all necessary water-injection information was obtained in 15 min and manual readings could be obtained with adequate reliability.

PORE INDEX TEST APPARATUS AND PROCEDURE

Test Unit Apparatus

A modified Press-Ur-Meter is used to perform the pore index test. The pump, valve, and gauge were removed from the lid and replaced by a 320-mL plexiglas tube, graduated by 2-mL increments. The addition of a standard 60-psi (414-kPa) pressure gauge completes the lid modifications. A hole drilled through the side of the pot at the bottom and fitted with a valve is used for loading and unloading the pot with cold tap water. Two valves are located at the top of the plexiglas tube. One valve is connected to a line that supplies air at a constant 35 psi (241 kPa). The other valve is a vent valve and is opened while the unit is being charged with water.

Test Procedure

1. Place 9000 g (minimum of 4500 g) of oven-dried, 0.5x0.75-in (1.27x1.91-cm) aggregate in the pot. During the evaluation phase of the pore index test, samples ranging from 3000 to 10 000 g were accepted for testing. Since the secondary load (pore index test result) is directly proportional to the size of the sample, values were adjusted to reflect a projected 9000-g sample. Many of the adjusted test results were from small samples received from the districts, but in a few cases half-samples were necessary because of high absorption. If the capacity of the 320-mL tube is exceeded during the test, the test is rerun with a 4500-g sample.
2. Attach the lid, open the vent valve, and fill the base and plexiglas tube with cold tap water to the 0-mL mark. The pressure gauge on the lid must remain at the zero pressure mark during this filling stage.
3. Close the water supply and vent valves and then open the 35-psi (241-kPa) air supply valve as soon as possible. The air valve remains open throughout the duration of the test.
4. Take a water-level reading at 1 min. The amount of water injected during this first minute fills the aggregate's macropores and is referred to as the primary load. A large primary load is considered to be an indication of a beneficial limestone property. A well-developed macropore system may function in a manner similar to air-entrainment voids in concrete paste. The primary load is not used in calculations of the pore index test result.
5. Take a water level reading at 15 min. The volume of water injected between 1 and 15 min is the secondary load and represents the amount of water injected into the aggregate's micropore system. A secondary load of 27 mL or more indicates a negative limestone property that correlates with a saturated aggregate's incapacity to withstand internal pressures caused by freezing. The secondary load in milliliters is reported out as the final pore index test result.

PORE INDEX CORRELATION

Routine aggregate testing began in 1978. The pore index was determined for aggregates from 28 different sources. These were compared with the service record and the ASTM C666 method B concrete durability results. The pore index test correlated very well. Aggregates with a history of producing D-cracking concrete consistently yielded indices greater than 27 mL. There were a few tests that did not initially appear to correlate with service record. Further investigation of these samples revealed variations in material and verified the pore index results.

NONHOMOGENEOUS COARSE AGGREGATE

Possibly the major problem in developing a reliable test to identify coarse aggregate that causes D-cracking is the variation in both the composition and the structure of the material. Stark of PCA (2) notes that "nearly all rock types known to be associated with D-cracking are of sedimentary origin" and "materials of igneous origin are not known to be associated with D-cracking." River gravels are probably the best example of nonuniform composition. In Iowa, gravel deposits can have from 30 to 80 percent particles of igneous origin. The remaining 20-70 percent are predominately limestone and dolomite particles, but Iowa gravels may contain from 1 to 10 percent deleterious particles such as shale, siltstone, chert, and iron oxides. Samples from gravel deposits have been manually separated, and laboratory freeze-and-thaw testing (ASTM C666 method B) of the igneous fraction has yielded excellent durability factors. The capacity of a gravel to produce durable concrete depends on the carbonate fraction. Where the carbonate fraction was nondurable, D-cracking has been identified in as few as eight years.

Even though it is not readily apparent to the casual observer, both the composition and the structure of carbonates can exhibit extreme variations. The dolomites (calcium-magnesium carbonates) generally have much larger grain sizes and pore

sizes than the limestones (calcium carbonates). The dolomites are generally not associated with D-cracking, but there are exceptions.

Kaneuji (5) in a Purdue University study recognized the variability of aggregate of a quarry face and recommended the sampling of individual ledges instead of stockpiles. Adjacent beds can vary tremendously in pore structure, and consequently one may be very durable while the other may result in severe D-cracking. Pertinent characteristics of the aggregates used in this paper are given in Table 1.

Figure 4. Pore volume versus pore size for nondurable aggregates.

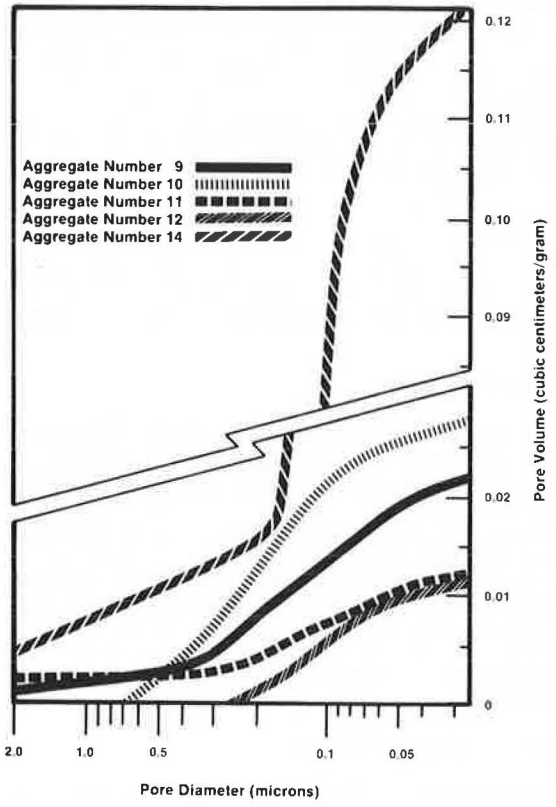

Figure 5. Pore volume versus pore size for durable aggregates.

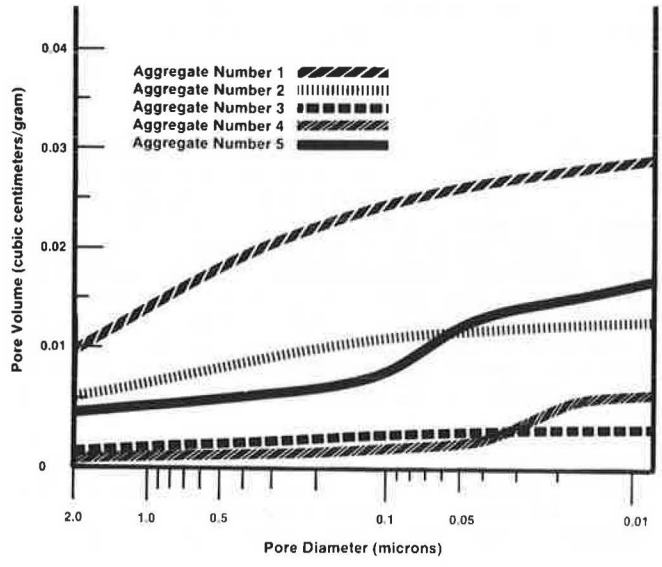

In general, the aggregates are listed from those with the best service record to those with the poorest service record. It should also be noted that the aggregates listed are either very good or very bad in regard to D-cracking. This is true because the middle range generally results from a nonuniform blend of aggregates and test results are more variable depending on the proportion of good and bad particles. Only relatively consistent and uniform coarse aggregates are included in the table, since a small fraction of nondurable aggregate can produce concrete that is susceptible to freeze-and-thaw distress.

A laboratory study of concrete beams made by blending coarse aggregates was conducted by using an evaluation by the ASTM C666 method B concrete freeze-and-thaw test. A coarse aggregate associated with severe D-cracking was blended with two sources of coarse aggregate that had an excellent service record. The poor aggregate constituted 15, 30, and 45 percent of the total coarse aggregate. When 15 percent of an aggregate with a durability factor of 54 was blended with 85 percent of an aggregate with a durability factor of 90, the result was a durability factor of 78. This agrees with a conclusion by Lindgren (6) in Purdue University research that "greater than 10% nondurable aggregate present in a pavement has a detrimental effect on the pavement." One relatively thin bed of nondurable stone in a quarry face may cause the coarse aggregate to result in D-cracking. The pore index test can be used to identify rapidly these nondurable beds. Benching a quarry so as to remove these nondurable beds from coarse-aggregate production can improve the final product.

DURABLE AGGREGATE THAT FAILS THE PORE INDEX TEST

As stated previously, Iowa specifications for coarse aggregate exclude materials with a method A freeze-and-thaw loss greater than 6. Materials with a low freeze-and-thaw loss are consistently classified correctly by the pore index test. The State of Illinois is using the pore index test and has indentified Western Materials (Kankakee, Illinois) coarse aggregate (aggregate 5 in Table 1) as having a very good service record and exhibiting a failing pore index of 44. Iowa testing has since confirmed Illinois data. This aggregate is an argillaceous dolomite that would have been excluded from further testing by the Iowa method A freeze-and-thaw test. Subsequent testing has identified an Iowa aggregate that is similar to the Illinois aggregate (aggregates 7 and 8 of Table 1). Mercury porosimeter testing included later in this paper supports pore index results by identifying pore sizes that normally coincide with aggregates associated with D-cracking. The Illinois aggregate (aggregate 5) contains 10 percent nonexpansive clay (illite or glauconite) finely dispersed in a dolomite matrix, which may be a factor in the very good service record.

MERCURY POROSIMETER STUDIES

A Quantachrome Scanning Porosimeter has been used on all of the aggregates in Table 1 to determine the pore sizes and volumes. An oven-dried 3-g sample of material passing the 0.25-in (0.64-cm) sieve and retained on the no. 4 (0.48-cm) sieve was used for the analysis of each source. All aggregates were scanned from 0 to 60 000 psi (414 MPa). The porosimeter is computer controlled and makes all necessary corrections and automatically plots the pore volume/pore radius output. The pore radii are changed to diameters for presentation in this paper. With one exception, all nondurable aggre-

gates analyzed to date exhibit a predominance of pore sizes in the 0.04- to 0.2-μm-diameter range, which is indicated by the steep slope in the plots shown in Figure 4. With the exception of aggregate 5 (discussed earlier), the aggregates with good to excellent service records do not exhibit a predominance of the 0.04- to 0.2-μm-diameter pore sizes (see Figure 5). Mercury porosimeter testing has shown that the pore index test is very effective in identifying aggregates with substantial pores of the 0.04- to 0.2-μm size.

SCANNING ELECTRON MICROSCOPE STUDIES

Durable coarse aggregates have been observed and photographed with a scanning electron microscope (SEM). All photographs included in this paper were magnified 1000 times. Aggregates 1 and 2 have excellent service records. The very coarse grain size and large pore size are shown in Figures 6 and 7, respectively. Nondurable aggregates 9, 10, and 12 (see Figures 8-10, respectively) generally exhibit a fine-grained texture. Figure 8 shows some coarse grains in a predominately fine-grained matrix. Comparison of the pore-size data from the mercury porosimeter with the grain-size data from the SEM would indicate that a coarse-grained structure generally results in larger pore sizes.

The SEM also has the capability of identifying localized elements at high magnification, and current studies will use this capability in the analysis of D-cracking or other rapid failure mechanisms.

Figure 6. SEM photograph (1000x) of aggregate 1 (Weaver, Alden, Iowa).

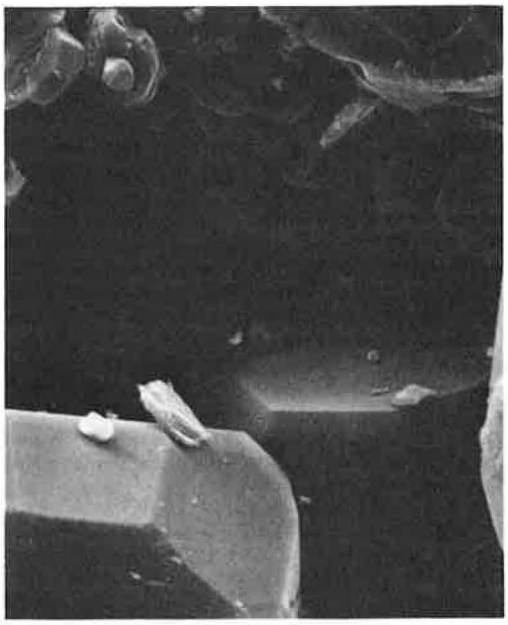

Figure 7. SEM photograph (1000x) of aggregate 2 (Niemann, Lamont, Iowa).

Figure 8. SEM photograph (1000x) of aggregate 9 (Columbia, Ullin, Illinois).

Figure 9. SEM photograph (1000x) of aggregate 10 [Alpha, Prairieburg, Iowa (Plower)].

Figure 10. SEM photograph (1000x) of aggregate 12 (Schildberg, Crescent, Iowa).

ANALYSIS OF INSOLUBLE FRACTION

Aggregate 5 has been acidized to remove the carbonate fraction. Mercury porosimeter, SEM, and chemical analyses of the residue are in progress. The analysis of the insoluble fraction of other aggregates is being initiated to determine whether they may contribute to the resulting aggregate durability.

CONCLUSIONS

1. The pore index test is very effective in identifying aggregates with a substantial system of pores in the 0.04- to 0.2-μm-diameter size.
2. The pore index test correlates very well with service records of nonargillaceous coarse aggregates used in PCC.
3. If 15 percent or more of the coarse aggregate is nondurable, the PCC will probably exhibit D-cracking.
4. Pore index tests of nonuniform material are not conclusive.
5. If possible, homogeneous fractions of coarse aggregates should be evaluated separately. Gravel should be separated into igneous and carbonate fractions for analysis. Individual beds of carbonate materials should be sampled separately.
6. Nondurable, nonargillaceous carbonate aggregates associated with D-cracking pavements exhibit a predominance of 0.04- to 0.2-μm-diameter pore sizes.
7. Nondurable coarse aggregates are generally fine grained and aggregates with a good to excellent service record are generally coarse grained or extremely fine grained.

ACKNOWLEDGMENT

We wish to thank Charles L. Huisman and James D. Myers of the Iowa DOT for their assistance in the durability research. The assistance of Turgut Demirel and Jerry Amenson in the use of the Iowa State University mercury porosimeter and SEM was very much appreciated.

This paper does not constitute a standard, specification, or regulation.

REFERENCES

1. D. Stark and P. Kleiger. Effects of Maximum Size of Coarse Aggregate on D-Cracking in Concrete Pavements. Portland Cement Assn., Skokie, IL, R&D Bull. RD023.01P, 1973.
2. D. Stark. Characteristics and Utilization of Coarse Aggregates Associated with D-Cracking. Portland Cement Assn., Skokie, IL, R&D Bull. RD-47.01P, 1976.
3. P. Kleiger, G. Monfore, D. Stark, and W. Teske. D-Cracking of Concrete Pavements in Ohio. Portland Cement Assn., Skokie, IL, Rept. OHIO-DOT-11-74, Oct. 1974.
4. J.D. Myers and W. Dubberke. Iowa Pore Index Test. Iowa Department of Transportation, Ames, Interim Rept., Jan. 1980.
5. M. Kaneuji. Correlation Between Pore Size Distribution and Freeze Thaw Durability of Coarse Aggregate in Concrete. Purdue Univ., West Lafayette, IN, Joint Highway Research Project, Rept. JHRP-78-15, Aug. 1978.
6. M.N. Lindgren. The Prediction of Freeze/Thaw Durability of Coarse Aggregate in Concrete by Mercury Intrusion Porosimetry. Purdue Univ., West Lafayette, IN, Joint Highway Research Project, Rept. FHWA-IN-JHRP-80-14, Oct. 1980.

Publication of this paper sponsored by Committee on Performance of Concrete.

Concrete Evaluation by Radar Theoretical Analysis

A.V. ALONGI, T.R. CANTOR, C.P. KNEETER, AND A. ALONGI, JR.

The operating principles of a mobile high-resolution radar system that has been optimized for inspection of pavements such as highways, bridge decks, and runways are described. The waveforms generated by the high-resolution radar are illustrated as well as the interaction of these waveforms with the pavement structure. Graphic derivations of representative radar waveforms for varying conditions are shown by using time-domain analysis. This simplified method of analysis enables useful models to be made for a range of separation thicknesses and pavement base materials. The results of laboratory tests are presented in which radar illuminates a double slab of concrete and the spacing between the two slabs is varied discretely and precisely from 0 to 30 cm (0 to 12 in). For spaces up to 7.5 cm (3 in) between two similar materials, the amplitude of the radar echo appears to be nearly proportional to the same dimension. As the space increases to 15 cm (6 in), the signal increases primarily in width. For spaces greater than 15 cm, the radar signal splits into two separate waveforms, thereby resolving the upper and lower boundaries of the space. These laboratory data are related to in situ void data taken on airport runways. Finally, a detailed analysis of a single concrete slab, illuminated by the radar, is performed. The amplitude and phase properties of the reflected signal waveforms are derived independently based on time-delay measurement and a mathematical method. Both methods agree with each other and with the experimental data.

As soon as a concrete structure in the infrastructure is poured, aging and accompanying deterioration start. The earlier the regression or impending fault can be discovered by nondestructive techniques, the easier and less costly it is to correct and the better is the chance of reducing user inconvenience. Such a system of maintenance is highly desirable.

Early in the 1970s, it was realized that radar, developed in the 1960s under contract with the U.S. Army to detect nonmetallic mines, might be modified for concrete evaluation and void detection. In its currently modified form, it is referred to as concrete inspection radar (CIR).

This paper deals with the theoretical concepts that form the basis for currently successful operation of CIR. An analysis is made of the synthesization of the received wave shape as well as a determination of the energy levels reflected at the various interfaces, such as air and concrete or concrete and base material. In addition, determination of space signals between two 15-cm (6-in) concrete blocks is demonstrated.

It should be noted that the word "voids" is used in this paper for illustrative purposes, and in the case of concrete it generally refers to small separations, cracks, or microcracks that determine the condition or serviceability of concrete.

OPERATING PRINCIPLES OF HIGH-RESOLUTION RADAR

Materials either man-made or occurring in nature are conveniently classified as metal or dielectric from an electromagnetic viewpoint. Metallic substances are generally good conductors, both electrical and thermal, whereas dielectric substances are poor conductors. Radio frequency (RF) waves are capable of penetrating and propagating through dielectric materials and tend to be almost totally reflected from metallic materials. Thus, an RF wave from a radar transmitter at an airport, for example, propagates through a dielectric medium, the air in this case, strikes a metallic boundary such as the skin of the aircraft, and is reflected back to the radar receiver; the aircraft angle and distance can then be identified. Similarly, an electromagnetic radio wave emitted by high-resolution radar into a dielectric material such as a pavement structure will propagate through the material until it intercepts a boundary. A boundary is any discontinuity or differing dielectric, such as air to asphalt, asphalt to concrete, change in concrete, and fractures and separations. At the boundary, a portion of the incident energy will be reflected and a portion will be transmitted through the boundary. These phenomena are governed by well-established physical laws, as illustrated later in this paper. Field application of the principle is discussed in the paper by Cantor and Kneeter elsewhere in this Record.

RADAR WAVEFORMS

A brief explanation of the waveforms generated and transmitted by high-resolution radar will assist in understanding the results and analysis of the interaction of the radar waveform with materials. The radar generates a repetitive pulse, of which a single radar cycle waveform is shown in Figure 1 (waveform 1a). The signal is radiated by the antenna into air and, when received, the return signal looks like waveform 1b. If the radiated waveform happens to intercept a boundary, such as air to concrete or air to metal, the reflected waveform that is received looks generally like waveform 1c. Boundaries between different materials have different reflection coefficients (1), from 0.2 for sand to 1.0 for metal, thus giving different amplitudes for the return echo. The reflection coefficient (ρ) determines the amount of energy returned from the material surface, top, bottom, or internal. The amplitude of the surface echo is indicative of its reflection coefficient, which allows classification of the surface material--i.e., concrete or blacktop. Waveform 1d in Figure 1 is more representative of the actual surface echo when the antenna is 20 cm (8 in) from the surface, the preferred operating distance. The pulling down of the first negative peak is caused by antenna end effect, and the true surface echo or return is measured from the large positive peak and the second negative peak (first negative peak after positive peak).

Subsequent echoes arising from boundaries within the pavement are further separated in time from the antenna end effect, and the shapes of their echoes are not affected by it. Note that measurements made in the laboratory are more susceptible to "multiple time around effects"--i.e., internal "re"-reflections (see waveform 2c in Figure 2)--because the samples under test are not terminated with an infinite thickness of base material, which greatly reduces the multiple time around effect. This can be noted in the laboratory test data but does not affect the analysis or interpretation of the data, since it is later in time and can be ignored or considered as noise.

GRAPHIC DERIVATION BY TIME-DOMAIN ANALYSIS

One of the chief advantages of a high-resolution radar is that it generates a very short pulse in time, approximately 1 ns (10^{-9} s), thereby allowing maximum resolution of boundaries or objects. Although one-half of a pulse width, or 15 cm (6 in) in air and approximately 5.5 cm (2.2 in) in asphalt or concrete, is an apparent theoretical limit of resolution, by taking advantage of the algebraically summed overlapped and time-displaced signal, it is possible to resolve distances down to crack widths.

Figure 1. Radar waveforms.

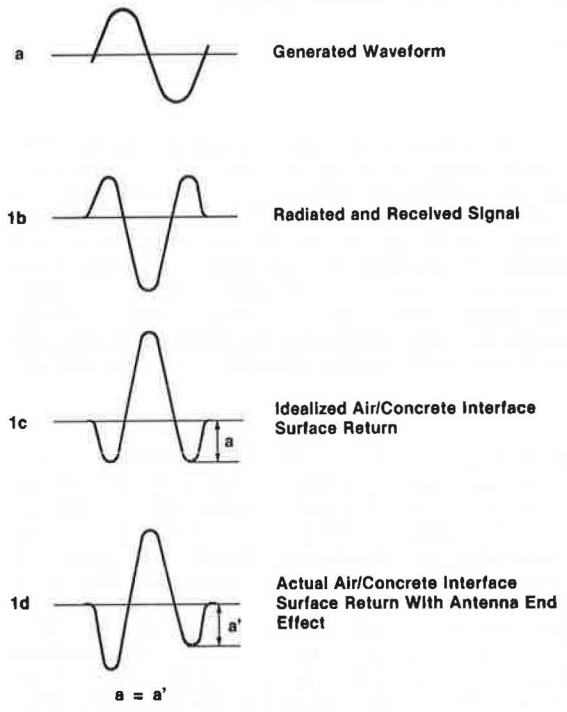

Figure 2. Graphic separation analysis.

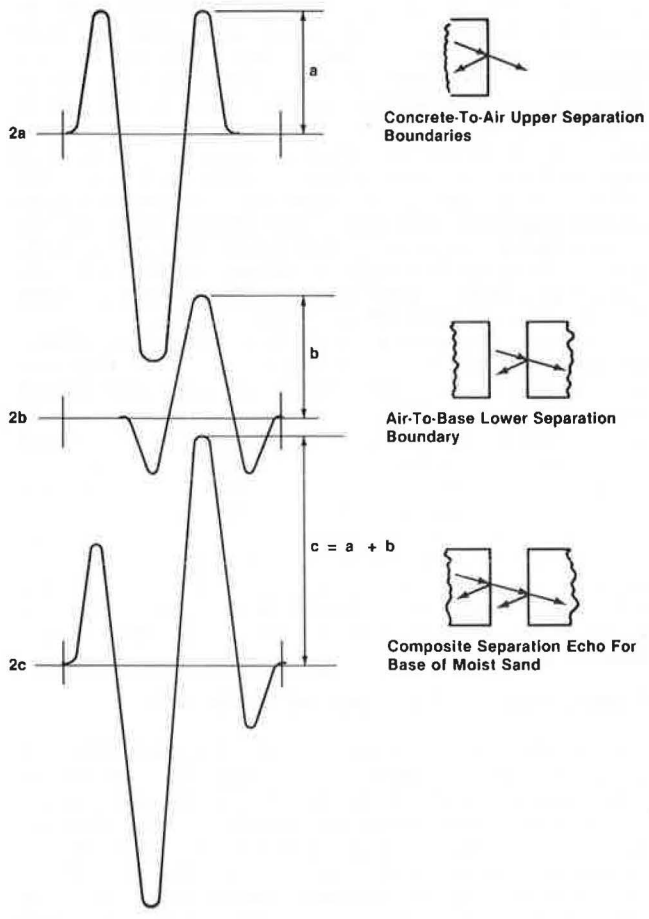

The amplitudes of the signal of the upper and lower void boundaries are derived by means of the reflection and transmission coefficients related to the dielectric materials encountered. In the analysis, it is assumed that the materials are "lossless", homogeneous, and frequency independent for the frequency spectrum of the transmitted waveform. This method can easily accommodate "lossy" materials by adjusting the transmission coefficient for the ray through the slab to include a loss factor. One other assumption is made--that the relative permeability is unity, which is the case for almost all pavement materials.

As an example, for an air space, a typical composite echo can be synthesized from two radar echoes that are less than half a pulse width apart. Given the waveforms shown in Figure 1, and by applying the principles of reflection and transmission of electromagnetic waves when they interact with dielectric substances, one can perform direct time-domain analyses that yield excellent results and correlate well with laboratory and field tests on voids (2). This simplified method of analysis is helpful in understanding the separation echo waveshape as a function of thickness and the dielectric properties of the space boundary. Thickness of void is constant at 6.25 cm (2.5 in).

In Figure 2, waveform 2a is the radar waveshape from the top of a concrete-to-air separation. For the separation chosen, 6.25 cm or about one-third of the radar pulse width, the isolated echo from the bottom boundary of the separation would be as shown in waveform 2b. Note the time displacement phase shift to waveform 2b with respect to waveform 2a. The algebraic sum of the two waveforms is as shown in waveform 2c. This resultant separation waveshape has the following properties: It is larger in amplitude than the other two; its width extends from the beginning of waveshape 2a to the end of waveshape 2b; it has a strong negative peak followed by a strong positive peak. These characteristics are almost always found in a separation echo. Waveform 2a is thus the echo of an infinite separation; that is, there is no bottom boundary echo to sum with it. Waveform 2b represents the reflection from the bottom boundary of the separation whose base material is slightly moist sand.

In Figure 3, waveform 3a shows the graphically derived composite separation echo for a totally dry sand base. This represents a limiting case since, in situ, the base would always have some moisture content. Observe that the composite echo is slightly smaller, peak to peak, than the previous echo in waveform 2c. However, the waveshape is still similar--negative and then positive major peaks; the first small positive peak is larger than the last small negative, and the complete echo waveform still has the same width.

Waveform 3b in Figure 3 is for two concrete slabs. This represents a pavement delamination if the separation is allowed to become very small. As the void approaches 0 cm, the echo from the upper and lower boundaries would cancel out because of phase relationship and spacing. Note that the peak-to-peak amplitude of waveform 3b is larger than that of waveforms 2c and 3a because the bottom reflection is stronger. The waveshape is first negative going, in its major peak, and this is then followed by a positive going major peak. The small leading and trailing positive and negative waveform components are almost equal. This case may also be representative of separations (voids) beneath pavements when the base material is crushed stone and sand.

If the bottom boundary of the separation is water saturated, or water, then the composite waveform would be like waveform 3c. The peak-to-peak ampli-

tude is much greater, about 1.5 times that of dry sand. However, the pulse width is still the same since it is determined solely by the separation distance. Note that the small negative trailing waveform is now larger than the small positive leading waveform; the major waveform peaks are still first negative and then positive, characteristic of separations.

Figure 3. Graphic separation analysis: base material variation.

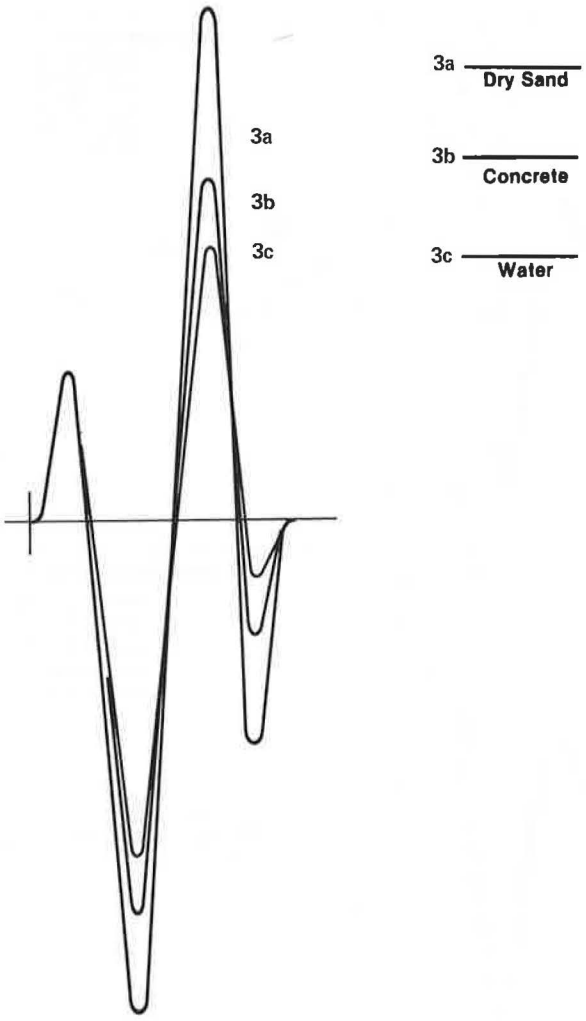

Although this technique has been illustrated for a single separation, it can be used directly for other distances by changing the time displacement between the top and bottom echoes.

For a given pavement thickness, when no separation is present beneath it, an estimate can be made of the material property of the base. The radar data show the time delay between the surface and the boundary echoes. They also show the ratio of the surface to boundary echo amplitudes that permits this determination.

SIGNAL MODIFICATION BY SPATIAL CHANGE

Two 0.9-m-square (3-ft-square) concrete slabs, both 15 cm (6 in) thick, were moved from 0 to 30 cm (0-12 in) apart, one behind the other, and the radar antenna was positioned perpendicular to the 0.9-m (3-ft) face. The radar return waveforms are shown for the various distances in Figures 4-7.

In Figure 4, the radar separation echoes are shown superimposed for 0-, 6-, 12-, 18-, and 25-mm (0-, 0.25-, 0.5-, 0.75-, and 1-in) spacings. These waveforms have features identical to those of the graphically derived waveforms 2c through 3b shown earlier in Figures 2 and 3, especially waveform 3b, since it was derived for two concrete slabs. The echoes all start at the same point in time. There is a leading edge minor peak followed by the leading major negative peak, the characteristic of a void, and this is then followed by a major positive peak and then by a trailing minor negative peak. As the separation is increased, the pulse width is increased, as shown by the slope in the positive and negative peaks.

Figure 5 very clearly shows the point in time at which the composite separation echoes start and the point at which the internal "re"-reflections occur. Figure 6 shows the difference in ending for the various echoes from 75 to 175 mm (3-7 in) and broadening of the waveform. Figure 7 shows the splitting of the waveform at 200-mm (8-in) separation, which resolves the boundary closest to the antenna from the boundary farthest from the antenna. In Figure 8, the echo waveform further splits as the separation goes from 250 mm to 300 mm (10-12 in).

The data demonstrate signal change as the separation increases. The first echoes arising from the bottom of the first 15-cm (6-in) block are all in phase due to the fixed thickness of the slab. The echoes from the bottom boundary, the top of the

Figure 4. Radar separation echoes for two 15-cm blocks: 0- to 25-mm air separation.

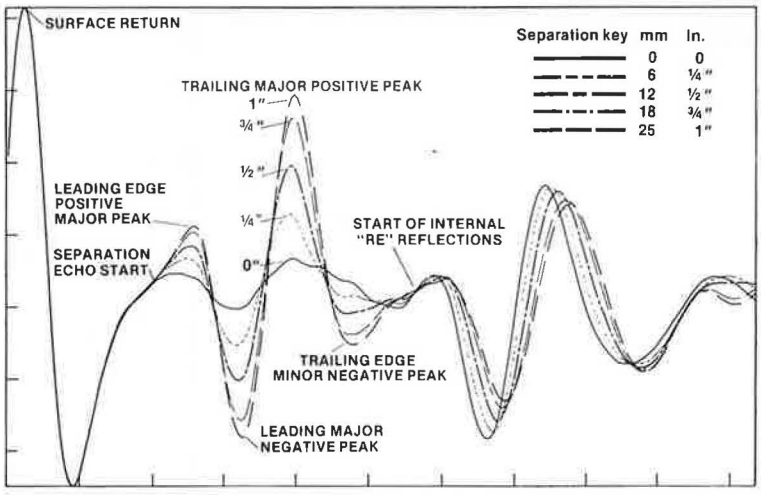

second 15-cm (6-in) block, discretely define the 2.5-cm (1-in) displacements for the 25-, 27.5-, and 30-cm (10-, 11-, and 12-in) spacing between slabs. The "two time around" or internal "re"-reflections of the first echo in the block closest to the radar interfere with the echo from the bottom boundary, which produces a characteristic effect. For an alternative presentation of these data, see the paper by Cantor and Kneeter elsewhere in this Record.

The data shown in Figure 9 were taken at an airport runway and are shown to illustrate the manner in which the laboratory knowledge was carried into field investigations. The two correlated well. Observe the spacing waveforms increasing with depth, which indicates an increasing separation, as was found in the field.

An inspection was made by means of high-resolution radar to determine the location of suspected

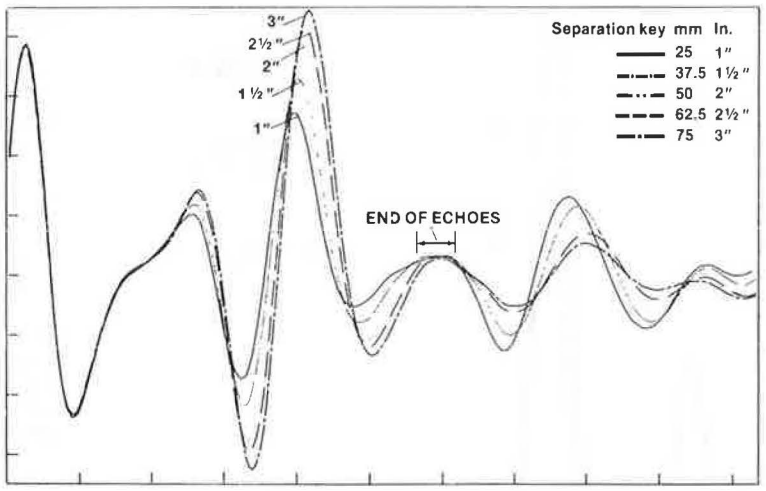

Figure 5. Radar separation echoes for two 15-cm blocks: 25- to 75-mm air separation.

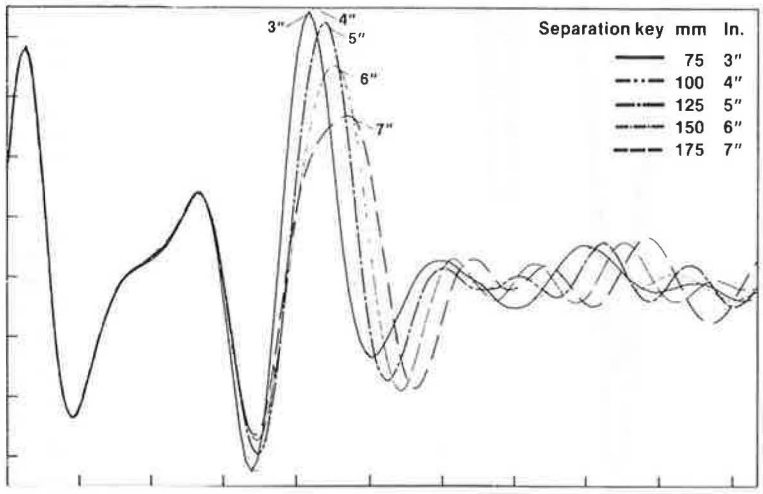

Figure 6. Radar separation echoes for two 15-cm blocks: 75- to 175-mm air separation.

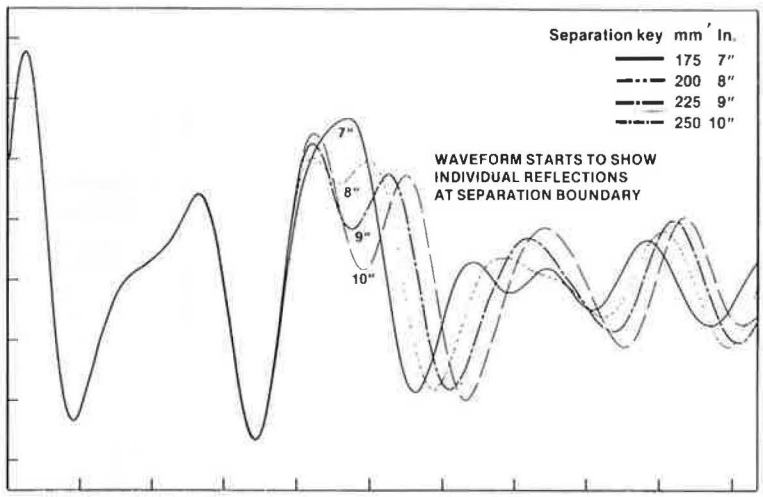

Figure 7. Radar separation echoes for two 15-cm blocks: 175- to 250-mm air separation.

Figure 8. Radar separation echoes for two 15-cm blocks: 250- to 300-mm air separation.

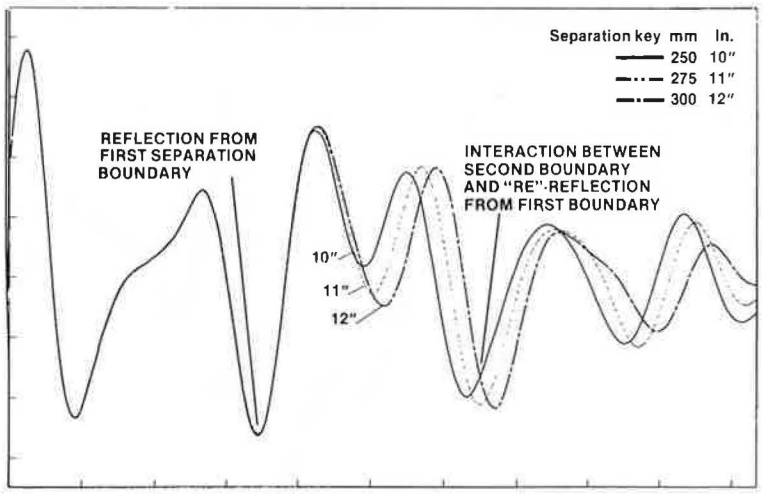

Figure 9. Void under runway.

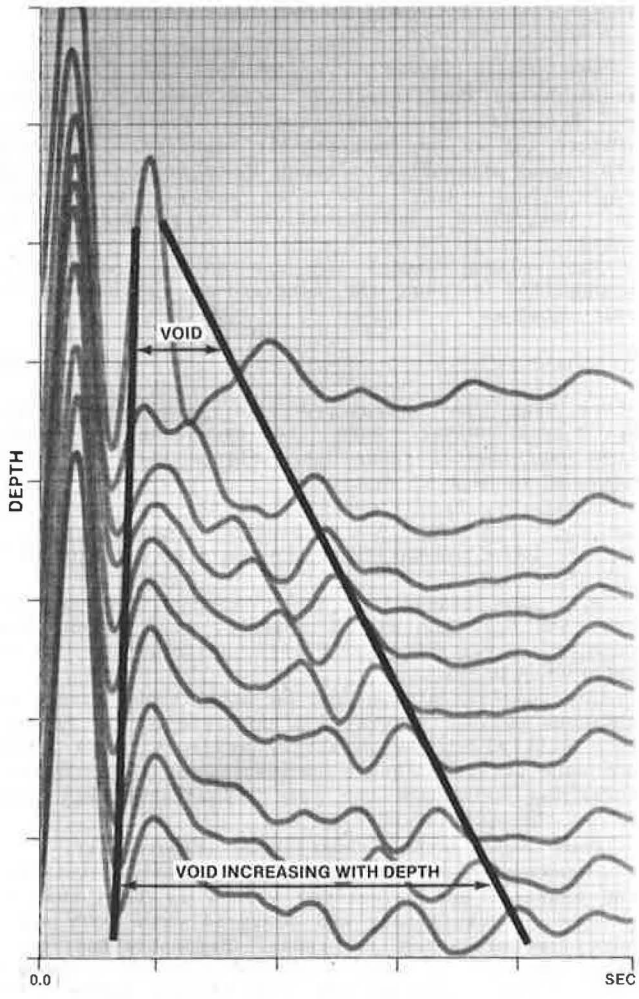

Figure 10. Ray diagram.

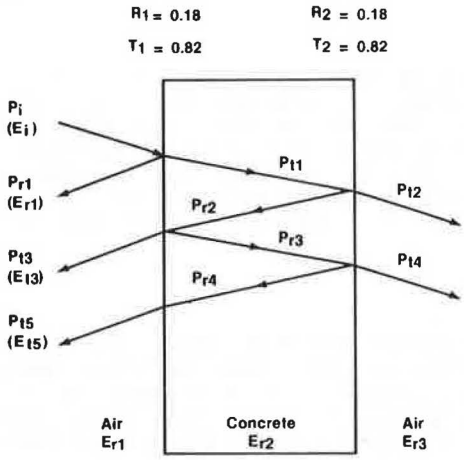

voids. Test borings made at the radar-indicated locations provided positive confirmation. The voids varied in thickness from 3 to 75 mm (0.125-3 in) although, as just reviewed, larger voids can be accommodated (3).

MATHEMATICAL ANALYSIS OF RADAR WAVES

The previously presented experimental data have been evaluated by analytical inductive and deductive methods. Quantitative methods are frequently helpful in explaining and corroborating this type of information. Therefore, a simplified mathematical method for analyzing radar data is discussed here that provides a data base for understanding and transferring knowledge for interpreting various waveforms.

The following assumptions and approximations are made: (a) All surface boundaries are in the plane perpendicular to the radar antenna, and (b) all dielectric materials are considered uniform, homogeneous, and frequency independent.

Figure 10 shows a ray diagram that depicts the transmissions through and reflections from the boundaries of different dielectric materials, air to concrete and concrete to air. Epsilon (ε) is the dielectric constant for the material and determines the time of travel of the electromagnetic wave through the medium, i.e., permittivity. Air has a known dielectric constant (ε_r) of approximately unity, and concrete has a calculated dielectric constant (ε_{r2}) of 6.11 (4). The voltage reflection coefficient (ρ) at the air-to-concrete boundary has also been calculated to be -0.424.

The power of the incident electromagnetic wave must be known to determine boundary reflection magnitude. The incident power, determined experimentally and normalized with respect to free-space (air) impedance, yielded a value of 33.06 units^2.

Figure 11. Experimental verification.

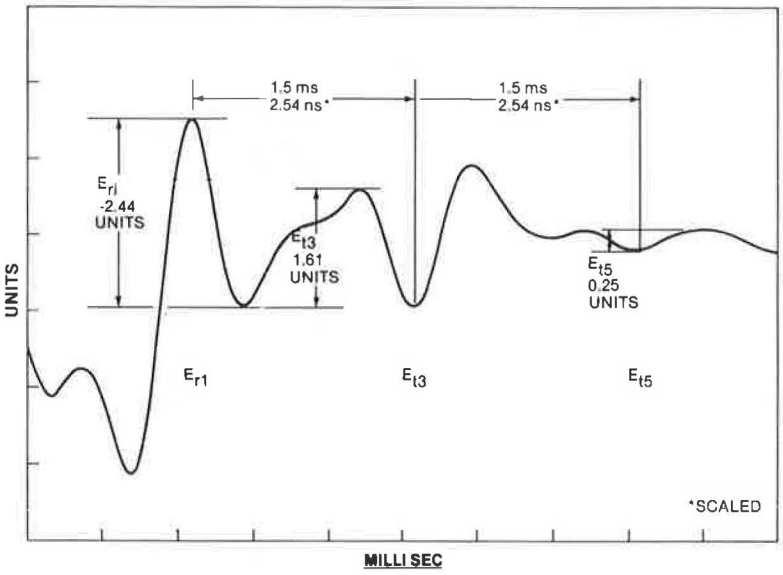

Ideally, the power transmitted (P_i) into a dielectric boundary or interface must equal the power reflected from the boundary (P_r) plus the power transmitted through the boundary (P_t)--i.e., $P_i = P_r + P_t$. At the air-concrete interface shown in Figure 9, the power reflected (P_r) can be solved if R, the power reflection coefficient, is known.

$$R_{n,n+1} = (\rho n, n+1)^2 \quad (1)$$

where n is the current medium and n+1 is the medium to be next penetrated. The voltage reflection coefficient ($\rho_{air/concrete}$) was calculated to be -0.424. $R_{air/concrete} = 0.18$. For this, the power transmission coefficient (T) can be determined:

$$T_{n,n+1} = 1 - R_{n,n+1} \quad (2)$$

$T_{air/concrete} = 0.82$.

The power P_{r1} reflected at the air-concrete boundary (Figure 9) can now be calculated: $P_{ri} = R_1 P_i = 5.95$ units^2.

The voltage signal E_{r1} due to the power P_{r1} reflected is determined to be and is calculated as

$$E_{r1} = (P_{r1})^{1/2} \quad (3)$$

where P_{r1} is normalized with respect to air impedance. The negative sign corresponds to a voltage polarity inversion. Thus, $E_{r1} = -2.44$ units. From experimental data (Figure 2), E_{r1} was measured at -2.44 units.

The magnitude of P_{t1}, transmitted power, can be calculated from the relation, $P_{t1} = T_1 P_i = 27.11$ units^2.

The signal attenuation for this concrete was calculated to be -0.154 dB/in of concrete from the flat plate experiment. Therefore, 15 cm (6 in) of concrete attenuation (A) is -0.924 dB for a power ratio of 0.806 and a signal decrease of about 20 percent. P_{t1} (Figure 10), at the concrete-air boundary, after traversing 15 cm of concrete, will then be $P_{t1} = T_1 P_i A = 21.85$ units^2.

Next, calculate P_{r2}, the power reflected back from the concrete-air boundary. It can be shown that the voltage reflection coefficient at the concrete-air interface will be the negative of that at the air-concrete interface: $\rho n, n+1 = -\rho n+1, n$.

The power reflection coefficient R_2 and power transmission coefficient T_2 will remain the same as R_1 and T_1, respectively. Therefore, P_{r2} (Figure 10) at the concrete-air boundary, including the signal attenuation through 15 cm of concrete, is $P_{r2} = R_2 P_{t1} A = 3.17$ units^2. P_{t3} can now be determined analytically: $P_{t3} = T_1 P_{r2} = 2.6$ units^2.

The voltage signal E_{t3} due to the power P_{t3} transmitted through the concrete-air interface is calculated as

$$E_{t3} = (P_{t3})^{1/2} \quad (4)$$

where P_{t3} is normalized for air impedance: $E_{t3} = 1.61$ units. Note the excellent agreement from experimental radar data (Figure 11): E_{t3} was measured to be 1.63 units.

Similarly, P_{r3} (Figure 10) at the back boundary is $P_{r3} = P_{r2} \cdot R_1 \cdot A = 0.46$ units^2. Likewise, P_{r4} at the front boundary is $P_{r4} = P_{r3} \cdot R_2 \cdot A = 0.0667$ units^2.

P_{t5}, the transmitted power through the boundary, and E_{t5}, the signal voltage, can now be determined: $P_{t5} = P_{r4} T_1 = 0.0547$ units^2, and $E_{t5} = (P_{t5})^{1/2} = 0.234$.

The polarity of E_{t5} can be established since an incident voltage wave from a concrete-to-air interface will always be partially reflected back with the same polarity as the incident wave (5). Therefore, E_{t5} will have the same polarity as E_{t3} and E_i but the opposite of E_{r1}.

From experimental radar data (Figure 11), E_{t5} was measured to be 0.25 unit. The deviation between the measured and calculated values is less than 6 percent. Thus, theory and measured data both support the abilities of radar, demonstrating that radar data can be analyzed through simplified mathematical means with results that closely agree with the experimental. Although we have taken a simplified example for illustrative purposes, the method of data analysis outlined here can be extended to a variety of more complicated cases.

CONCLUSIONS AND RECOMMENDATIONS

Based on data developed in this paper, which consist of examination of waveforms, graphic evaluations, mathematical analysis, and laboratory and field

experiments, it can be concluded that CIR is an appropriate technology for evaluating the condition of concrete up to 75 cm (30 in) in depth by differentiating between serviceable concrete and deteriorated concrete, which consists of delaminations, deteriorations, microcracks, and cracks up to and including small voids. This is further supported by the field experiences described in the paper by Cantor and Kneeter elsewhere in this Record.

The following recommendations are made:

1. Theoretical analyses followed by field tests have successfully demonstrated the ability of radar to detect changes in materials and locate where these changes occur. It is therefore recommended that the system be enhanced for field operations.
2. It is further recommended, as considered in the paper by Cantor and Kneeter in this Record, that the CIR be made completely automatic, including signal processing and data handling, so that the radar system can be used as a maintenance management tool to provide greater cost benefit for roadway repair with minimum inconvenience to the riding public.

ACKNOWLEDGMENT

The contents of this paper reflect our views and do not necessarily reflect the views of Penetrader Corporation or the Port Authority of New York and New Jersey.

REFERENCES

1. A.R. Von Hippel. Dielectrics and Waves. M.I.T. Press, Boston, MA, 1966.
2. J.A. Stratton. Electro-Magnetic Theory. McGraw-Hill, New York, 1941.
3. A. Alongi. Model PS-24 Penetradar and Technical Notes PTN-001 and 002. Penetradar Corp., Niagara Falls, NY, 1981.
4. A.G. Kandoian and others. Reference Data for Radio Engineers, 4th ed. International Telephone and Telegraph, New York, 1956.
5. L.F. Woodruff. Electric Power Transmission. Wiley, New York, 1946.

Publication of this paper sponsored by Committee on Performance of Concrete.

Radar as Applied to Evaluation of Bridge Decks

T.R. CANTOR AND C.P. KNEETER

Approximately 90 percent reliability has been achieved in nondestructively identifying good and deteriorated concrete on a bridge deck, based on experimental research in the laboratory and field. The ability of concrete inspection radar to function reliably and repeatably in identifying the condition of concrete is established. Ability to detect voids is commented on. Present signal processing, data analysis, and interpretation via cluster analysis constitute a lengthy manual operation. However, with computer-assisted data automation, the system should be a viable field instrument operable by a technician.

Concrete inspection radar (CIR) has demonstrated its capability to reliably perform in the field as a nondestructive evaluation (NDE) tool for determining the condition of concrete (1-3). CIR has identified good and distressed concrete with 90 percent confidence (4).

Physical laboratory studies performed to calibrate the equipment and understand physical parameters include detection of voids, effects of steel, multiple material layers, antenna direction and angularity, water, temperature, and edge (5).

Included in the laboratory analytical studies were various signal-processing techniques, among which were topographic displays, photographic superimposition, graphic signature identification techniques, and mathematical models (3). Of the mathematical models, cluster analysis has resulted in the most reliable and least time-consuming classification of concrete (6).

The field operations were conducted on several major structures. Among the factors studied were reproducibility, influence of reinforcing steel, and varying void depths. The field investigation culminated in the physical verification of the concrete condition as interpreted by the analysis of the radar data (4).

To verify the radar-predicted conditions of distressed and good concrete, a physical evaluation was undertaken by field drilling. Depth of drilling was ranked and statistically analyzed and led to a physically verified confidence of 90 percent (4).

Automation of the present manual data processing by direct computer operation will make CIR a field system operable by a technician and capable of identifying and differentiating good and distressed concrete.

INTRODUCTION TO CIR

Starting at pouring of concrete, every structure in the infrastructure begins to deteriorate with time. The first evidence of this, generally, is surface cracking. With roads, riding surfaces may hide these defects until, in many cases, serious problems exist. Once water enters the cracks, deterioration increases more rapidly, because of either freeze-thaw stresses or rebar corrosion. The earlier the fault or impending fault can be detected, the less costly and easier it is to repair, with minimum inconvenience to the users of the facility (7).

The search to obtain an NDE tool capable of detecting deterioration as early as possible led Port Authority of New York and New Jersey (PANYNJ) Engineering Research and Development engineers down many paths, the most successful of which has been CIR (8).

Interest in radar as a possible NDE tool stemmed from radar development work by Calspan Corporation (9) in the mid-1960s, under U.S. Army contract, to detect buried nonmetallic mines. Subsequent CIR modifications allowed it to be used in the early 1970s to detect voids under pavements (1,2). Follow-up studies of this radar development work by PANYNJ Engineering Research and Development staff in 1974 led to the program of radar NDE testing and development described in this paper (10).

Engineering Research and Development has developed techniques for using CIR to experimentally evaluate concrete pavement conditions. Radar NDEs made in 1977 on bridge-deck pavement were substantially confirmed by core samples (10). Since 1977, the radar NDE effort has been primarily concerned with acquiring equipment, developing equipment reliability, accumulating radar laboratory and field experience, and experimenting with techniques to speed up and eventually automate the signal analysis process. There now exists a high degree of confidence (90 percent) in the ability of CIR to function reliably in the field and to distinguish good from defective concrete in pavement traverses at speeds from 12.9 to 16.1 km/h (8-10 mph).

The signal analysis and interpretation process is not yet automated, although progress is being made. Currently, signal analysis is a lengthy procedure that requires fairly extensive use of research skills.

It is estimated that millions of dollars per year in benefits may be achieved by extensive use of radar for NDE (11). These potential benefits result from greater certainty in maintenance scheduling, minimizing emergency repairs, detecting developing weaknesses, effecting repairs before failure, and more exact determination by radar survey of the amount of work to be performed prior to preparing contracts or inviting bids. It is recommended that the radar NDE program continue to speed up the analysis and interpretation of the radar signals. The training of technicians to perform radar NDE will be the final step.

EXPERIMENTAL DATA

The following section considers a combination of laboratory experiments and field diagnostic tests that, along with data processing and analysis, were undertaken to reach the present state of 90 percent confidence in identifying the condition of concrete by use of CIR.

Laboratory

The laboratory operations were undertaken to understand how radar interacted with concrete to calibrate radar signals or signatures. Among the wide range of studies conducted were the following: resolution; multiple reflections; stability; repeatability; concrete block studies of various thicknesses, singly and in combination; surface location by metal target; separation determination; modeling of roadway, bridge decks, etc.; air standardization studies; equipment compatibility; antenna angularity and directionality; rebar, water, and boundary effects; effect of temperature; and low power supply voltage. Space limitations allow only the following study examples to be developed here.

In one major study, two 15.2-cm (6-in) thick concrete blocks were positioned vertically in front of the CIR, with the rear block on rollers so that it could be moved to create a separation that could be varied from 0 to 30.5 cm (0-12 in) (see Figure 1). This work was the key to evaluating field void data. This study is described and analyzed in considerable detail in the paper by Alongi and others elsewhere in this Record.

Another calibration study was the use of several concrete slabs of different thicknesses to determine the appearance and reflections caused by the interface (see Figure 2). Trace modifications due to rebar inclusion proved to be negligible (12,13).

Field

The field operations were undertaken, first, to prove feasibility and, second, to quantify the ability of CIR to assess concrete condition and locate voids.

Figure 1. Variable separation of two 6-in-thick concrete blocks.

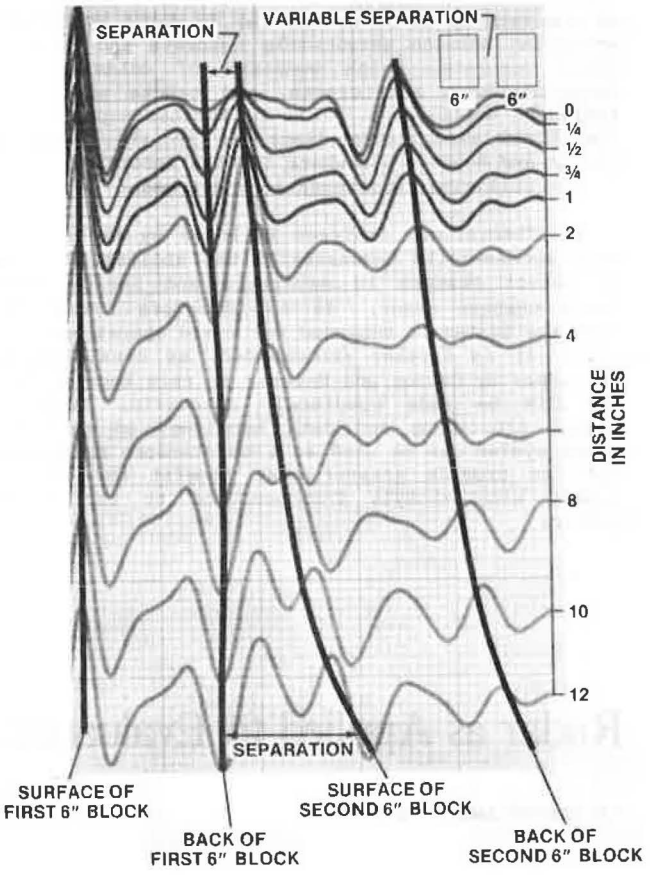

Several field studies follow: A 3-mile, four-lane, cantilevered truss bridge was the first structure to be field surveyed from a moving van at a speed of 12.9-16.1 km/h (8-10 mph) (see Figure 3) (10). At some locations, data were also taken with the vehicle stationary. The stationary data, when compared with data taken at the same location four years later, showed excellent repeatability (see Figure 4) (4) and the possibility of the onset of aging.

At the same speed, two wheel tracks in each of the four lanes of a 1.6-km (1-mile) long bridge were surveyed in about 3 h. This provided a trace for every 7.6 cm (3 in) of bridge deck.

In earlier work, trace superimposition (see Figure 5) was used to select some 60 locations to core. Where the traces overlaid each other, the concrete was found to be good--i.e., in good condition. Where there was poor superimposition of the traces, the quality of the concrete was poor--i.e., distressed. The excellent correlation achieved between CIR predictions and actual physical condition verified radar feasibility (10).

In a recent study covering 213 m (700 ft) of bridge deck, readings taken every 2.1 m (7 ft) accumulated more than 100 samples. The data were analyzed in the laboratory, and condition prediction was determined by cluster analysis (4). Physical verification of conditions was established by what is essentially a wearing test. The test consisted of measuring the depth drilled into the concrete by using a new 1.6-cm (0.625-in) carbide drill driven

at fixed speed and with a fixed force for 2 min (see Figure 6). The data displayed in Figure 7 show a correlation between radar and drilling (wearing) of 90 percent, which establishes the ability of CIR to determine concrete condition.

A subsurface void or washout was suspected to exist under a taxiway (1-4, 13). The topographic presentation of the radar data delineating the void is shown in Figure 9 of the paper by Alongi and others elsewhere in this Record.

The signature of a tunnel roadway was considerably different from that of a bridge deck. Each had a distinctive signature because of differences in support steel and physical design. It was demonstrated both in the field and the laboratory that these signature differences caused no difficulties in data analysis. This was also true for rebars spaced over a large area. Once the signature is established, the analysis is only negligibly affected.

Data Analysis and Processing

Perhaps the most challenging feature of converting theoretical CIR concepts into an operating NDE system was the data analysis and processing. This derives from two considerations: (a) the complexity of data analysis and (b) the huge quantity of data to be processed. For example, surveying pavement at 12.9-16.1 km/h (8-10 mph) provided a trace for every 7.6 cm (3 in) of linear roadway in a 33-cm (13-in) wide swath. For one study of a 1.6-km (1-mile) long, four-lane bridge surveyed at the above speed, all eight wheel tracks were surveyed in 3 h of field operation, 975 m (3200 reel ft) of magnetic tape was recorded, and more than 80 Polaroid oscilloscope photographs of unique features were generated.

Figure 2. Trace identification: model of 4-in overlay on 6-in base.

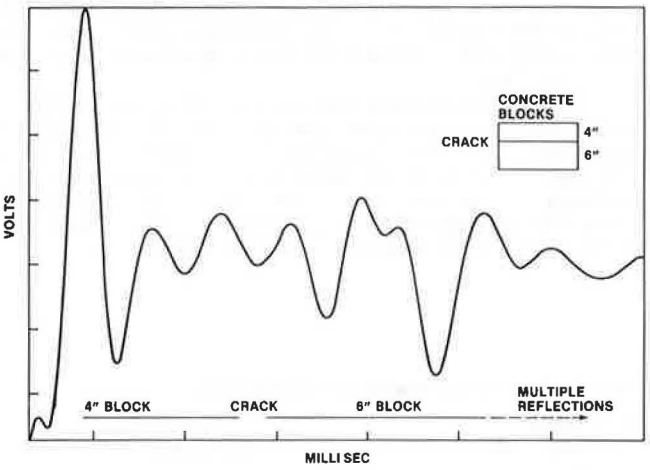

Figure 3. Van-mounted radar system.

Figure 4. Repeatability of data.

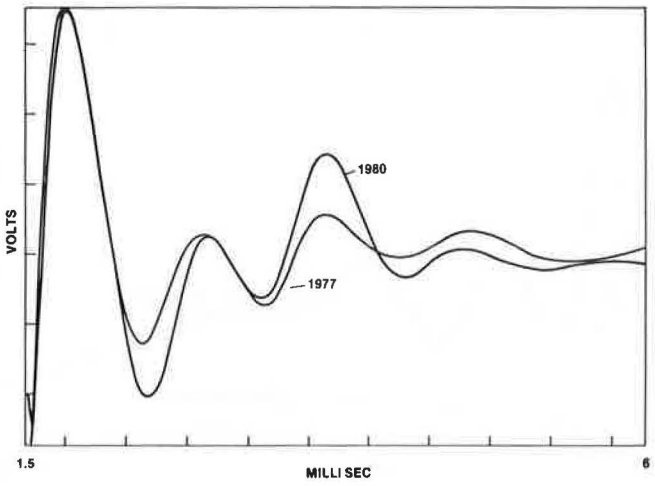

Figure 5. Radar conformation: (top) steady superimposable radar traces and good core and (bottom) erratic nonsuperimposable radar traces and poor core.

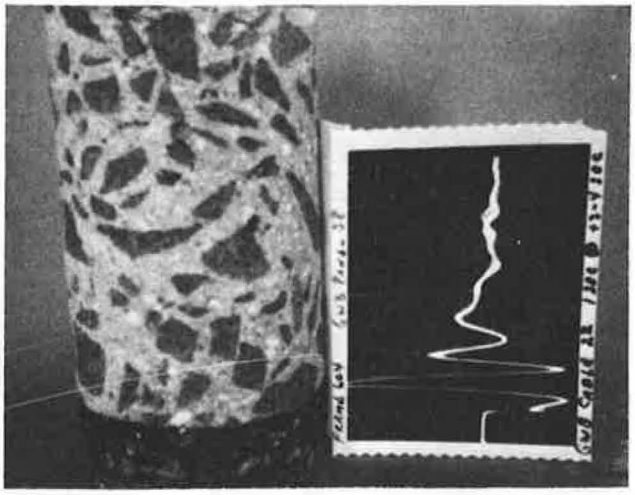

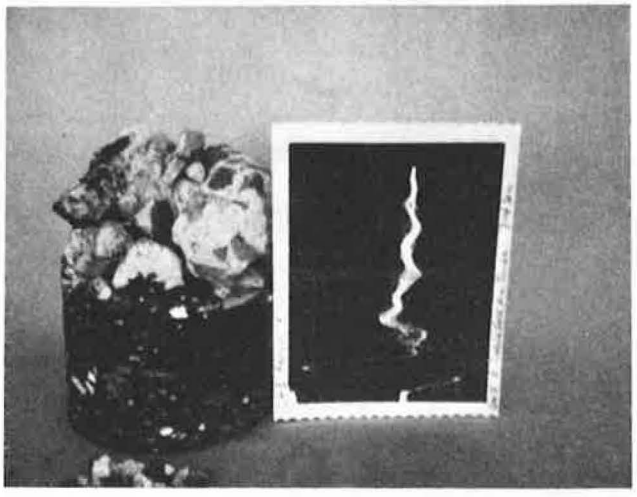

At least four major approaches have been tried: (a) topographic display, (b) photographic superimposition, (c) graphic signature identification techniques, and (d) mathematical modeling. Cluster analysis, a mathematical modeling technique, has proved to be most successful. A test of 213 m (700 ft) of bridge deck gave a 90 percent correlation between radar evaluation predictions of condition and actual field physical conditions.

Cluster Analysis

The field data are recorded in analog form on magnetic tape. In the laboratory, the analog data are converted to digital and "x-y" plotted. Manually derived information from the plot is fed to a computer and, via suitable programming, the traces are mathematically compared and placed in clusters of like morphology. The clustering results in three general groups of traces: good concrete, distressed concrete, and an intermediate, not clearly classified, group with possibly a limited number of outliers.

By using cluster analysis of a series of 100 traces from a bridge deck, radar predicted three groups: 72 percent good, 11 percent distressed, and 17 percent not clearly defined but generally lying between the other two groups. Physical verification was made by drilling 1.6-cm (0.625-in) holes into the deck at 21 locations. Ten of these locations were anticipated as distressed by CIR; 9, or 90 percent, of the drilled holes correlated. Eleven of the locations anticipated as good by CIR were also drilled and 10, or 91 percent, were judged good (Figure 7).

The range of concrete varied from very good to quite poor with no sharp break. This condition would normally be anticipated on a working maturing structure and is clearly and significantly shown in the drilling-depth distribution (Figure 7).

A 4.6-cm (1.8-in) depth was considered the dividing line; greater depth was considered distressed and lesser depth good (Figure 7). Only one good CIR signal gave a greater depth--5 cm (2 in)--and none were deeper than this. Conversely, there were no distressed CIR readings at holes shallower than 3.4 cm (1.75 in).

Further correlation was derived from the theoretical concept that good concrete should exhibit a smoother curve than distressed concrete (8). When 10 curves of good concrete were averaged, the resulting curve was quite smooth. This contrasted with the average of 10 distressed curves, which resulted in a more peaked curve (see Figure 8).

Figure 6. Standardizing drill rig.

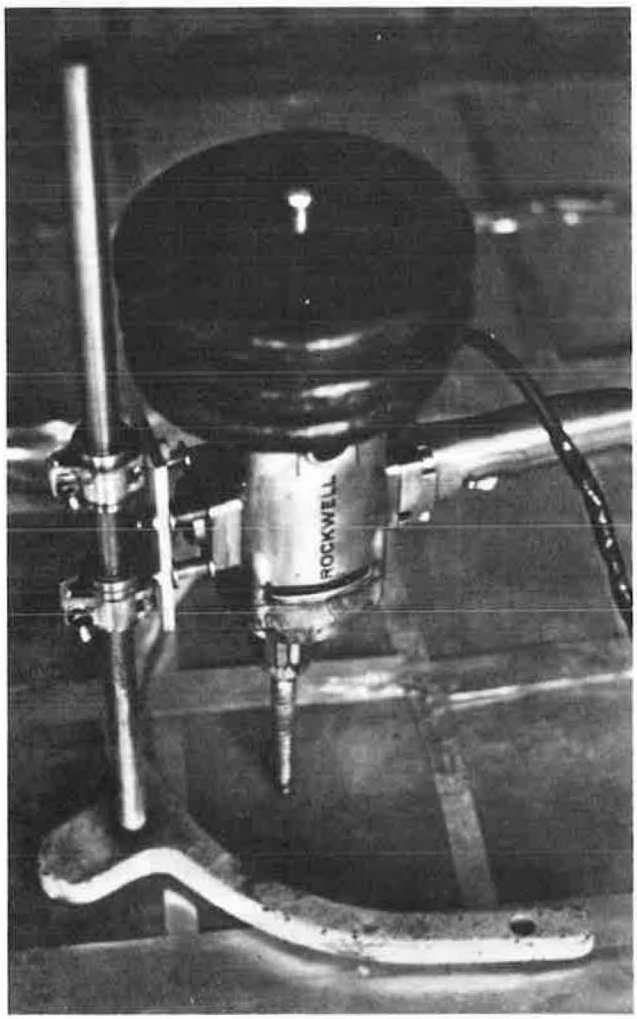

Figure 7. Radar field verification: cluster predictions.

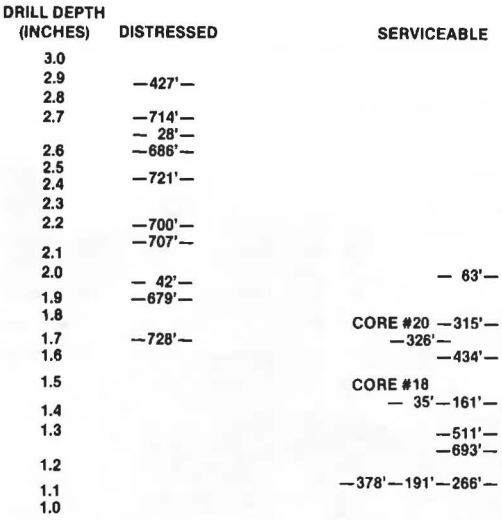

Figure 8. Generalized radar traces.

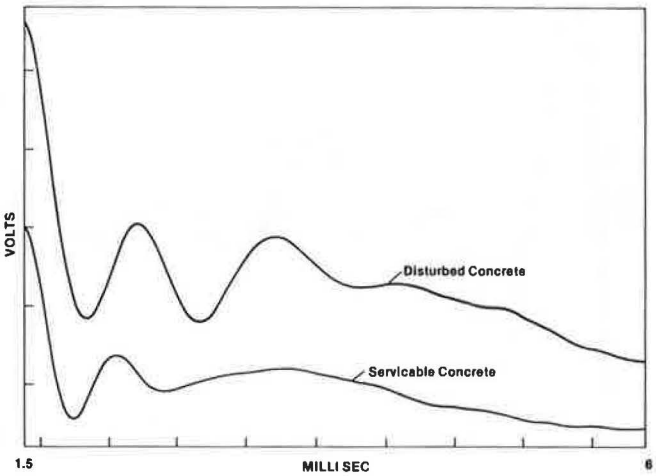

Figure 9. Topographic traces from moving vehicle.

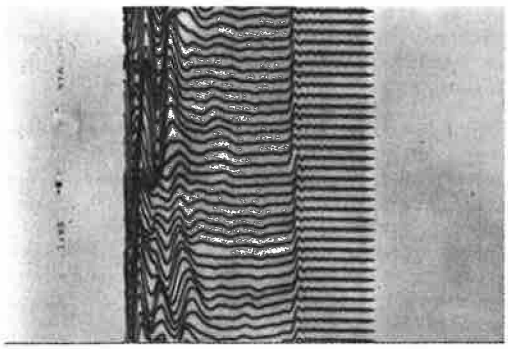

SERVICEABLE CONCRETE

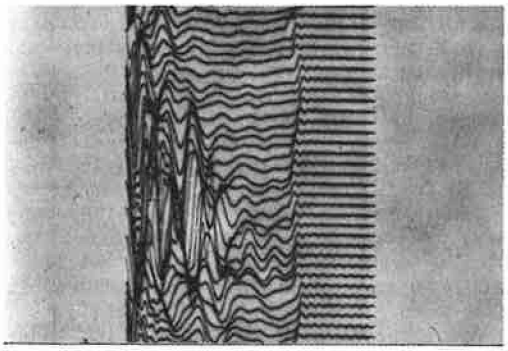

DISTURBED CONCRETE

Figure 10. System block diagram.

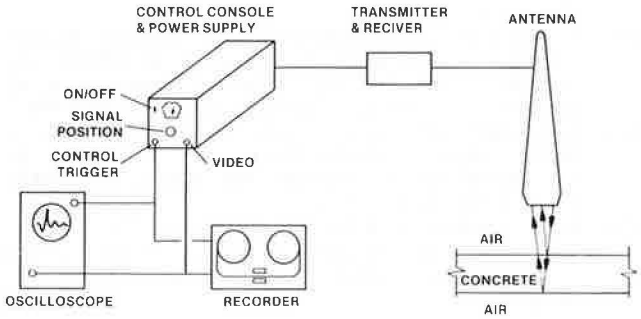

Topographic Display

The topographic display procedure (10) consisted of displaying the original analog data recorded on magnetic tape on an oscilloscope, photographing the display with a synchronized shutterless motion picture camera, and then projecting the film on a viewing screen. The results are shown in Figure 9. Disturbance can be easily recognized by eye, but the procedure is extremely tedious and time consuming and causes rapid operator fatigue. The method, although somewhat functional, cannot really be regarded as satisfactory.

Photographic Superimposition

In photographic superimposition (10) the shutter of a Polaroid camera is left open for 10 s as the traces are displayed on an oscilloscope and recorded as a multiple exposure. When the traces superimpose on each other, the concrete is good. When superimposition is poor, wavy, or noisy, the concrete is distressed (Figure 5). This technique was used effectively in locating distressed and good areas on a bridge deck and was verified by coring. Although it is a proven procedure, it is extremely slow.

Graphic Signature Identification Techniques

In theory, it is possible to determine the condition of the concrete at any location by examining the radar trace. In practice, this is difficult, because of both the complexity of the trace and the time required to dissect the trace and understand its component parts. The method is generally relegated to the laboratory to be used for calibrating or other special conditions.

EQUIPMENT AND OPERATING THEORY

Penetradar Model PS-24 (8) is a lightweight, low-power, all-solid-state, high-resolution, nondestructive, ground-penetrating radar device. It is mobile and can be mounted in a light truck or van (Figure 3). The monostatic antenna (for transmitting and receiving) illuminates a 0.09-m^2 (1-ft^2) area at 20 cm (8 in) above the surface for inspecting pavements at speeds up to 19.3-25.7 km/h (12-15 mph).

The radar transmitter couples short bursts of low-power radio frequency (RF) energy through the perpendicularly oriented antenna into the pavement or material under investigation (5). Each burst or pulse is about 1 ns (one-billionth of a second) in duration and occurs more than 1 million times per second. A portion of the RF energy is reflected whenever there is a change or discontinuity in the propagation medium--for example, air to asphalt to concrete to soil, etc. The RF reflection, or radar echo, is picked up by the antenna, connected to the receiver, and processed for display and recording (see Figure 10).

The receiver measures the time for the transmitted pulse to travel to a target discontinuity and for the echo to return. In free air the pulse will travel out 15.2 cm (6 in) and return in 1 ns, whereas in concrete the velocity of propagation is reduced so that the corresponding distance is about 5.7 cm (2.25 in) in 1 ns, depending on the quality and condition of the concrete or other material under investigation.

As the pulse travels in air (less dense material) to concrete (more dense material), the trace goes sharply positive, then negative at the interface, whereas the polarity swing is reversed as the pulse travels from concrete (more dense) to air (less dense), the typical void condition. In practice, these interface changes can be difficult to resolve because of reflections and interference patterns caused by multiple reflections.

The radar echo from a pavement surface (first return) is generally much stronger than echoes from beneath the surface (as shown in Figure 9 of the paper by Alongi and others in this Record). Theoretically, the depth of a discontinuity is derived from the time separation between the surface and fault echoes. Examples of fault-echo sources from within the pavement are delamination, voids, and fracturing. The last distinct echo is generally the reflection from the bottom boundary of the pavement. Usually, the return signal from poor concrete is more complex and may have higher amplitudes and more peaks than the return signal from good concrete (Figure 2).

For a more thorough treatment of the theory of radar and the principles involved, the reader is referred to the paper by Alongi and others in this Record.

In addition to the radar unit, the following minimal support equipment is required (Figure 10): a three-channel, reel-to-reel, high-quality magnetic tape recorder and an oscilloscope.

The radar generates data at a rate of approximately 1800 traces/min, which overloads the manual method of analysis and thus limits the value of the system. Therefore, the final configuration will consist of a high-speed analog-to-digital signal converter and a dedicated computer of sufficient capacity to process the data by using cluster analysis techniques. This will increase data analysis capacity; reduce analysis time, perhaps, to real-time conditions; increase the reliability of the analysis; and enable the fringe-area uncertainties to be resolved or reduced.

CONCLUSIONS

The following conclusions can be made based on laboratory and field studies of radar as an NDE tool for determining the condition of concrete:

1. Radar survey equipment has proved to be a functional and reliable field device capable of determining the condition of concrete pavements and structures.
2. A 90 percent correlation has been obtained between radar evaluation predictions and pavement physical condition.
3. Present analysis and interpretation of radar data require a research engineer and manual processing and constitute a time-consuming procedure. By developing a computerized, automated system of data interpretation, manual data processing will be eliminated. Time will be saved and real-time operation may be achieved.
4. Addition of automated-data-processing equipment will make radar a practical NDE tool for use by field technicians.
5. When the condition of concrete is slightly less than good but not appreciably deteriorated, radar comparisons with cluster analysis generally indicate an uncertain transition zone, which suggests that the material may be starting to show distress, thus "flagging" the locations for further observation and scheduling of least-cost maintenance.

RECOMMENDATIONS

The material presented in this paper has demonstrated the ability of CIR to determine the condition of concrete. Therefore, it is urged that further development of radar data-processing signal analysis and interpretation techniques to reduce the skill level and time required to make pavement condition evaluations be vigorously pursued.

ACKNOWLEDGMENT

We wish to express our thanks to Anthony Alongi of Penetradar Corporation for his invaluable consultation and assistance in planning and developing the project. We also wish to thank Patrick Quinn for his assistance in several phases of the work and various other PANYNJ staff members for help in the field and office.

REFERENCES

1. A.V. Alongi. Radar Examination of Condition of Two Interstate Highway Bridge Decks. Penetradar Corp., Niagara Falls, NY, 1973.
2. A.V. Alongi. Radar Survey of Wheeler Sack Airfield, Fort Drum, New York, to Locate Voids Beneath Runways. Penetradar Corp., Niagara Falls, NY, 1976.
3. R.M. Morey. Coal Thickness Profiling Using Impulse Radar. Geophysical Survey Systems, Hudson, NH, 1978.
4. T.R. Cantor and C.P. Kneeter. Verification of Radar NDE of 700 ft of the GWB. Port Authority of New York and New Jersey, Jersey City, NJ, Engineering R&D Rept. 81-3, May 1981.
5. E. Brookner. Radar Technology. Artech House, Inc., Dedham, MA, 1979.
6. J. Fowler. Short Pulse Radar Signal Processing. Ensco, Inc., Springfield, VA, 1977.
7. M.E. Harr and G.Y. Baladi. Non-Destructive Testing and Evaluation of Flexible Highway Pavements. Purdue Univ., West Lafayette, IN, Joint Highway Research Project C-36-63F, 1977.
8. Model PS-24 Operation and Maintenance Manual. Penetradar Corp., Niagara Falls, NY, 1980.
9. A.V. Alongi. Short Pulse High Resolution Radar for Cadaver Detection. Calspan Corp., Buffalo, NY, 1970.
10. T.R. Cantor and C.P. Kneeter. Radar and Acoustic Emission Applied to Study of Bridge Decks, Suspension Cables, and Masonry Tunnel. TRB, Transportation Research Record 676, 1978, pp. 27-32.
11. G. Baillot. Possibilities of Actual Utilization of Very High Frequencies in Civil Engineering (in French). Central Laboratory of Bridges and Highways, Paris, France, June 1980.
12. J.R. Moore and J.D. Echard. Radar Detection of Voids Under Concrete Highways. Institute of Electrical and Electronics Engineers, New York, Paper 6-80-0131, 1980.
13. W.J. Steinway, J.D. Echard, and C.M. Luke. Locating Voids Beneath Pavement Using Pulsed Electromagnetic Waves. NCHRP, Rept. 237, Nov. 1981.

Publication of this paper sponsored by Committee on Performance of Concrete.

Effects of Concrete Deterioration on Bridge Response

DAVID B. BEAL AND WILLIAM P. CHAMBERLIN

Two reinforced-concrete T-beam bridges, constructed in 1931 with similar cross-section dimensions and properties, now show major differences in the appearance of their concrete. As a result, inspectors have rated one as having "serious deterioration and not functioning as originally designed" and the other as being in "new condition". Bridge engineers are responsible for translating these subjective evaluations into predictions of the structures' load-carrying capacity, but little information is available to permit quantification of the consequences of concrete deterioration on bridge response. The two bridges were instrumented to determine tension reinforcement stress under an equivalent HS-20 truck positioned on the bridge deck. The results showed no difference in behavior attributable to concrete deterioration. Theoretical justification for this result was established by showing the variation in reinforcement stress expected as a function of compressive concrete loss and reduction in concrete strength. In both cases, the magnitude of the resulting stress change was shown to be small and generally less than the measurement accuracy of the electrical resistance strain gages used on the actual bridges. Differences in concrete properties determined from cores taken from the structural decks corresponded with those in the appearance of concrete in the two bridges. Nevertheless, it was concluded that inspectors did not identify those aspects of structural condition of these bridges that have a significant impact on their safe load-carrying capacity. It is suggested that this result is typical of inspections of a majority of reinforced-concrete T-beam bridges.

Federal Highway Administration (FHWA) national bridge inspection standards (1) require that highway bridges be inspected and rated for load-carrying capacity to ensure the public safety. Procedures and guidelines to assist state and local agencies in this task are given in the American Association of State Highway and Transportation Officials Manual for Maintenance Inspection of Bridges (2). In addition, the load-rating engineer will have available a detailed inspection report on the structure, which generally is prepared in accordance with specific standards (3).

For concrete structures, the qualitative information in the inspection report cannot be used directly to establish a load capacity, and it is the structural engineer's job to quantify the consequences of reported deterioration on the capacity of the bridge. Little information is available to guide this quantification, and, as a result, load ratings of reinforced concrete bridges are believed to be unduly conservative.

This paper analytically examines the probable significance of certain types of deterioration and presents experimental data on the response of two reinforced-concrete T-beam bridges to service loads. Specifically examined are the effects on bridge capacity of reduction in concrete strength and loss of section in the compression zone that result from freeze-thaw damage of non-air-entrained concrete and corrosion of steel reinforcement.

BRIDGES EXAMINED

The bridges discussed in this paper are two of five tested to evaluate the practicality of an inexpensive physical test to establish the safe load-carrying capacity of deteriorated structures (4). The conclusion of that work was that this objective was partially unobtainable, for reasons to be discussed.

The structures considered here were selected because of their similar design dimensions and ages and the difference in the inspection ratings of their primary structural members. Both are T-beam structures constructed in 1931. Their cross sections (see Figure 1) differ only in stem depth (bridge 2 is 2 in deeper) and the presence of parapets on bridge 1. In addition, bridge 2 has a 39.5-ft span compared with 37.5 ft for bridge 1, and both support lines are skewed at 22°. Because of these structural differences, measured bridge responses to applied loads were adjusted (as described in a later section of this paper) to permit comparison.

BRIDGE CONDITION

Both bridges were rated visually by state forces as part of a routine biennial inspection (3). On a scale of 1 (potentially hazardous) to 7 (new condition), the primary members of bridge 1 were rated 3 (serious deterioration or not functioning as originally designed) because of severe concrete deterioration (see Figures 2 and 3), particularly in T-beam stems and in the lower extremity of the fascia beams. By contrast, the primary members of bridge 2 were assigned a condition rating of 7 because of their generally sound appearance (see Figures 4 and 5).

The New York rating scale is similar to a 10-point scale suggested by FHWA (5), which is widely used throughout much of the United States. On the FHWA scale, the primary members of bridge 1 would

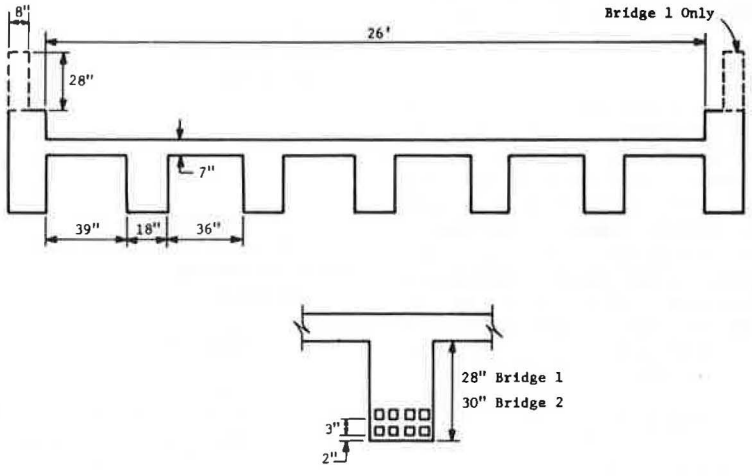

Figure 1. Bridge cross sections.

Figure 2. Bridge 1.

Figure 3. Deterioration of T-beams in bridge 1.

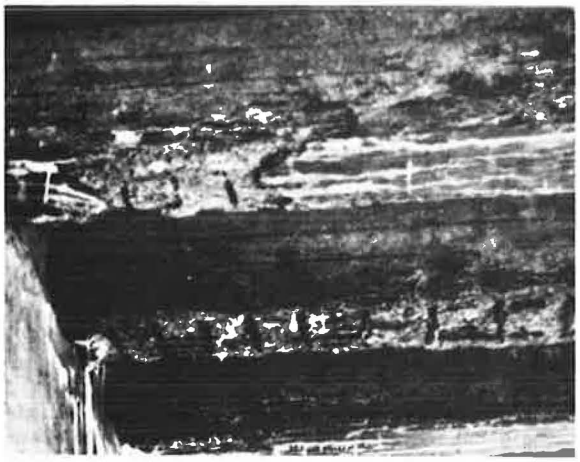

Figure 4. Bridge 2.

Figure 5. Condition of T-beams in bridge 2.

have been rated 4 (minimum adequacy to tolerate present traffic, immediate rehabilitation necessary to keep open).

Because subsequent load tests (described later) resulted in a nearly identical structural response in the two bridges for the same level and configuration of load, in spite of the gross difference in the apparent condition of their primary structural members, a limited study was undertaken to further define the relative condition of their concrete.

Bridge 1

The overall appearance of the concrete in bridge 1 was one of advanced deterioration. Curbs and parapets were badly eroded due to paste damage (Figure 2), and large areas of concrete had spalled from the underside of T-beam stems and fascia beams (Figure 3), exposing rusted steel reinforcement. The vertical faces of all beams exhibited extensive cracking, which generally paralleled their axes. Efflorescence was common. Measurements of sonic pulse velocity through the stems of three girders yielded values in the 1700- to 4400-ft/s range, which indicates concrete with generally low strength and elastic properties.

The deck was covered with a bituminous wearing course and thus was visible only from the underside. No scaling or spalling was evident, but severe cracking and efflorescence were present in many areas. Four pairs of 4-in-diameter cores drilled through the deck (at about one-quarter span) indicated that the 7-in structural deck was highly fractured throughout and that the cement paste was severely deteriorated locally. Otherwise, the concrete was well compacted but not air entrained. The results of the tests on the deck cores were as follows:

Item	Test Result
Structural deck	
Condition	Highly fractured, severe paste deterioration
Air entrainment	Non-air-entrained
Absorption (%)	5.6 (mean of seven values)
Sonic velocity (ft/s)	Not measurable
Compressive strength (psi)	5195 (single value)
Wearing course	
Condition	Severe paste deterioration
Absorption (%)	6.7 (single value)

The only core segment long enough to test in compression (ASTM C39-72) yielded a strength of 5195 psi. Seven core segments tested for absorption (ASTM C642-75, immersion method) yielded a mean

value of 5.6 percent, which is greater than about 80 percent of values measured in cores from other New York bridge decks (6). An earlier concrete wearing surface of undeterminable thickness, probably dating from the bridge's initial construction, was totally disintegrated in all but one of the eight cores. A segment from this single core had an absorption of 6.7 percent.

Bridge 2

By contrast, the concrete in bridge 2 was in excellent condition (Figures 4 and 5). No scaling or spalling was evident on structural elements or on the underside of the deck, and both were free of cracking. Pulse-velocity measurements through the stems of two girders were in the 12 400- to 14 200-ft/s range, which indicates concrete of at least moderate quality.

A set of cores were drilled through the deck, similar to those from bridge 1. Results of tests on these cores were as follows:

Item	Test Result
Structural deck	
Condition	Generally sound, slight paste deterioration
Air entrainment	Non-air-entrained
Absorption (%)	4.1 (mean of eight values)
Sonic velocity (ft/s)	12 020 (mean of four values)
Compressive strength (psi)	5160 (mean of five values)
Wearing course	
Condition	Absent
Absorption (%)	--

The results indicated that the concrete was generally sound and unfractured and there was only slight paste deterioration immediately beneath the bituminous wearing surface. No evidence of a concrete wearing surface remained. Membrane waterproofing was present beneath the wearing course in two of the cores. The concrete from bridge 2 was also well compacted and not air entrained. Five core segments sufficiently long to test in compression yielded a mean strength of 5160 psi. Sonic pulse velocity measured through four of these core segments was in the 10 400- to 15 000-ft/s range. All eight cores were tested for absorption and yielded a mean value of 4.1 percent, which is greater than only 12.5 percent of values measured in cores from other New York bridge decks.

Comparison of Bridges 1 and 2

Both experimental bridges were built in 1931 from the same basic design, with well-compacted, non-air-entrained concrete of comparable strength. Yet their relative condition is markedly different. Although it was beyond the scope of this investigation to determine the causes for this difference, several contributing factors are apparent.

The absorption of bridge 1 concrete appears to be higher than that in bridge 2, possibly by as much as 1.5 percent when measured after 48 years of service. This suggests a higher initial water-cement ratio in the bridge 1 concrete that could have resulted in a higher permeability to both water and dissolved chlorides. Failure of concrete in the structural deck is judged to have resulted from freezing of water in the pores of saturated cement paste, aggravated by the presence of chlorides in solution. Failure of concrete in the lower portion of the T-beam stems and fascia girders is judged to have resulted from the same causes plus corrosion of steel reinforcement near the concrete surface. Both mechanisms are facilitated by increased concrete permeability. Differences in deterioration of concrete in other bridge decks in New York have been shown to be measurably related to differences in concrete absorption within the range encountered here (7).

A second factor that may have contributed to the superior performance of bridge 2 is the possible presence of a protective waterproofing membrane between the structural concrete deck and the wearing surface at some time during the bridge's life. A membrane of the bituminous-epoxy type was found in two of the eight cores removed from this bridge. No evidence of a coating was found on the cores from bridge 1. Though such membranes have generally been found to be imperfect barriers to the passage of water and dissolved chlorides (8), they certainly inhibit such passage significantly, even in the least-effective applications.

THEORETICAL CONSIDERATIONS

Despite the emphasis on concrete strength in design calculations and construction inspection, this property has only a modest influence on structural capacity. In working stress design, which was in use in the era when the concrete bridges that are now causing load-rating difficulty were constructed, variations in concrete strength are reflected in the concrete modulus of elasticity and allowable stress. For sections of constant dimension under equal magnitude of bending moment, loss of concrete strength (reduction in modulus) results in an increase in the neutral axis depth, since a greater concrete area is needed to balance the steel. This increase is reflected in a decrease in the moment arm of internal forces and, consequently, an increase in steel stresses (see Figure 6). Because modulus varies as the square root of concrete strength, the change in steel stress is small over the probable range of concrete strengths. In contrast, concrete stress decreases under these conditions, since the decrease in internal moment arm is more than compensated by the increase in compression area. This decrease is also small, however.

Despite these modest effects on stress levels, the consequences of reduced concrete strength can be significant from the point of view of working stress. Allowable stress levels are a constant percentage of concrete strength (2), and thus, in certain cases, theoretical member capacity will vary directly with concrete strength. These cases occur when the amount of reinforcement is large and limiting stress levels are attained first in the concrete. Although each structure should be checked on an individual basis, this compression control situation is unusual and reductions in concrete strength will be of no consequence, except in the case of very weak concrete.

Figure 6. Variation in steel stress with concrete compressive strength.

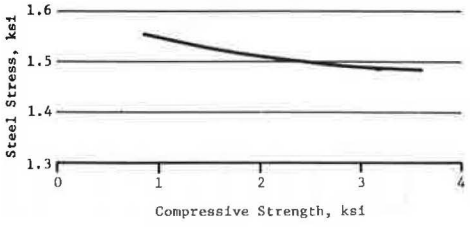

If more recent methods of strength design are used, concrete strength also has little influence on capacity as long as this strength is above some limiting value. This limit is determined by calculating the concrete strength at which the failure mode changes from yielding of the reinforcement to compression failure. The latter is unacceptable because of the lack of visible signs of impending collapse. A specific section can be easily analyzed to determine this limit.

Figure 7. Variation in steel stress with slab thickness.

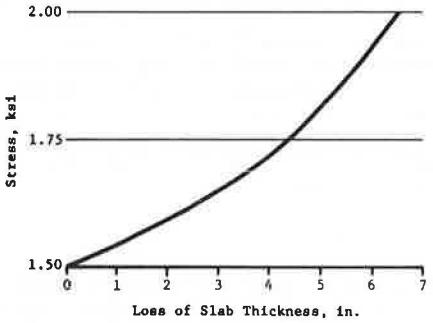

Figure 8. Effect of support skew on transverse influence line.

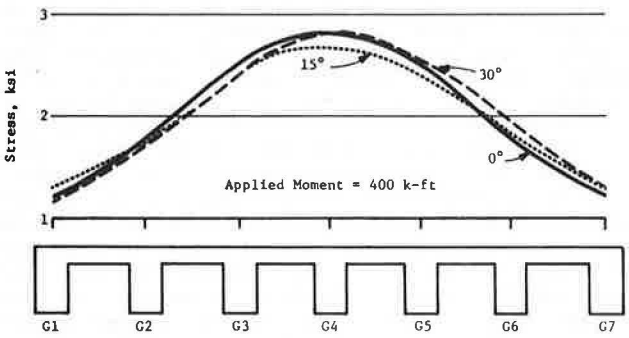

Figure 9. Effect of parapets on transverse influence line.

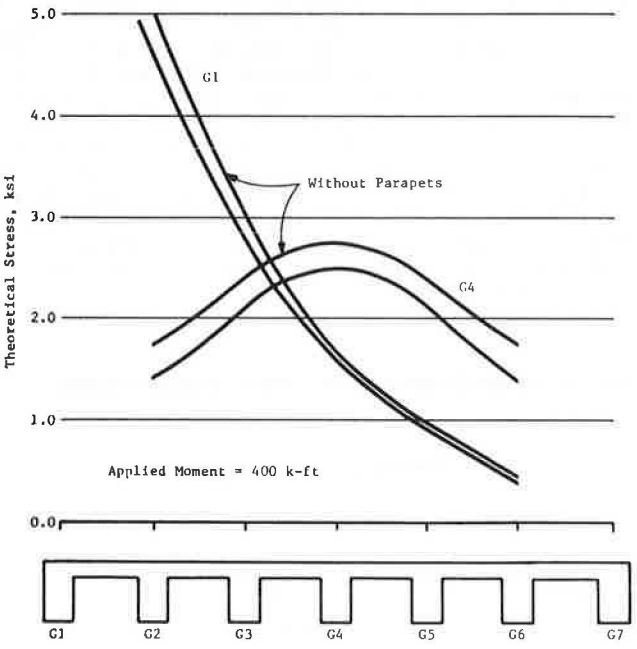

The consequences of loss of compression area can be evaluated by considering a specific T-beam section representative of the bridges tested. The section is subjected to a constant moment, and the variation in steel stress with decrease in slab thickness is evaluated. It can be seen in Figure 7 that steel stresses increase at an increasing rate. Although the variation in stress over the range of thicknesses shown is great, it should be realized that losses greater than about 3 in would weaken the ability of the slab to perform its primary function of resisting wheel loads.

From these two examples, it should be apparent that the consequences of loss of concrete strength or compression concrete area are small at working stress levels. Because of this result, observations of concrete deterioration in a conventional inspection report are of limited use to the structural engineer in making a rational estimate of safe load-carrying capacity.

FIELD TEST

Despite the analytical findings regarding the influence of concrete deterioration on structure response, it was still felt that there should be a measurable difference between the behavior of sound and deteriorated structures. The two structures were instrumented with electrical-resistance strain gages bonded to the tension steel reinforcement at midspan. The test load was a dump truck weighing about 40 000 lb, which, when positioned at bridge midspan, produced a maximum bending moment close to the current HS-20 design load. The truck was positioned at several transverse locations across the widths of the structures, and strain in the reinforcement was measured. With these data, a transverse influence line was produced for each girder that gave the variation in reinforcement stress with transverse position.

Because of structural differences in the bridges, direct comparison of measured values is not possible. However, differences in response due to span length and support skew angle can be eliminated by normalizing the result to a constant level of midspan bending moment. Although support skew causes a marked change in the bending moment resisted by individual girders, there is an accompanying change in the total bending moment. Because of these changes, the variation in transverse distribution of bending moment is small for skew angles less than 30° (see Figure 8).

An analytical adjustment has also been made for the different stem depths. Conventional theory for reinforced concrete at working stress levels predicts that the stress induced in the reinforcing steel is proportional to the resisted bending moment. This factor of proportionality--the reciprocal of the section modulus--can be calculated from properties of the section. With knowledge of section modulus, measured strains can be adjusted to a common basis. The justification for this adjustment is the assumption that, although the effective section is poorly defined, if both structures were in new condition the only difference in the relation between moment and steel stress would be caused by the difference in stem depth.

An analytical adjustment for the effect of the parapets on the measured values cannot be made. Figure 9 shows the effect of the increased fascia stiffness that results from the parapets. Because of this increased stiffness, a greater proportion of total moment is carried by the fascia, which causes a reduction in stress in the interior girders. Because the section modulus of the fascia is increased, stress levels at this location are also

Figure 10. Experimentally determined influence lines.

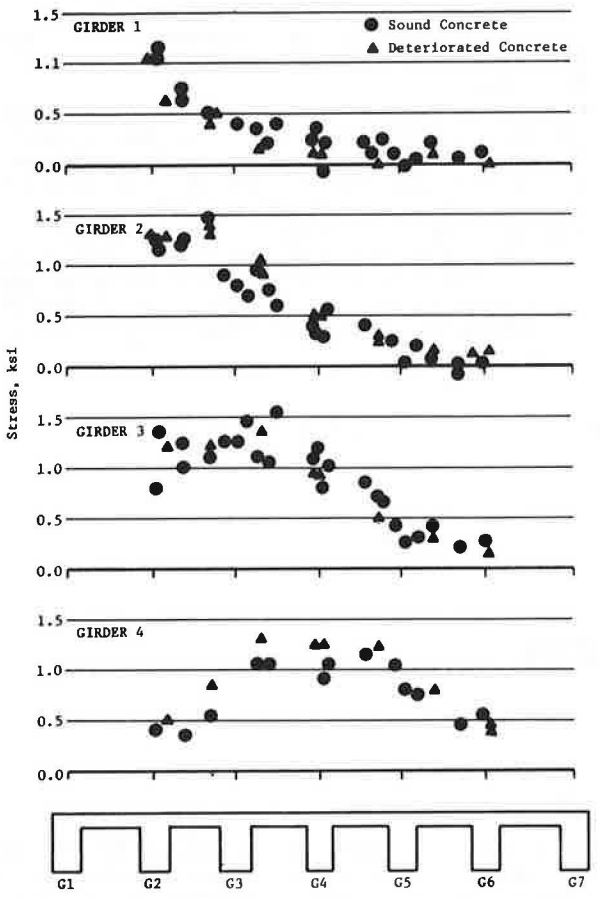

reduced despite the larger moment. This effect cannot be removed from the data because the stiffness of the heavily deteriorated parapets cannot be reliably estimated.

The adjusted data are plotted in Figure 10 as influence lines showing the variation in stress in a particular girder as a function of load position. Data from symmetrical girders have been superimposed (i.e., the plot for girder 1 contains data from girders 1 and 7) since the raw data showed no evidence of unsymmetrical behavior. Except for the centerline member (girder 4), there are no differences in either the magnitude or trend of the influence lines for the two bridges. For girder 4, the response of the deteriorated structure (bridge 1) is slightly greater for loads near the centerline. Since this is the structure with parapets, and since analysis shows that stress levels would be decreased by the action of these elements, it is concluded that the parapets are inactive. In addition, the higher stresses imply weaker concrete or a reduced section resisting load.

The significance of the observed difference in response should be assessed in terms of the reliability of electrical strain gage measurements and the consequences to the load capacity of the structure. Data for each of the four girders scatter substantially. This scatter is the result of the joint variability of the load placement and the strain gages (and associated data-acquisition equipment). In addition, variation due to a lack of complete structural symmetry is a contributing factor. In view of the variability shown here, and experience with this type of measurement on other structures (9), claiming an accuracy better than ±200 psi would be unrealistic.

The maximum stress induced in girder 4 is 1300 psi in the deteriorated structure and 1150 psi in the sound structure. These stresses are the result of a 400-kip•ft moment resisted by the cross section. Based on these values and accounting for the dead-load stresses, these bridges could support 5.6 and 6.2 HS-20 trucks, respectively, with 30 percent impact at the steel working stress of 18 000 psi. Less conservatively, if one considers the effects of trucks in two lanes (the design load), the most heavily loaded girder is girder 2. For this design loading condition, the structures can support 3.0 and 3.2 times the design load, respectively. Thus, based on the evidence from these tests, neither structure is in any danger of flexural failure under highway loads.

OTHER STRENGTH CONSIDERATIONS

Clearly, the testing and analyses performed for these structures do not comprehensively evaluate their strength. Other forms of failure, such as fatigue, loss of bond between reinforcement and concrete, and punching shear in the slab, have not been evaluated. In general, these modes give no signs of impending failure, and testing short of destruction reveals no information on capacity. Analysis also falls short, particularly when it is necessary to factor in the existing condition of the concrete.

CONCLUSIONS

Despite an inspection report indicating that bridge 1 has severe deterioration, some testing that confirmed the presence of low-strength concrete, and rating by accepted procedures that suggested only minimal adequacy to tolerate present traffic, a comparison of physical test results from this and a geometrically similar but sound structure revealed only minor differences in flexural behavior. Estimates of flexural capacity, based on the field test results, show that both structures can support at least three times their design load without exceeding allowable stress in the steel reinforcement.

The results presented indicate that structural inspection and rating procedures used in New York and believed to be typical of national practice are deficient for evaluating deteriorated structural concrete elements. Apparently, bridge inspectors are not identifying those aspects of structural condition, which have a significant impact on safe load-carrying capacity. Although it is not an objective of this paper to identify appropriate inspection items, it is suggested that such things as length of exposed rebar (as an indication of bond loss) and loss of rebar cross section may be of greater significance to load-rating engineers than apparent overall quality of the concrete. Additional work is needed to identify types of bridge conditions that are detrimental to capacity and to develop procedures for converting these observed conditions into accurate load ratings that do not penalize the aesthetically deficient but structurally safe bridge.

ACKNOWLEDGMENT

This paper was prepared under the administrative supervision of William C. Burnett, Engineering Research and Development Bureau, New York State Department of Transportation, with the cooperation of FHWA.

REFERENCES

1. National Bridge Inspection Standards. Federal Register, Vol. 36, No. 81, 23 C.F.R., Chapter 1, Part 25, April 27 1971, pp. 7851-52.
2. Manual for Maintenance Inspection of Bridges. AASHTO, Washington, DC, 1974.
3. Bridge Inspection Manual for the Bridge Inventory and Inspection System. Structures Design and Construction Subdivision, New York State Department of Transportation, Albany, undated.
4. R.J. Kissane, D.B. Beal, and J.A. Sanford. Load Rating of Short-Span Highway Bridges. Engineering Research and Development Bureau, New York State Department of Transportation, Albany, Res. Rept. 79, May 1980.
5. Bridge Inspector's Training Manual. FHWA, 1970.
6. W.G. Leslie and W.P. Chamberlin. Effects of Concrete Cover Depth and Absorption on Bridge Deck Deterioration. Engineering Research and Development Bureau, New York State Department of Transportation, Albany, Res. Rept. 75, Feb. 1980.
7. W.G. Leslie, R.J. Irwin, and W.P. Chamberlin. Bridge Deck Deterioration: Two Case Studies. Engineering Research and Development Bureau, New York State Department of Transportation, Albany, Feb. 1979.
8. W.P. Chamberlin, R.J. Irwin, and D.E. Amsler. Waterproofing Membranes for Bridge Deck Rehabilitation. Engineering Research and Development Bureau, New York State Department of Transportation, Albany, Res. Rept. 29, May 1975.
9. D.B. Beal and R.J. Kissane. Field Testing of Horizontally Curved Steel Girder Bridges: Second Interim Report. Engineering Research and Development Bureau, New York State Department of Transportation, Albany, Res. Rept. 1, Oct. 1971.

Publication of this paper sponsored by Committee on Performance of Concrete.

Abridgment

Accuracy of the Chace Air Indicator

MICHAEL M. SPRINKEL

Results of a study undertaken to quantify and improve the relation between air contents in concrete determined by using the Chace air indicator (CAI) and those determined by using the pressure method are reported. The study revealed very poor agreement between air contents determined by the two methods. The pressure method gave values typically 30 percent higher than anticipated based on the CAI readings. The poor agreement was found to involve relations between the volume of the stems, the volume of the bowls, and the mortar correction factors supplied by the manufacturers of the CAI. Consequently, it was recommended that AASHTO T199-72 be modified to account for these relations so that the CAI can be used to obtain a reasonably accurate indication of the air content of fresh concrete.

Inspection personnel like the Chace air indicator (CAI) (AASHTO T199-72) because of the relative ease with which it can be used. Unfortunately, very poor agreement has been noted between the air contents determined by the CAI and those determined by the pressure method (ASTM C231-75 and AASHTO T152-76). As shown in Figure 1 (1), concrete accepted with the CAI and noted as having an air content of 8 percent, which would be acceptable, could actually have an air content of 12 percent or more, which could cause the concrete to fail the strength test. Frequently, when concrete cylinders have failed the 28-day strength test, subsequent petrographic examinations of the hardened concrete have revealed that the air content was much too high.

The study reported here, which comprised the preparation and testing of 99 batches of pavement and bridge-deck concretes (2, p. 145), was conducted to quantify and improve the relation between air contents determined by the CAI and those determined by the pressure method. The air content of each batch was determined once by using the pressure method, twice by using the CAI to measure the air content of each of two mortar samples obtained by passing a portion of the concrete through a no. 10 sieve (screened samples), and twice by using the CAI to measure the air content of each of two samples obtained by removing mortar from the concrete with a putty knife (unscreened samples).

RESULTS

Figure 1 shows the plots of the average of the CAI determinations on the two unscreened samples as a function of the air content determined by the pressure method, after the data for the CAI have been corrected for the mortar content of the concrete based on the manufacturer's recommended mortar correction factors (MCFs). A relation similar to that shown in Figure 1 was obtained by plotting the average of the CAI determinations on the two screened samples as a function of the air content determined by the pressure method. The data obtained for the screened mortar samples were slightly more variable than those for the unscreened samples: The standard deviation was 0.81 percent as compared with 0.71 percent (1).

Chace Factor

To determine why the CAI was indicating air contents that were much too low, measurements were made of the volumes of the bowls and stems of 36 randomly selected indicators from three manufacturers. The important consideration was the Chace factor, which is defined here as the volume of one graduation on the stem, which represents 1 percent air, expressed as a percentage of the volume of the bowl, which contains the sample of mortar. The measurements revealed that, for CAIs supplied by manufacturers H and C, the average Chace factor was 2.30 and the uniformity was good, exhibiting standard deviations of 0.05 and 0.03, respectively. The CAIs from manufacturer L had an average Chace factor of 1.87, but the variation among the instruments was broad: The standard deviation was 0.46. In fact, one CAI from manufacturer L had a Chace factor of 1.43 (the inside diameter of the stem was relatively small and would produce high stem readings) and another had a Chace factor of 2.51 (the inside diameter was relatively large and would produce low readings). For

example, if one used the manufacturer's MCF, which is accurate for a Chace factor of 1.8, a sample of mortar exhibiting an air content of 8.0 percent when checked with the CAI that had the Chace factor of 1.43 would provide an air content of 4.5 percent when checked with the CAI that had the Chace factor of 2.51. It is interesting to note that the American Association of State Highway and Transportation Officials (AASHTO) requires the CAI to be manufactured so that the Chace factor is 2.2. The CAIs from manufacturers H and C are in reasonable compliance with the AASHTO specification (AASHTO T199-72).

Figure 1. Air content determined by pressure method versus mortar-corrected CAI air content based on manufacturer's recommended mortar correction.

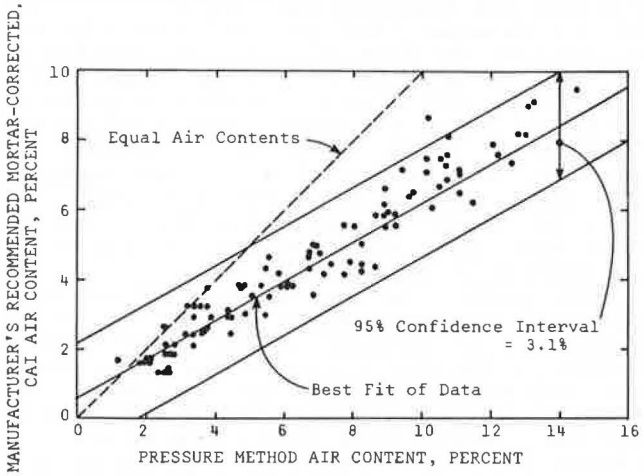

Table 1. Mortar correction factors.

Mortar Content by Volume		Chace Factor[a]				
Amount (ft^3/yd^3)	Percent	1.6	1.8[b]	2.0	2.2	2.4
27	100	1.60	1.80	2.00	2.20	2.40
20	74	1.19	1.33	1.48	1.63	1.78
19	70	1.13	1.27	1.41	1.55	1.69
18	67	1.07	1.20	1.33	1.47	1.60
17	63	1.01	1.13	1.26	1.39	1.51
16	59	0.95	1.07	1.19	1.30	1.42
15	56	0.89	1.00	1.11	1.22	1.33
14	52	0.83	0.93	1.04	1.14	1.24
13	48	0.77	0.87	0.96	1.06	1.16
12	44	0.71	0.80	0.89	0.98	1.07
11	41	0.65	0.73	0.81	0.90	0.98
10	37	0.59	0.67	0.74	0.81	0.89

[a]Volume of one graduation on stem as a percentage of the volume of the bowl.
[b]Factors supplied by the manufacturers.

Figure 2. Air content determined by pressure method versus Chace-factor-based mortar-corrected CAI air content.

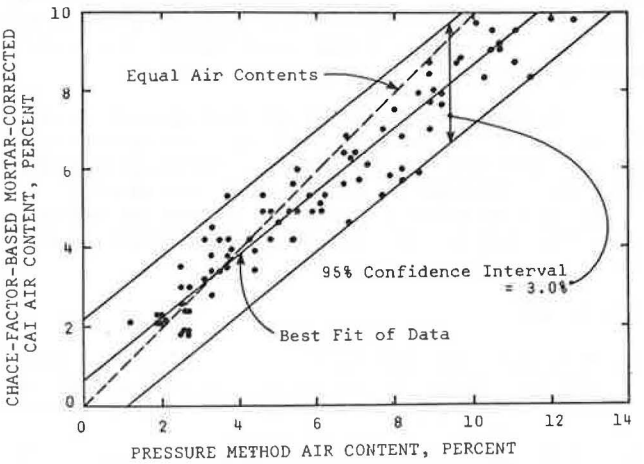

The MCFs given in Table 1 were tabulated for use with the typical range of Chace factors. Reading from the left column, on the first line of Table 1 it can be seen that, for a Chace factor of 1.8 and a mortar content of 100 percent by volume (27 ft^3/yd^3), the stem reading is multiplied by 1.8 to get the volume of air. On the seventh line it can be seen that, if the concrete has a mortar content of 56 percent by volume (15 ft^3/yd^3), the air content is read directly since the MCF is 1.0.

The relation shown in Figure 2 is the result of the modification of the stem readings by applying the MCFs to take into account the particular Chace factors of the CAIs used to produce the data. It can be seen in Figure 2 that, once the Chace-factor-based MCFs were applied to the stem readings, there was fairly good agreement between the air contents determined by the CAI and the pressure method, and there was a magnitude of improvement in comparison with the relation shown in Figure 1, which is based on the manufacturer's MCFs.

Curve Correction

The dashed line in Figure 2 is the line of equality, and it can be seen that, even after the Chace-factor-based MCFs are applied, the CAI reads slightly high at low air contents and low at high air contents. The application of another correction, designated "curve correction", improves the agreement between the air contents determined by the CAI and the pressure method. For example, if the Chace-factor-based mortar-corrected air content of an unscreened sample is 8 percent, the curve correction is 1 percent and the actual air content is 9 percent. The curve correction for each Chace-factor-based mortar-corrected CAI air content was determined by subtracting this air content from the pressure-method air content as determined from the equation for the line representing the best fit of the data in Figure 2 by using the data from the CAIs as the independent variable. The equation is

$$PM = (SR)(CF)(MC)(1.164)/27 - 0.308 \quad (1)$$

where

PM = air content determined by pressure method (%),
SR = stem reading, and
MC = mortar content (ft^3/yd^3).

A similar equation for the line representing the best fit of the data for screened samples is

$$PM = (SR)(CF)(MC)(1.138)/27 - 0.869 \quad (2)$$

It is interesting to note that curve corrections based on these two equations are similar to ones reported by the Virginia Highway and Transportation Research Council, the Federal Highway Administration, and the U.S. Army Corps of Engineers in studies made 20 years ago (3).

As can be seen in Figure 3, once the Chace-factor-based MCFs and the curve corrections are applied, the air content determined by the CAI agrees with that determined by the pressure method. Because of the inherent variability of concrete and the small size of the sample used with the CAI, for

one operator the standard deviation for the average air content for two unscreened samples, compared with the air content determined by the pressure method, is 0.97 percent. The standard deviation for two screened samples is 1.08 percent, which is 11.0 percent greater than for unscreened samples. Therefore, screening should be avoided if the samples can be obtained without it. A generally accepted standard deviation for a pressure test is 0.6 percent; therefore, the average CAI air content of five unscreened samples provides a confidence level equal to that provided by one pressure test.

Figure 3. Air content determined by pressure method versus Chace-factor-based mortar-corrected and curve-corrected CAI air content.

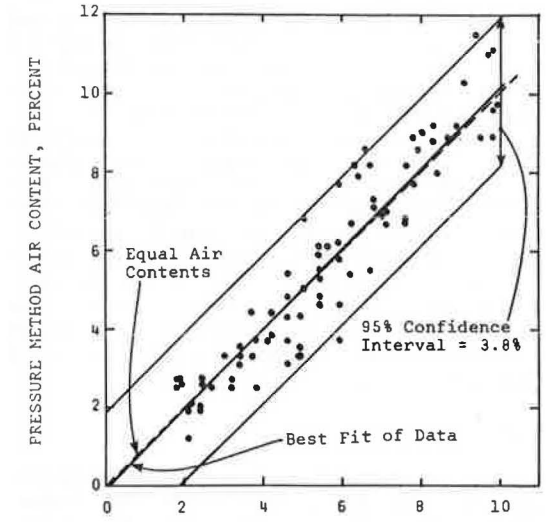

Figure 4. Chace conversion nomograph.

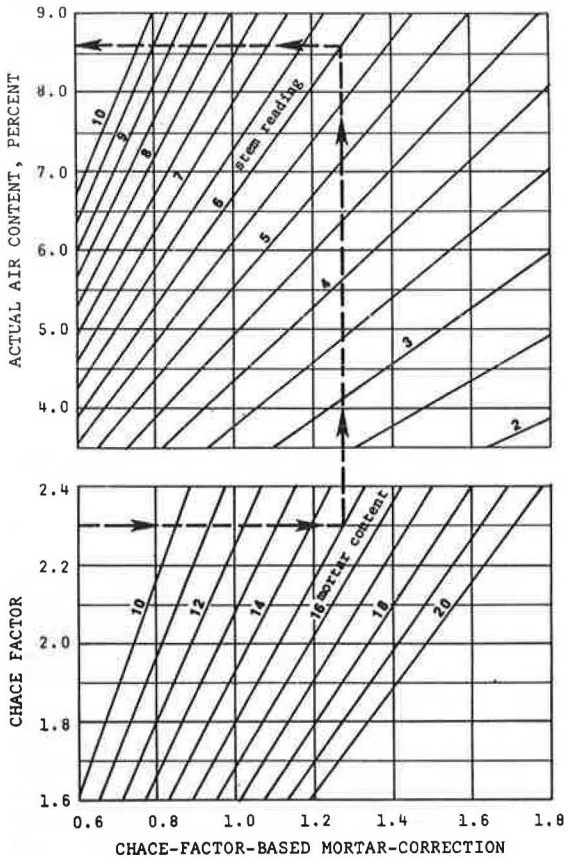

IMPLEMENTATION OF RESULTS

The Virginia Department of Highways and Transportation currently determines the Chace factor of each CAI and furnishes field personnel with CAIs inscribed with the Chace factors. The Chace factor for a CAI can be determined in a few minutes with a 1-mL syringe, such as an insulin syringe, by noting the quantity of alcohol injected into 10 graduations on the stem. Although the volume of the metal cup should not be overlooked, the cups have typically been found to be reasonably uniform in size. The stems tend to vary in size because they consist of drawn glass tubing that is difficult to control in the manufacturing process.

Field personnel are also supplied with the Chace conversion nomograph shown in Figure 4 (1), which allows them to determine the air content without multiplying the stem reading by the Chace-factor-based MCF and without adding the curve correction. As an example of how to use the nomograph, assume that the indicator has a Chace factor of 2.3, the concrete has a mortar content of 56 percent by volume (15 ft^3/yd^3), and the stem reading is 6.0 percent; then the actual air content would be 8.6 percent (Figure 4). If one used the MCF supplied by the manufacturer, the stem reading of 6.0 percent would be reported for the air content, which is 2.6 percent less than the actual air content and represents an error of 30 percent.

Test results for the acceptance of concrete are based on the average air content of two samples and, if the results differ by more than 2 percent, a third sample is taken and test results are based on the average of the three samples. Concrete determined to be unacceptable by the CAI is not rejected unless a test with the pressure method confirms that it is unacceptable. The pressure method is used to determine whether concrete to be placed in bridge decks meets Department specifications. The current practice allows the Department to minimize the work load on the inspector and at the same time to have an acceptable level of assurance regarding the air content of the concrete.

CONCLUSIONS

1. The CAI can be used to provide a reasonably accurate indication of the air content of fresh concrete, when results are based on the average of tests of a minimum of two samples and the results are corrected by using a Chace conversion nomograph that takes into account the Chace factor, curve correction, and MCF.

2. A test result based on the average Chace-factor-based mortar-corrected and curve-corrected CAI air contents of five samples typically provides the same confidence as one pressure test result.

3. AASHTO T199-72 should be revised to incorporate the findings of this study (the revisions will be in the 1982 edition).

REFERENCES

1. M.M. Sprinkel and B. Lee. The Chace Air Indicator. Virginia Highway and Transportation Research Council, Charlottesville, VHTRC 81-R37, Feb. 1981.
2. Road and Bridge Specifications. Virginia De-

partment of Highways and Transportation, Richmond, Jan. 1, 1978.
3. H.H. Newlon, Jr. A Field Investigation of the AE-55 Air Indicator. Virginia Council of Highway Investigation and Research, Charlottesville, Rept. 35, Oct. 1962.

Publication of this paper sponsored by Committee on Batching, Mixing, Placing, and Curing of Concrete.